THE

LONDON, EDINBURGH, AND DUBLIN

PHILOSOPHICAL MAGAZINE

AND

JOURNAL OF SCIENCE.

[SEVENTH SERIES.]

DECEMBER 1937.

LXXXVIII. *The Diamagnetic Susceptibilities of some Complex Ions.* *By* Dr. S. RAMACHANDRA RAO *and* S. SRIRAMAN, *Annamalai University, Annamalainagar, South India* *.

1. *Introduction.*

THE most comprehensive investigation of the susceptibilities of chemical compounds and ions was first carried out by Pascal [1]. He discovered that the law of additivity was generally obeyed in the case of organic compounds, while for inorganic compounds no such simple relation was applicable. Joos [2] and Ikenmeyer [3] calculated the susceptibilities of some ions belonging to the alkali and halogen groups on the assumption that for those ions possessing the same inert gas electronic configuration the susceptibility was inversely proportional to the square of the nuclear charge. Reicheneder [4] determined the susceptibilities of halogen ions by finding out the susceptibilities of the corresponding acids, the diamagnetic contribution of the hydrogen ion being taken as zero. Weiss [5] pointed out the necessity of taking into account this contribution, and estimated the ionic contribution of H^+ to be 1·0 (paramagnetic) [6]. We owe to Kido [7] an elaborate

* Communicated by the Authors.

investigation of the magnetic susceptibility of chemical compounds and ions. He compared the ionic values deduced theoretically by Angus [8] with those obtained from experiment, and observed a systematic difference between the sets of values. He attributed this difference, which depended on the valency of the ion, to the paramagnetic term arising from the Van Vleck distortion of the orbits [9].

More recently Hoare and Brindley [10] have determined the diamagnetic susceptibilities of salts composed of ions with inert gas configurations, using a large electromagnet and adopting the Gouy method. They made a careful test of the additivity law from the results obtained, and found that it did not hold good for the halides of lithium and cæsium. They have adduced special reasons, both theoretical (Pauling [11], Stoner [12] and Angus [8]) and experimental, in support of deducing all ionic susceptibilities with 0·7 as the standard value for Li^+. The susceptibility of this ion being small, no large error will be involved in the determination of the values for other ions.

The influence of the deforming power of ions on each other when they combine to form compounds does not seem to have been taken into account in the estimation of ionic susceptibilities. Flordal and Frivold [13] showed that large changes of susceptibilities took place when some alkaline earth halides were dissolved in water. Such a change had already been observed by Hocart [14], who obtained a 2 per cent. increase of susceptibility on dissolving calcium chloride in water. The influence of the deforming power of ions on magnetic susceptibilities has been considered at length by Varadachari [15] and Subramaniam [16]. Fajans [17] has shown that the deforming power of the cation is large when its size is small and the charge is great. Ions possessing inert gas configurations produce less deformation than those which do not possess such closed configurations. Anions, on the other hand, suffer much deformation when both their charge and size are large. These conclusions were shown to be applicable to the case of some metallic halides by Subramaniam [16].

These considerations make it clear that in the estimation of susceptibilities of free ions a careful investigation of ionic deformation and the consequent departure from

the law of additivity must be made in every case. This point is emphasized by the work of Subramaniam[16], who obtained as much as 22 per cent. increase on dissolving cadmium iodide and 11 per cent. increase on dissolving zinc iodide in water.

One method of studying ionic deformations which follows from the experimental work of Varadachari [15] and Subramaniam [16] is to determine the susceptibilities of salts in the solid state and in the state of solution. The change of susceptibility on dissolving the salt may be attributed to the release of ionic deformations. There is, however, the problem of hydration of the ions in solution. The ions may attach themselves to the solvent molecules, bringing about new constraints. But careful investigations by Hocart [14], Flordal and Frivold [13], and Subramaniam [16] indicate that such interaction in the solution does not cause more than 1 per cent. change in the total susceptibility. It is most likely that in many cases the change is much less.

The problem becomes more complicated when we proceed to determine the ionic susceptibilities of complex radicals. In salts formed by the combination of a simple ion with a complex radical we have to consider not merely the electronic interactions within the radical but also the constraints that may be formed or released due to the presence of the simple ion. When therefore we dissolve such salts in water the changes observed would depend on the nature of dissociation, the formation of polymers, and the release of deformation of the electronic system within the molecule. In this paper it is proposed to study the ionic susceptibilities of a few complex radicals by careful experiments on a few important salts (containing those radicals) in the solid and dissolved states. In Section 4 of this paper the measurements made here will be discussed in the light of our knowledge of their other properties.

2. *Experiment.*

A study has been made of the susceptibilities of formate, acetate, nitrite, nitrate, iodate, and selenite, ions. The salts used were of the highest purity, obtained from Kahlbaum or Merck. The solvent employed, namely water, was distilled several times before use,

and chemical tests showed the complete absence of any ferromagnetic impurity.

Measurements of susceptibility were made with a Curie balance [18]. Water was used as the standard for comparison, its susceptibility at 30° C. being taken to be 0·72.

The containers were thin spherical bulbs blown from glass tubing having a low diamagnetic susceptibility. The deflexions obtained with the bulbs were about 2 mm. (in no case more than 5 mm.), while they were nearly 15 cm. for the substances taken. The retorsion method was employed, the specimen being brought to the identical position in presence of the magnetic field. After determining the deflexions with the solutions contained in the bulbs the water was evaporated away by keeping them open in an air-oven at about 70° C. Knowing the initial masses of the bulbs, it was thus possible to determine the masses of the salt and solvent in each case. The weights were determined with a Sartorius balance correct to the tenth of a milligram. A careful estimate of the various errors involved in these observations indicates a probable error of $\frac{1}{2}$ per cent. in the susceptibility values.

3. *Results.*

(a) *Magnetic Susceptibilities of the Salts in the Solid State.*

In the following table are given the results obtained for the different substances in the solid state (except formic acid). The values obtained by other investigators are also given wherever these are available. Most of the substances investigated do not seem to have been studied before.

(b) *Formates and Acetates.*

Sodium formate of extra pure quality was available. Barium formate was rendered extra pure by careful recrystallization from an aqueous solution and subsequent drying in a water-bath for 15 minutes, and keeping in an air-oven for more than half an hour. Calcium formate was very pure, but since its solubility is low investigations could be made only for a few concentrations. The acetates studied were specimens "for analysis" from Kahlbaum. Great care was taken to prevent atmospheric

moisture from being absorbed by the salts. The measurements made are given in the following tables The concentrations given are expressed as the mass in grams of the salt dissolved in 100 grams of the solution.

TABLE I.

No.	Substance.	Mol. wt.	No. of trials.	χ.		χ_M.	
				Authors.	Others.	Authors.	Others.
1...	Formic acid HCOOH	46·02	6	0·4464	0·432* 0·434‡	20·5	20·0‡
2...	Sodium formate NaCOOH	68·01	6	0·3642	..	24·8	
3...	Barium formate $Ba(COOH)_2$	227·39	6	0·2927	..	66·6	
4...	Calcium formate $Ca(COOH)_2$	130·09	5	0·3033	..	39·5	
5...	Sodium acetate $NaCH_2COOH$	82·02	6	0·4584	0·50*	37·6	
6...	Barium acetate $Ba(CH_2COOH)_2$, H_2O	273·42	6	0·3662	..	100·1	
7...	Iodic acid HIO_3	175·94	6	0·2666	..	46·9	50·41†
8...	Lithium iodate $LiIO_3$	181·87	5	0·2660	..	48·4	
9...	Sodium iodate $NaIO_3$, H_2O	215·93	5	0·2978	..	64·3	
0...	Potassium iodate KIO_3	214·03	4	0·2783	..	59·6	63·1†
1 ..	Sodium nitrite $NaNO_2$	69·01	7	0·2097	..	14·5	
2...	Potassium nitrite KNO_2	85·11	5	0·2741	..	23·3	
3...	Barium nitrite $Ba(NO_2)_2$, H_2O	247·40	5	0·2372	..	58·7	
4...	Sodium nitrate $NaNO_3$	85·01	4	0·2941	0·280*	25·0	25·6‡
5...	Potassium nitrate KNO_3	101·10	4	0·3333	0·326*	33·7	34·0‡
6...	Selenious acid H_2SeO_3	129·22	3	0·3219	0·360*	41·6	
7...	Sodium selenite Na_2SeO_3	173·20	4	0·2992	..	51·8	

χ. Specific diamagnetic susceptibility.
χ_M. Molecular diamagnetic susceptibility.

No systematic variation of the susceptibility was observed when the concentration was varied. An examina-

* Int. Crit. Tables, vi. p. 356.
† Gray and Farquharson, Phil. Mag. x. p. 191 (1930).
‡ Kido, ref. 6.

tion of the above table shows that the additive law is obeyed in all the cases investigated. The deviation is small and the largest obtained is only +0·005. This is due obviously to the error in the value of the concentration of the solution (which is likely to be less than 1 per cent.) and the errors in the observed values of the specific

TABLE II.

No.	Substance.	Range of concentrations studied.	Number of measurements.	Change of susceptibility per gram of substance on dissolving in water.
1...	Sodium formate	25 to 52	9	+0·005
2...	Barium formate	20 to 30	9	+0·002
3...	Calcium formate	2 to 8	8	+0·003
4...	Sodium acetate	17 to 37	9	+0·004
5...	Barium acetate	10 to 25	6	+0·002

susceptibilities of the salt and the solution. We may therefore conclude that there is very little change in susceptibility when formates and acetates are dissolved in water. The small changes observed may also be attributed to depolymerization of complex water molecules.

(c) *Iodic Acid and Iodates.*

The iodic acid and iodates used in this investigation were of the purest specimens available from Kahlbaum. The results are given below.

TABLE III.

No.	Substance.	Range of concentrations studied.	Number of measurements.	Change of susceptibility per gram of substance on dissolving in water.
1...	Iodic acid	17 to 76	10	−0·031
2...	Lithium iodate ..	30 to 60	7	−0·036
3...	Potassium iodate	10 to 20	4	−0·017

The susceptibility shows a definite decrease when the substances are dissolved in water. No systematic variation was obtained when the concentration was varied. The mean changes observed are given in the last column.

(d) *Nitrites and Nitrates.*

Merck's extra pure nitrites were used. The glass bulbs used as containers were made sufficiently large and had wide mouths to facilitate rapid filling up with the substances. The salts are deliquescent, and hence the bulbs with the freshly filled substances were placed in a desiccator under very low pressures before the magnetic measurements were made. Consistent results were then

TABLE IV.

No.	Substance.	Range of concentrations studied.	Number of measurements.	Change of susceptibility per gram of substance on dissolving in water.
1...	Sodium nitrite ..	27 to 45	4	+0·046
2...	Potassium nitrite	30 to 35	4	+0·043
3...	Sodium nitrate ..	30 to 42	4	+0·016

obtained. The monohydrate of barium was dried at atmospheric pressure in a desiccator, but this made very little difference in the observed susceptibilities. The nitrites were dissolved out with dilute hydrochloric acid in order that the mass of the substance could be determined. The results are given in Table IV.

Much interest attaches to the study of nitrates, since it is well known from Raman effect studies [19] and other investigations [20] that these salts dissociate completely at moderate concentrations. Hence in the solutions we have clearly two types of ion only. The change of specific susceptibility on dissolving the salt may almost wholly be attributed to dissociation.

The specific susceptibility of the nitrate increases very little on dissolving it in water, but the increase is much larger in the case of the nitrites.

(e) *Selenites.*

The aqueous solutions of sodium selenite were studied, and the results are tabulated below :—

TABLE V.

No.	Substance.	Range of concentrations studied.	Number of measurements.	Change of susceptibility per gram of substance on dissolving in water.
1...	Sodium selenite	18 to 35	4	+0·045

The specific diamagnetic susceptibility of sodium selenite increases on dissolving the substance in water.

(f) *Molecular Susceptibility Changes on Solution.*

Table VI. gives the molecular diamagnetic susceptibility values of the salts studied in the foregoing pages in the solid and dissolved states.

TABLE VI.—Collected Data.

Substance.	χ_M solid state.	χ_M dissolved state.
Sodium formate	24·8	25·1
Barium formate.....	66·6	67·0
Calcium formate	39·5	39·9
Sodium acetate	37·6	37·9
Barium acetate	100·1	100·6
Iodic acid	46·9	41·3
Lithium iodate	48·4	41·8
Sodium iodate	64·3	—
Potassium iodate	59·6	56·0
Sodium nitrite	14·5	17·6
Potassium nitrite	23·3	27·0
Barium nitrite	58·8	—
Sodium nitrate	25·0	26·4
Potassium nitrate	33·7	—
Selenious acid	41·6	—
Sodium selenite	51·8	59·6

To calculate susceptibilities of the various acid radicals it is necessary to know the susceptibilities of the metallic

ions. The values determined by various investigators are given below :—

TABLE VII.—Ionic Susceptibilities.

Ion.	Theoretical.			Experimental.				
	P.	S.	A.	I.	K.	HB.	FF.	
							(A).	(B).
Li^+	0·63	0·665	0·665	4·0	1·6	0·7	0·7	0·7
Na^+	4·2	4·17	3·74	10·4	7·6	6·1	6·9	6·9
K^+	16·7	14·40	13·06	16·0	13·6	14·6	15·6	15·0
Ca^{++} ...	13·3	11·38	10·42	11·0	6·5	—	7·0	8·8
Ba^{++} ...	46·0	33·30	31·59	39·9	23·6	—	25·4	29·3

P. Pauling [11]. I. Ikenmeyer [3]. S. Slater [12].
K. Kido [7]. A. Angus [8]. HB. Hoare and Brindley [10].
FF (A). Flordal and Frivold [13]. Values calculated from magnetic measurements in the solid state.
FF (B). Flordal and Frivold [13]. Values calculated from magnetic measurements in the dissolved state.

We have taken the values given in the last column as the most probable ones, and calculated the susceptibilities of the complex ions on this basis.

The ionic susceptibilities of the formate $(COOH)^-$, acetate $(CH_2COOH)^-$, iodate $(IO_3)^-$, nitrite $(NO_2)^-$, nitrate $(NO_3)^-$, and selenite $(SeO_3)^{--}$ ions obtained from the foregoing tables are given in the following table. The molecular susceptibilities of the salts in the dissolved state have been taken for the calculations. Where two or more values for the ions were available the average has been given.

4. *Discussion.*

We shall first consider the susceptibilities of the formate and acetate ions. The molar susceptibility of formic acid is seen from Table I. to be 20·5, whereas Kido's experimental value is 20·2. According to Varadachari [15] the molar susceptibility of acetic acid is 32·3, Kido's value being 32·0. The susceptibility of the formate

ion is 17·3 and that of the acetate ion 29·8. It is thus evident that the value of the formate ion is nearly 16 per cent. less than that of formic acid. In the case of the acetate this change is much smaller, being less than 7 per cent. The replacement of one of the hydrogens in the formic acid by a metal ion seems to bring about some change in the internal structure which decreases definitely the diamagnetic susceptibility of the formate ion. Since the change is rather considerable, and apparently independent of the nature of the metal ion introduced, it looks most likely that the replacement

TABLE VIII.—Ionic Susceptibilities.

Ion.	Ionic susceptibility.		
	Calculated from solid data.	Calculated from solution data.	Kido.
$(COOH)^-$	17·3	17·6	20·2*
$(CH_2COOH)^-$	29·8	30·2	31·4*
$(IO_3)^-$	47·3	41·1	52·2
$(NO_2)^-$	8·0	11·4	15·0
$(NO_3)^-$	18·1	19·5	20·1
$(SeO_3)^{--}$	44·9	52·7	47·5

of one of the H ions by the metal ion is accompanied by a change in the internal structure.

Recently Ray [21] put forward the view that the ionizable hydrogen in it is not the hydrogen of the hydroxyl group but the hydrogen attached to the carbon atom. Seshadri [22], on the other hand, suggested that this view was untenable from the well-known chemical properties of the fatty acid and that the CH group persists in the formate ion. Venkateswaran [23] verified by investigations on the Raman effect the presence of the CH group in the solutions of metallic formates. This suggests that the binding of the H^+ ion to the carbon atom is stronger than that of the other H^+ ion to the oxygen atom. Magnetic data support this evidence very clearly.

* Calculated values same as for the respective acids.

If we assume that the formic acid molecule has the following structure, after Lewis and others [24],

$$HCOOH \rightarrow H^{+1} + C^{+2} + O'' + O^{-2} + H^{+1},$$

we note that one oxygen atom (O″) is linked to the carbon atom with a double bond while the other oxygen atom is attached to it with a covalent linkage. The hydrogen ion attached to the oxygen ion should be covalently linked and the attachment should be loose. Kido has calculated the molecular susceptibility of formic acid from the known susceptibilities of the constituent ions. According to him we have for the susceptibility of formic acid

$$\begin{aligned} HCOOH \rightarrow H^{+1} + C^{+2} + O'' + O^{-2} + H^{+1} \\ = -1{\cdot}2 + 7{\cdot}7 + 13{\cdot}7 \\ = 20{\cdot}2, \end{aligned}$$

while the observed value of the molecular susceptibility of formic acid is 20·5. It will be noted that the contribution of the oxygen atom linked by a double bond is only 7·7, for which assumption Kido has given much experimental support. The last two ions are taken separately and not as $(OH)^{-}$, for which the ionic susceptibility is, according to Kido, 8·5 and not 13·7 as we have assumed in the above calculation. We know that the $(OH)^{-1}$ ion possesses very strong binding, the paramagnetic component due to this binding being 5·2; but in formic acid such a binding does not exist, as the magnetic evidence makes it very clear.

When we proceed from formic to acetic acid we find that the hydrogen ion attached to the carbon atom is replaced by $(CH_3)^{+}$. Kido finds that the calculated value of 31·4 for the molecular susceptibility of acetic acid agrees satisfactorily with his experimental value of 32·0. As in the case of formic acid the susceptibility of the acetate decreases slightly when the hydrogen attached to oxygen is replaced by a metallic ion.

It is well known that aqueous solutions of formic acid and formates are weak electrolytes. It is likely therefore that a good part of the metal formates studied here exists undissociated in the solution. This might explain the fact that no change of susceptibility is noticed when formates and acetates are dissolved in water.

Iodates and iodic acid are of special interest since their Raman spectra in the solid and dissolved states have been studied [25], [26]. Concentrations varying from 18N to 0·15N of iodic acid in water were investigated by Venkateswaran [26]. He found that progressive dissociation took place as the dilution was increased, but, unlike nitric acid, dissociation was incomplete even at large dilutions. He has also established evidence to show that polymerization takes place in aqueous solutions and that $(I_2O_8)^{--}$ ions exist even at concentrations of 0·5N.

For our study concentrations varying from nearly 1·2N to 18N have been employed. The diamagnetic susceptibility of iodic acid was found to decrease as the solid was dissolved in water. This change per unit concentration remained the same in the range investigated. This is just what would happen if a definite proportion of the solid dissolved breaks up into H^+ and $(IO_3)^-$ ions. The solution contains, besides these ions, the molecules of HIO_3, which have not dissociated, and a small quantity of polymerized $(I_2O_6)^{--}$ ions. It looks almost definite that the decrease of diamagnetic susceptibility should be due to the dissociation of HIO_3 molecules into the corresponding ions.

The quantitative estimation of the dissociation constant at different concentrations is a matter of some difficulty, but our magnetic measurements show that this constant should be fairly large at the concentrations studied in this investigation. In the dissolved condition the $(IO_3)^-$ ion has a susceptibility of 41·1, although this is likely to be a little less. Kido obtains a value of 52·2, which is much higher than our value.

Using Kido's arguments we shall now show that our value is nearer the calculated value than 52·2. Assuming $(IO_3)^- = I^{+5} + 3O^{-2}$, he determined the value of the I^{+5} ion by assuming the susceptibility of the $(IO_3)^-$ ion to be 52·2 and that of O^{-2} ion 13·7. His value of the susceptibility of the pentavalent iodine ion is in harmony with the values of the other incomplete ions of this element. It seems to us essential that due weight should be given to the fact that iodine pentoxide is more stable than any of the oxides of the other halogens. The attachment of at least two of the three oxygen ions to the iodine ion is very strong, and hence it is likely

that the ionic susceptibility is less than the estimated value. Further, Kido's values are derived from the susceptibility measurements on solids, and we have shown that on dissolving iodic acid and iodates there is an effective decrease in susceptibility. If two of the three oxygen atoms are supposed to possess a double bond, then, assuming the value of the I^{+5} ion to be 11·1, we obtain for the IO_3^- ion 40·2, which is near the value 41·1 obtained by us.

Some support may be had for the above conclusions by the formula proposed by Blomstrand [27] for the anhydride I_2O_5, namely

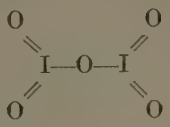

The middle oxygen atom can be replaced by two equivalent hydroxyl groups to form $I_2O_4(OH)_2$ or $2HIO_3$. The nature of binding of two of the oxygen atoms is different from that of the third in the acid molecule.

If we make iodine trivalent in iodic acid, and write the formula for HIO_3 as

then, substituting Kido's ionic values, we obtain for the molecular diamagnetic susceptibility the value 64·9; but since our value for the acid is 46·9 and that for the iodate ion is 41·8, it is clear that the above formula is not the correct one.

We shall next consider the nitrates and nitrites. Important experimental work of Ramakrishna Rao on the Raman effect in aqueous solutions of nitric acid and nitrates has established the conclusion that dissociation is strong even at moderate concentrations [19], [28]. There is evidence to show the absence of any polymerization in the aqueous solution. Hence the observed change of susceptibility, if any, should be due almost completely to dissociation. The ionic susceptibility of NO_3 is found to be 19·5, Kido's value being 20·1. The increase of susceptibility when a nitrate is dissolved in water

is small, being 1·4. We shall show presently that the symmetric structure of the nitrate ion will suffer a very small disortion due to combination with a positive ion.

Kido has calculated the susceptibility of the nitrate ion by assuming that $NO_3^- \rightarrow N^{+5} + 3\,O^{-2}$, in which one of the oxygen atoms is linked to the nitrogen by a double bond. By substituting the ionic values he obtains 20·1 as the calculated value. This is in agreement with his and our experimental values. There is thus conclusive proof that nitrogen is pentavalent in the nitrates.

X-ray studies on the structure of nitrates are of particular interest in this connexion [29]. It has been shown that, like other stable groups, the nitrate ions enter as fixed building units into all their crystals. Each ion is found to be strictly planar, with the central atom 1·26 Å distant from surrounding oxygen ions at the corners of an equilateral triangle 2·18 Å. on one side. In view of the fact that the ionic radii of O^{-2} and N^{+5} are nearly 1·32 and 0·1 Å., much distortion of the oxygens is to be expected. The combination of such a symmetric structure with a positive ion must produce a small effect so far as further distortion is concerned. The fact that the change of susceptibility when a nitrate is dissolved in water is small is in agreement with our knowledge of the structure of crystalline nitrates. The order of increase obtained in this investigation is the same as that obtained by Hocart and others in the investigation of electrovalent salts such as the alkaline halides. It is likely therefore that the increase of diamagnetic susceptibility is due to causes other than mere dissociation. It has also been shown that such small changes may be due to the changes in the diamagnetism of the solvent due to the breaking of complexes.

Nitrates give oxygen when heated and are converted into nitrites. Further and more intense heating breaks up the nitrites. This suggests that the first decomposition is an easy one. When this oxygen is liberated the symmetry of the structure round the nitrogen is no longer as perfect as before. Hence combination of the nitrite ion with a metallic ion should result in some distortion involving the presence of a paramagnetic component. Our results show that on dissolving the nitrites in water the change of susceptibility is much more than in the case of the nitrates.

More experiments are necessary with selenites and selenates before any general conclusions are drawn. Our investigation with sodium selenite shows that the ionic susceptibility of $(SeO_3)^{--}$ increases from 44·9 to 52·7 when the substance is dissolved in water. It has been shown [30] that the molecular conductivity of aqueous solutions increases gradually as the dilution is increased, reaching a limiting value of 112·6 at infinite dilution in the case of sodium selenite. The degree of hydrolysis has been shown to be fairly small in such solutions. Venkateswaran [31] has studied the Raman spectra of selenious acid and its sodium salts. The spectra of aqueous solutions of different concentrations indicate that the dissociation of the acid is weak and that the proportion of molecules dissociated to $HSeO_3^-$ ions remains almost constant. From the changes in the relative intensities of the two lines, 706 and 597, Venkateswaran infers that in the solid selenious acid selenium is hexavalent and that in aqueous solutions it becomes tetravalent. The corresponding formulæ are given below :

(1) 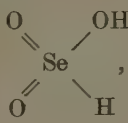

(2) 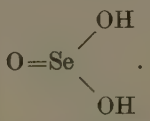

According to Kido the ionic susceptibilities of Se^{+6} and Se^{+4} are $-3·1$ (paramagnetic) and 6·4 (diamagnetic) respectively. A change therefore from the first type to the second type of molecule would be accompanied by an increased diamagnetic susceptibility of 9·5. If we assume that there exists a greater binding effect in the first type than in the second type, this would give rise to a further increase of diamagnetic susceptibility. An increase of this order is obtained when solid sodium selenite is dissolved in water. There is therefore every reason to attribute this increase to an alteration in the valency of the selenium when the salt is dissolved in water.

Summary.

The diamagnetic susceptibilities of some formates and acetates, nitrites and nitrates, iodates and selenites, have been determined in the state of solid and in solutions in water. Formates and acetates do not show any change of susceptibility when dissolved in water. Experiments with iodic acid and iodates showed that the specific diamagnetic susceptibility was greater in the solid state than in the state of solution. In the light of Raman effect data it looks most likely that these changes should be due to dissociation of iodic acid and iodate molecules, but the matter seems to require further investigation. Nitrates show very small changes in susceptibility when dissolved in water because of the stable structure of the nitrate ion as revealed by X-ray studies. Nitrites show a larger increase on dissolving in water than nitrates. Magnetic data support the view that the nitrogen in the nitrite ion is trivalent. In the case of selenites the diamagnetic susceptibility increased when they were dissolved in water. These results support Venkateswaran's inference from Raman effect investigations that in the solid selenious acid selenium is hexavalent and in aqueous solutions it becomes tetravalent. Attention is drawn to the necessity of studying salts in aqueous solutions before definite inferences could be drawn regarding the susceptibilities of the ions concerned.

References.

(1) *Compt. Rend.* clviii. p. 37 (1914); clix. p. 429 (1914); clxxiii. p. 144 (1921).
(2) *Zeits. f. Phys.* xix. p. 347 (1923); xxiii. p. 835 (1925).
(3) *Ann. der Phys.* i. p. 169 (1929).
(4) *Ann. der Phys.* iii. p. 58 (1929).
(5) *Journ. de Phys.* i. p. 185 (1930).
(6) Susceptibility values given in this paper (unless otherwise stated) are diamagnetic and in 10^{-6} units.
(7) Sc. Rep. Tohoku Imp. Univ. xxii. p. 835 (1933).
(8) Proc. Roy. Soc. A, cxxxvi. p. 573 (1932).
(9) 'Electric and Magnetic Susceptibilities,' p. 302 (1932).
(10) Proc. Roy. Soc. A, cxlvii. p. 88 (1934); clii. p. 342 (1935).
(11) Proc. Roy. Soc. A, cxiv. p. 18 (1927).
(12) Proc. Leeds Phil. Soc. i. p. 484 (1929).
(13) *Ann. der Phys.* xxiii. p. 425 (1935).
(14) *Compt. Rend.* clxxxviii. p. 1151 (1929).
(15) Proc. Ind. Acad. Sc. ii. p. 16 (1935).
(16) Proc. Ind. Acad. Sc. iv. p. 404 (1936).
(17) 'Radio elements and Isotopes, etc.,' p. 74 (1931).
(18) For a detailed account see Rao, Proc. Ind. Acad. Sc. i. p. 123 (1934).

(19) Proc. Roy. Soc. A, cxxvii. p. 279 (1930).
(20) Int. Crit. Tables, vi. p. 237.
(21) 'Nature,' cxxxiii. p. 646 (1934).
(22) Cur. Sc. iii. p. 353 (1934); iv. p. 650 (1936); iv. p. 812 (1936).
(23) Proc. Ind. Acad. Sc. ii. p. 615 (1935).
(24) Journ. Am. Chem. Soc. xxxv. p. 1448 (1913).
(25) Woodward, *Phys. Zeits.* xxxii. p. 690 (1931).
(26) Proc. Ind. Acad. Sc. ii. p. 119 (1935).
(27) Mellor, Comp. Treatise, ii. p. 321.
(28) Rao, Kon. Acad. Amsterdam, xxxiii. no. 6 (1931).
(29) Wyckoff, 'The Structure of Crystals,' p. 272 (1931).
(30) Mellor, Comp. Treatise, x. p. 822.
(31) Proc. Ind. Acad. Sc. iii. p. 533 (1936).

LXXXIX. *The Frequencies and Nodal Systems of Circular Plates.* *By* R. C. Colwell *and* H. C. Hardy, *West Virginia University* *.

[Plates X. & XI.]

THE solution of the circular vibrating plate was obtained by Kirchhoff † in 1850, but only the simplest modes have been computed by his method. This is because of the difficulty in making the complicated calculations in the absence of complete tables of the Bessel functions involved. Another method which avoids the use of the Bessel functions was proposed by Lord Rayleigh ‡ and extended by Ritz §. They assume a deflexion curve represented by a series of terms

$$y=[a_1\phi_1(x)+a_2\phi_2(x)+a_3\phi_3(x)+\dots]\cos\omega t, \quad . \quad (1)$$

in which the coefficients a_1, a_2, a_3, etc., are so determined that the equation of the fundamental frequency is reduced to a minimum. A series of linear equations in these coefficients are found whose determinant is made to vanish and the coefficients thereby calculated. Even this method becomes unwieldy at higher frequencies, because the number of coefficients increases with the succeeding modes, n equations being necessary to obtain the nth mode. It is proposed in the following analysis to simplify Kirchhoff's solution and give a comparatively easy method of calculating the frequencies and the nodal systems.

* Communicated by the Authors.
† Rayleigh, 'Sound,' vol. i. p. 352.
‡ *Ibid.* p. 261.
§ Ritz, *Ann. der Physik*, vol. xxviii. p. 737 (1909).

The solution of the circular plate obtained by Kirchhoff may be summarized as follows. The differential equation of the circular vibrating plate is

$$\nabla^4 w = k^4 w, \quad . \quad . \quad . \quad . \quad . \quad . \quad (2)$$

where

$$k = \frac{\sqrt{\omega}}{c}, \quad c^4 = \frac{Eh^2}{3\rho(1-\sigma^2)} \quad . \quad . \quad . \quad (2a)$$

and w is the deviation from the normal position of any point on the plate, ω is the angular frequency, E Young's modulus, $2h$ the thickness of the plate, ρ the density, and σ Poisson's ratio. The equation derived from (2) gives a nodal system of diameters distributed about the centre described by

$$\cos(n\theta - \alpha) = 0, \quad . \quad . \quad . \quad . \quad . \quad . \quad (3)$$

and a system of nodal circles given by

$$J_n(kr) + \lambda J_n(ikr) = 0. \quad . \quad . \quad . \quad . \quad (4)$$

In order to evaluate λ it is necessary to put in the boundary conditions for a plate with a free edge. These are

$$\left.\begin{aligned} \frac{\partial}{\partial r}\left(\frac{\partial^2 w_n}{\partial r^2} + \frac{1}{r}\frac{\partial w_n}{\partial r}\right) - n^2\left(\frac{2-\sigma}{a^2}\frac{\partial w_n}{\partial r} - \frac{3-\sigma}{a^3}w_n\right) &= 0, \\ \frac{\partial^2 w}{\partial r^2} + \sigma\left(\frac{1}{a}\frac{\partial w_n}{\partial r} - \frac{n^2}{a^2}w_n\right) &= 0. \end{aligned}\right\} \quad . \quad . \quad . \quad (5)$$

Substituting (5) in (4), we obtain for $r = a$

$$\left.\begin{aligned} -\lambda &= \frac{n^2(\sigma-1)[kaJ_n'(ka) - J_n(ka)] - k^3a^3J_n'(ka)}{n^2(\sigma-1)[ikaJ_n'(ika) - J_n(ika)] + ik^3a^3J_n'(ika)}, \\ -\lambda &= \frac{(\sigma-1)[kaJ_n'(ka) - n^2J_n(ka)] - k^2a^2J_n(ka)}{(\sigma-1)[ikaJ_n'(ika) - n^2J_n(ika)] + k^2a^2J_n(ika)}. \end{aligned}\right\} \quad . \quad . \quad . \quad (6)$$

If the values of λ in (6) are equated, we obtain

$$\begin{aligned} &[n^2(\sigma-1)^2ka - n^4(\sigma-1)^2ka - k^5a^5][iJ_n(ka)J_n'(ika) \\ &\quad - J_n(ika)J_n'(ka)] - 2k^3a^3n^2(\sigma-1)[J_n(ika)J_n'(ka) \\ &\quad + iJ_n(ika)J_n'(ika)] + 2k^4a^4(\sigma-1)iJ_n'(ka)J_n''(ika) \\ &\quad + 2k^2a^2n^2(\sigma-1)J_n(ka)J_n(ika) = 0. \quad . \quad . \quad . \quad . \quad . \quad (7) \end{aligned}$$

For high values of ka ($ka > 10$) provided $ka >> n$ all

terms containing less than the third power of ka may be neglected. Equation (7) then reduces to

$$[k^2a^2-2(1-\sigma)n^2]\frac{J_n(ka)}{J'_n(ka)}-[k^2a^2+2(1-\sigma)n^2]\frac{J_n(ika)}{iJ'_n(ika)}+2ka(1-\sigma)=0. \quad . \quad (8)$$

When $n=0$, this further reduces to the equation given by Rayleigh *

$$2(1-\sigma)+ika\frac{J_0(ika)}{J'_0(ika)}+ka\frac{J_0(ka)}{J'_0(ka)}=0. \quad . \quad . \quad (9)$$

Putting $I_n(ka)/I'_n(ka)$ for $J_n(ika)/iJ'_n(ika)$ where I represents the modified Bessel function of the first kind, we obtain (8) in the more convenient form

$$\frac{J_n(ka)}{J'_n(ka)}=\frac{[k^2a^2+2(1-\sigma)n^2]\frac{I_n(ka)}{I'_n(ka)}-2ka(1-\sigma)}{k^2a^2-2(1-\sigma)n^2}. \quad (10)$$

Now the graph of $I_n(x)/I'_n(x)$ against n for different values of x (fig. 1) shows that this ratio approaches unity as x increases. The graph may be used to determine the values of the I functions. By successive approximations $J_n(ka)$ is found in terms of $J'_n(ka)$ and the permissible values of ka checked in the tables. As a first approximation Kirchhoff has given the value

$$ka=\frac{\pi}{2}(n+2s), \quad . \quad . \quad . \quad . \quad . \quad (11)$$

where s equals the number of circles.

As n becomes greater the approximation in equation (10) is inaccurate for the smaller modes. Some of the values in Table I. have been worked out by Timoshenko †, using the Ritz method. The other values have been calculated by another arrangement of equation (7) which contains all the terms This equation is

$$\frac{J_n(ka)}{J'_n(ka)}=\frac{[k^4a^4+2(1-\sigma)n^2k^2a^2+n^2(n^2-1)(1-\sigma)^2]\frac{I_n(ka)}{I'_n(ka)}-2k^3a^3(1-\sigma)}{k^4a^4-2(1-\sigma)n^2k^2a^2+n^2(n^2-1)(1-\sigma)^2}.$$
$$+2n^2(1-\sigma)ka\frac{I_n(ka)}{I'_n(ka)}$$
$$. \quad . \quad . \quad (12)$$

* Rayleigh, *ibid.* p. 361.

† Timoshenko, ' Vibration Problems in Engineering,' p. 317 (1928).

Fig. 1.

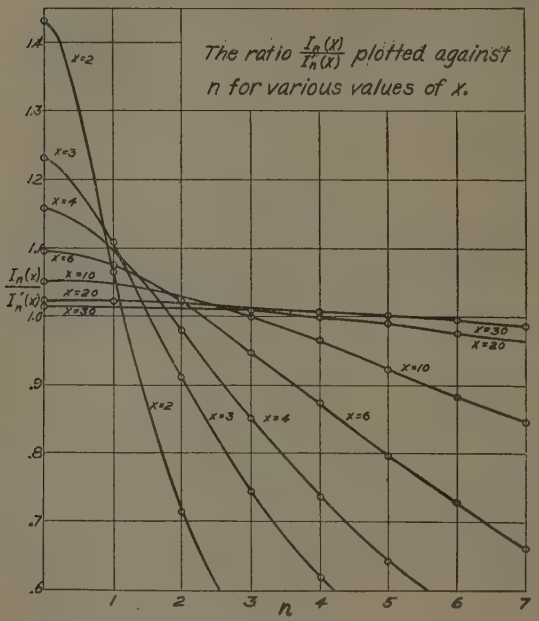

TABLE I.

Values of ka for Various Nodal Systems.

n is the number of diameters ; S the number of circles.
σ is taken equal to 0·33 in all calculations.

S.	$n=0$.	$n=1$.	$n=2$.	$n=3$.	$n=4$.	$n=5$.	$n=6$.
0	..	..	2·292*	3·497	4·65†	5·75†	6·80†
1	3·014	4·530*	5·937*	7·274	8·55†	9·79†	11·00†
2	6·209	7·737*	9·16	10·55	11·95	13·23	14·50
3	9·370	10·91*	12·41	13·86	15·24	16·57	17·88
4	12·53	14·08	15·58	17·05	18·45	19·81	21·15
5	15·68	17·23	18·73	20·21	21·63	23·01	24·37
6	18·83	20·38	21·89	23·37	24·80	26·20	27·57
7	21·98	25·53	25·04	26·52	27·96	29·40	30·86
8	25·12	26·67	28·19	29·67	31·12	32·58	34·04
9	28·26	29·81	31·33	32·81	34·28	35·74	37·21
10	31·40	32·95	34·47	35·95	37·43	38·90	40·38

* Values also given by Timoshenko (*cf.* reference above).
† Values true within 2 per cent.

It can be seen from this equation that if n is small and ka large $J_n(ka)=J'_n(ka)$ approximately.

A second method for calculating the values of ka in high frequency systems can be developed from the fact that the curves for $J_n(x)$ and $J'_n(x)$ intersect at the point midway between the s root of $J_n(x)=0$ and the s root of $J_n(x)=0$ provided hat the succeeding maxima are nearly equal. This is true for all save the first few roots. It has been shown by McMahon * that the s root in order of magnitude of the equation $J_n(x)=0$ is

$$x_n^s=\beta-\frac{m-1}{8\beta}-\frac{4(7m^2-38m+31)}{3(8\beta)^3}, \quad . \quad . \quad (13)$$

where $\beta=\frac{\pi}{4}(2n+4s-1), \quad m=4n^2.$

Further, the s root in order of magnitude of the equation $J'_n(x)=0$ is

$$x'^s_n=\nu-\frac{m+3}{8\nu}-\frac{4(7m^2+82m-9)}{3(8\nu)^3}, \quad . \quad . \quad (14)$$

where $\nu=\frac{\pi}{4}(2n-4s+1), \quad m=4n^2.$

The average values of these roots will give the values of ka approximately; thus

$$(ka)^s_n=\frac{x^s_n+x'^s_n}{2}=\frac{\pi}{2}(n+2s)-\frac{4(112n^4+88n^2+11)}{3[4\pi(n+2s)]^3}.$$

If we set $\alpha=\frac{\pi}{2}(n+2s)$ and $m=4n^2$, we obtain

$$(ka)^s_n=\alpha-\frac{m+1}{8\alpha}-\frac{4[7m^2+22m+11]}{3[8\alpha]^3}. \quad . \quad . \quad (15)$$

The first term is that given as an approximation by Kirchhoff. The series converges rapidly and gives accurate results.

Calculation of the Nodal Circles.

Substituting the second value for λ in equation (6) into equation (4) we obtain

$$J_n(kr)=\begin{matrix}(\sigma-1)[kaJ'_n(ka)-n^2J_n(ka)]-k^2a^2J_n(ka)\\ (\sigma-1)\left[ka\frac{I'_n(ka)}{I_n(kr)}-n^2\frac{I_n(ka)}{I_n(kr)}\right]+k^2a^2\frac{I_n(ka)}{I_n(kr)}\end{matrix}. \quad (16)$$

* Gray, Mathews, and MacRobert, 'Bessel Functions,' p. 260, MacMillan Co.

Now the modified Bessel function I_n is similar to a hyperbolic function in that it starts at small values and increases rapidly to infinity (see Table II.). Since r is considerably less than a for all values except those circles near the edge,

$$I_n(ka) >> I_n(kr)$$

and also

$$I'_n(ka) >> I_n(kr).$$

TABLE II.

x.	$I_0(x)$.
0	1·000
1	1·266
5	27·240
10	2816·000
20	$4{\cdot}36 \times 10^7$
30	$5{\cdot}70 \times 10^{11}$

TABLE III.

Roots of $J_n(x)=0$.

S.	$n=0$.	$n=1$.	$n=2$.	$n=3$.	$n=4$.	$n=5$.
1	2·405	3·832	5·135	6·379	7·586	8·780
2	5·520	7·016	8·417	9·760	11·064	12·339
3	8·624	10·173	11·620	13·017	14·373	15·700
4	11·792	13·323	14·796	16·224	17·616	18·982
5	14·931	16·470	17·960	19·410	20·827	22·220
6	18·071	19·616	21·117	22·583	24·018	25·431
7	21·212	22·760	24·270	25·749	27·200	28·628
8	24·353	25·903	27·421	28·909	30·371	31·813
9	27·494	29·047	30·571	32·050	33·512	34·983
10	30·636	32·160	33·720	35·192	36·654	38·148

The right side of equation (16) becomes vanishingly small as r becomes smaller. Hence J (kr) approaches zero. This means that at high frequencies the values of kr giving nodal circles will be the values of $J_n(kr)=0$ except very near the edge. This is the same result as obtained for the membrane at all frequencies.

The radii of the nodal circles for any desired mode is obtained by dividing the value of ka (Table I.) into

the succeeding roots of $J_n(x)=0$. These roots are given in Table III. The radius of the pth circle will be

$$\frac{r_p}{a}=\frac{x_n^p}{x_n^s}=\frac{p\text{th root of } J_n(kr)}{\text{boundary value of } (ka)_n^s} \quad . \quad . \quad . \quad (17)$$

Fig. 2 *a*.

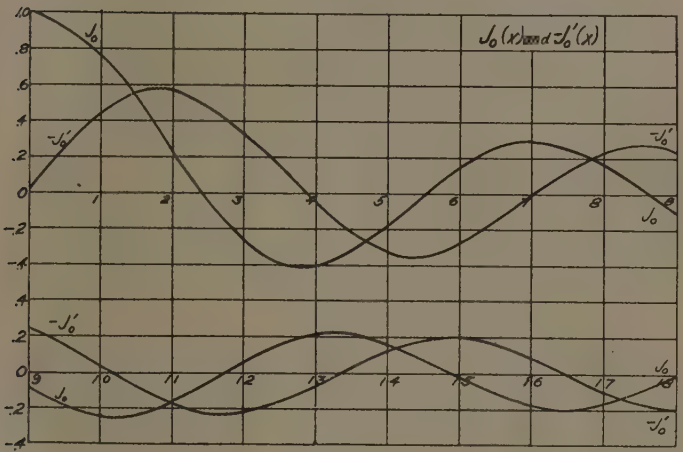

Fig. 2 *b*.

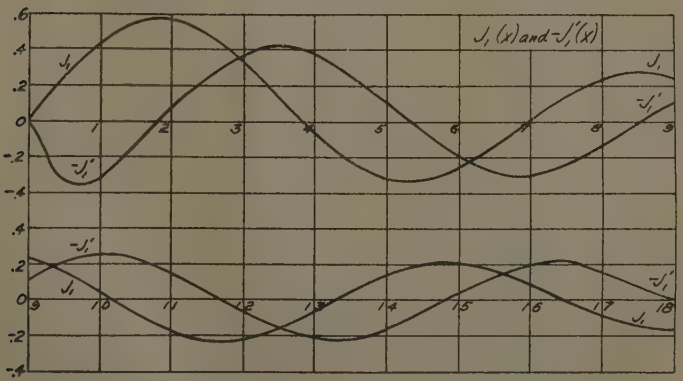

The graphs of $J_n(x)$ and $-J_n(x)$ are given in fig. 2 for values of n from 0 to 5. From these it is possible

to find the nodal circles with a fair degree of accuracy. It can be seen at once from these curves that when $n=0$ and there are no diameters, the circles given by

Fig. 2 c.

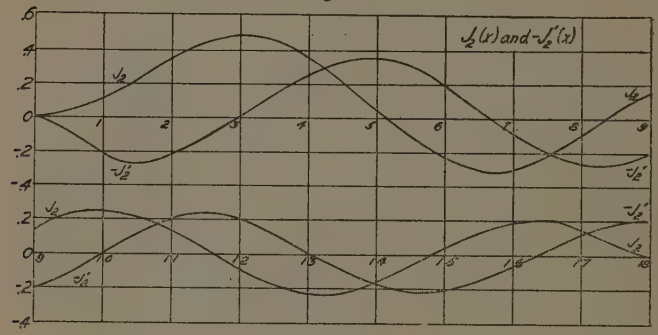

Fig. 2 d.

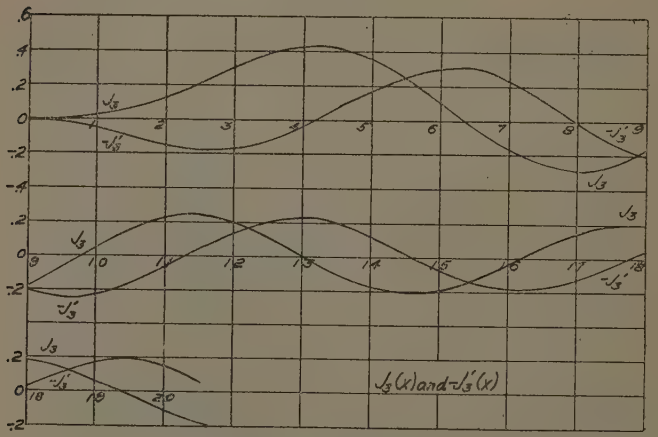

equation (4) [Kirchhoff's solution] will not be correctly spaced unless the plate is properly supported. If n has an integral value, the diameters will be present and equation (4) will give the correct solution. Photographic reproductions of these cases are shown in fig. 3 (Pl. X.

All these sand patterns were formed by balancing the plates at the centre upon the top of a vibrating magneto-strictive rod. Since the radius of the circular hole at the

Fig. 2*e*.

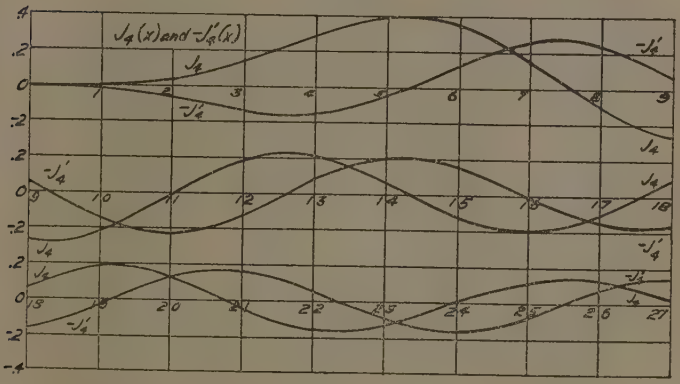

Fig. 2*f*.

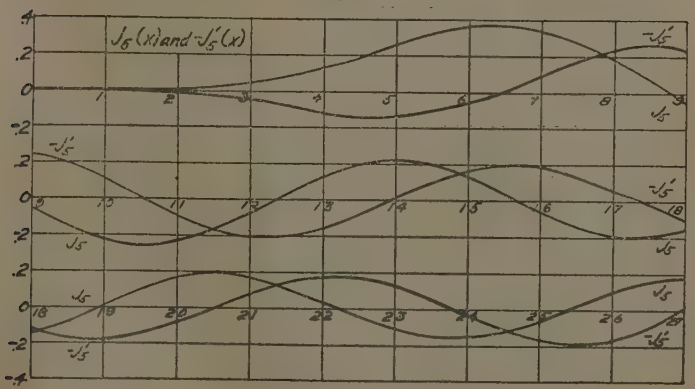

centre is not negligible, the radii of the circles in figs. 3*a*, 3*b*, and 3*c* (Pl. X.) do not agree with equation (4). The circle of fig. 3*d* (Pl. X.) has two diameters and the radii of the circles agree with the theory. Figs. 3*e* and 3*f* (Pl. X.) show that the circular plate will vibrate in segments and that many figures can be produced which are not covered

by Kirchhoff's theory. The calculations for the plates in fig. 4 (Pl. XI.) are shown in Table IV.

TABLE IV.

Pl. XI. fig. 4*a* (7 circles, 4 diam.).

Radius calculated.	Radius observed.
·271	·271
·396	·399
·514	·516
·631	·632
·746	·749
·860	·863
·973	·965
Frequency calc....	9820
Frequency obs.	10,900

Pl. XI. fig. 4*b* (7 circles, 5 diam.).

Radius calculated.	Radius observed.
·299	·298
·420	·420
·534	·538
·646	·650
·756	·757
·866	·869
·974	·967
Frequency calc. ..	11,120
Frequnecy obs.	11,740

Pl. XI. fig. 4*c* (7 circles, 9 diam.).

Radius calculated.	Radius observed.
·381	·378
·489	·492
·591	·595
·688	·695
·782	·788
·876	·833
·970	·969
Frequency calc....	9930
Frequency obs.	10,800

Pl. XI. fig. 4*d* (9 circles, 6 diam.).

Radius calculated.	Radius observed.
·268	·266
·366	·361
·457	·454
·546	·546
·633	·634
·721	·724
·809	·810
·894	·896
·979	·973
Frequency calc....	11,120
Frequency obs.	12,220

Pl. XI. fig. 4 *e*
(10 circles, 8 diam.).

Radius calculated.	Radius observed.
·288	·280
·373	·365
·454	·446
·533	·523
·612	·602
·689	·681
·763	·755
·838	·838
·913	·910
·988	·973
Frequency calc. ... 7830	
Frequency obs. ... 5960	

Pl. XI. fig. 4 *f*
(13 circles, 0 diam.).

Radius calculated.	Radius observed.
..	..
·167	..
·240	·240
·314	·306
·388	·386
·462	·464
·537	·540
·612	·615
·685	·691
·760	·764
·833	·836
·908	·911
·983	·980
Frequency calc. ... 7310	
Frequency obs. ... 5430	

All these calculations have been made from equations (4) except the last (Pl. XI. fig. 4 *f*), because the first five figures (Pl. XI. figs. 4 *a*–4 *e*) have nodal diameters and. therefore, act as though they were clamped at the centre with a very small clamp. However, when circles only appear, as in Pl. XI. fig. 4 *f*, it is necessary to take account of the dimensions of the clamp. This case has been worked out by Southwell *. On account of the discontinuity at the clamp, the general solution becomes

$$w=\alpha \mathrm{J}_n(kr)+\beta \mathrm{Y}_n(kr)+\gamma \mathrm{I}_n(kr)+\delta \mathrm{K}_n(kr), \quad . \quad (18)$$

where α, β, γ, and δ are constants to be determined by the boundary conditions of equation (5) along with the inner conditions at the clamped edge, which are

$$\left.\begin{aligned} w&=0,\\ \frac{\partial w}{\partial r}&=0,\end{aligned}\right\} \quad . \quad . \quad . \quad . \quad . \quad . \quad (19)$$

* R. A. Southwell, Proc. Roy. Soc. ser. A, vol. ci. p. 113 f (1922).

for $r=b$, the radius of the clamping circle. Southwell's boundary conditions then take the form

$$\alpha\left[J_0(ka)-\frac{1-\sigma}{ka}J_1(ka)\right]+\beta\left[Y_0(ka)-\frac{1-\sigma}{ka}Y_1(ha)\right]$$
$$-\gamma\left[I_0(ka)-\frac{1-\sigma}{ka}I_1(ka)\right]$$
$$-\delta\left[K_0(ka)-\frac{1-\sigma}{ka}K_1(ka)\right]=0. \quad . \quad . \quad . \quad (20)$$

$$\alpha J_1(ka)+\beta Y_1(ka)+\gamma I_1(ka)+\delta K_1(ka)=0. \quad . \quad (21)$$

$$\alpha J_0(kb)+\beta Y_0(kb)+\lambda I_0(kb)+\delta K_0(kb)=0. \quad . \quad (22)$$

$$\alpha J_1(kb)+\beta Y_1(kb)-\gamma I_1(kb)-\delta K_1(kb)=0. \quad . \quad (23)$$

When the significant terms in the series expansions are used, the relation between the constants is found from (22) and (23)

$$\beta=\delta=-\frac{\alpha+\gamma}{E}, \quad . \quad . \quad . \quad . \quad . \quad . \quad (24)$$

where E=log 2−Euler's Constant=0·11593.

Substituting (24) in (20) and (21), we get the following relations:

$$\frac{\alpha}{\gamma}=-\frac{EI_1(ka)-K_1(ka)-Y_1(ka)}{EJ_1(ka)-K_1(ka)-Y_1(ka)}. \quad . \quad . \quad (25)$$

$$\frac{\alpha}{\gamma}=\frac{EI_0(ka)-K_0(ka)+Y_0(ka)-\frac{1-\sigma}{ka}[EI_1ka-K_1(ka)+Y_1(ka)]}{EJ_0(ka)+K_0(ka)-Y_0(ka)-\frac{1-\sigma}{ka}[EJ_1(ka)+K_1(ka)-Y_1(ka)]} \quad . \quad . \quad (26)$$

$$\frac{\beta}{\gamma}=\frac{\delta}{\gamma}=-\frac{J_1(ka)-I_1(ka)}{EJ_1(ka)-K_1(ka)-Y_1(ka)}. \quad . \quad (27)$$

$$\frac{\beta}{\gamma}=\frac{\delta}{\gamma}=-\frac{J_0(ka)+I_0(ka)-\frac{1-\sigma}{ka}[J_1(ka)+I_1(ka)]}{EJ_0(ka)+K_0(ka)-Y_0(ka)-\frac{1-\sigma}{ka}[EJ_1(ka)+K_1(ka)-Y_1(ka)]} \quad . \quad (28)$$

Now in these equations (25–28), the only significant terms in the numerators at high frequencies are the

I terms. For instance, when $ka=10$, $I_0(ka)=2816$, while the absolute value of $J_0(ka)$ is always less than unity. Also the K terms are negligible. For instance, when $ka=10$, $K_0(ka)=17{\cdot}8\times10^{-7}$. Therefore all these terms are dropped and the two values of β/γ in (27) and (28) are equated thus:

$$\frac{-I_1(ka)}{EJ_1(ka)-Y_1(ka)} = \frac{I_0(ka)-\frac{1-\sigma}{ka}I_1(ka)}{EJ_0(ka)-Y_0(ka)-\frac{1-\sigma}{ka}[EJ_1(ka)-Y_1(ka)]}. \quad (29)$$

which may be written

$$\frac{EJ_0(ka)-Y_0(ka)}{EJ_1(ka)-Y_1(ka)} = 2\frac{1-\sigma}{ka} - \frac{I_0(ka)}{I_1(ka)}. \quad (30)$$

The right-hand side of equation (30) is approximately -1, hence

$$\frac{J_0(ka)+J_1(ka)}{Y_0(ka)+Y_1(ka)} = \frac{1}{E}. \quad (31)$$

This is a convenient form for finding the permissible values of ka. The values of (ka) for the first ten modes of a plate with free edge are (s=number of circles)

s.	ka.	s.	ka.
0.....	1·937	6.....	20·41
1.....	4·573	7.....	23·56
2.....	7·82	8.....	26·70
3.....	10·98	9.....	29·84
4.....	14·13	10.....	32·98
5.....	17·27		

The first two values are also given by Southwell *.

In order to find the radii of the various nodal circles, we set $w=0$.

Then

$$\alpha J_0(kr)+\beta Y_0(kr)+\gamma I_0(kr)+\delta K_0(kr)=0. \quad (32)$$

* Southwell, *ibid.* p. 143.

Substituting the values of α/γ, β/γ, δ/γ from (25) and (27), we obtain

$$-[EI_1(ka)-K_1(ka)-Y_1(ka)]J_0(kr)$$
$$+[I_1(ka)-J_1(ka)]Y_0(kr)$$
$$+[EJ_1(ka)-K_1(ka)-Y_1(ka)]I_0(kr)$$
$$+[I_1(ka-J_1(ka)]K_0(kr)=0. \quad (33)$$

When the insignificant terms are dropped equation (33) becomes

$$-EI_1(ka)J_0(kr)+I_1(ka)Y_0(kr)=0, \quad . \quad . \quad (34)$$

or

$$\frac{J_0(kr)}{Y_0(kr)}=\frac{1}{E} \quad . \quad . \quad . \quad . \quad . \quad . \quad . \quad (35)$$

The first ten roots of this equation are

Root.	*kr*.	Root.	*kr*.
1.....	3·97	6.....	19·61
2.....	7·08	7.....	22·75
3.....	10·20	8.....	25·90
4.....	13·33	9.....	29·04
5.....	16·49	10.....	32·18

The values for the radii are then found by dividing each of the successive roots by (ka) for the system. Exactly the same process was followed in calculating Pl. XI. fig. 4*f*.

Summary.

Kirchhoff has given the equation for the radii of the nodal circles in terms of Bessel's functions, and an approximate formula for ka (equation 11). For very high values of ka ($ka>10$) approximate solutions are given in equations (9), (10), and (12). When n has an integral value, diameters are always present and the plate behaves as though it were fixed at the centre, and Kirchhoff's solution is applicable. When $n=0$ the plate has nodal circles only, and equation (4) cannot be applied unless the plate is clamped on a nodal circle and vibrated at the proper place. When the plate is clamped at the centre and n has an integral value Kirchhoff's solution still applies ; but if $n=0$ and there are no diameters Southwell's

solution must be used. It will be seen from Table IV. that the calculated radii agree very closely with the radii observed. On the other hand, because of the approximations made, the observed frequencies differ very much from those calculated, particularly for the modes with a large number of circles.

XC. *Fourier Expansions obtained operationally.*

By N. W. McLachlan, *D.Sc.**

1. LET $(a), f(t)$ be a function of period $2h$ commencing at $t=0$, being single-valued, except at its discontinuities, where it is finite †; (b) the discontinuities and maxima and minima in the interval be limited in number. Then the operational form (O.F.) of $f(t)$ for the range $t=0$ to ∞ is given by

$$\text{(O.F. of zeroth period)}/(1-e^{-2ph})=\phi_0(p)/(1-e^{-2ph}). \quad (1)$$

For the zeroth period ‡

$$\phi_0(p)=p\int_0^{2h} e^{-pt}f(t)\,dt, \quad . \quad . \quad . \quad . \quad . \quad (2)$$

and for the nth period

$$\phi_n(p)=p\int_{2nh}^{(2n+2)h} e^{-pt}f(t)\,dt. \quad . \quad . \quad . \quad . \quad (3)$$

Writing $t=\tau+2nh$ in (3), we get

$$\phi_n(p)=pe^{-2nph}\int_0^{2h} e^{-p\tau}f(\tau+2nh)\,d\tau \quad . \quad . \quad (4)$$

$$=e^{-2nph}\phi_0(p), \quad . \quad . \quad . \quad . \quad . \quad . \quad . \quad . \quad . \quad (5)$$

since $f(t)$ is periodic. Hence the O.F. from $t=0$ to ∞ is

$$\phi(p)=p\int_0^{\infty} e^{-pt}f(t)\,dt=\phi_0\sum_{n=0}^{\infty} e^{-2nhp} \quad . \quad . \quad . \quad (6)$$

$$=\phi_0/(1-e^{-2hp}), \quad . \quad . \quad . \quad . \quad . \quad . \quad . \quad . \quad . \quad (7)$$

* Communicated by the Author.

† $f(t)$ is piecewise continuous (stückweise glatt), as exemplified in fig. 1 *a*.

‡ This nomenclature, borrowed from electrical filter circuit theory, is convenient in the present case.

provided the real part of $p>0$. Now if the operators conform with the Mellin inversion theorem this condition is satisfied when $c>0$ in the Bromwich-Wagner integral

$$f(t)=\frac{1}{2\pi i}\int_{c-i\infty}^{c+i\infty} e^{zt}\phi(z)\frac{dz}{z}, \quad t>0. \quad . \quad . \quad . \quad (8)$$

To conform with the M. theorem for the range $t=0$ to ∞, $|\phi(p)|p|$ must $\to 0$ uniformly as $|p|\to\infty$, $-\frac{1}{2}\pi \leqslant$ phase $p \leqslant \frac{1}{2}\pi$. Integral (8) is then zero for $t<0$.

By (7) and (8)

$$f(t)=\frac{1}{2\pi i}\int_{c-i\infty}^{c+i\infty}\frac{e^{zt}\phi_0(z)\,dz}{z(1-e^{-2zh})}, \quad t>0. \quad . \quad . \quad (9)^*$$

On evaluation this integral will usually yield a trigonometric series. In this respect it should be observed that integral (9) is zero when $t<0$, so we have not proved that $f(t)$ will be repeated when $t<0$, as it would be in the case of a Fourier expansion. It is not intended, of course, that the foregoing should be used as a substitute for the usual procedure when obtaining a Fourier expansion. In practical applications like § 4 below it is useful in order to determine the initial transient.

2. *Example.*—If the iterated curve is $|\sin t|$, *i. e.*, a rectified sine wave †, we have

$$\phi_0=p\int_0^{\pi} e^{-pt}\sin t\,dt=\frac{p}{(p^2+1)}(1+e^{-\pi p}). \quad . \quad (10)$$

Hence by (9) and (10)

$$f(t)=\frac{1}{2\pi i}\int_{c-i\infty}^{c+i\infty}\frac{e^{zt}(1+e^{-\pi z})\,dz}{(z^2+1)(1-e^{-\pi z})} \quad . \quad . \quad (11)$$

$$=\frac{2}{\pi}\left(1-2\sum_{n=1}^{\infty}\frac{\cos 2nt}{(4n^2-1)}\right). \quad . \quad . \quad . \quad . \quad . \quad (12)$$

Formula (12) represents a Fourier expansion, the function being repeated when $t<0$.

* In the standard form of the Mellin inversion theorem the lower limit in the integral (6) is $-\infty$. This will be seen by writing $x=e^{-t}$ in formulæ (38), (39), pp. 87, 88, Courant and Hilbert, 'Methoden der Mathematischen Physik.' The restriction on $|\phi(p)/p|$ ensures that the lower limit $t=0$ can be used, since the double integral (see C. & H., p. 88) corresponding to the range $t=-\infty$ to 0 vanishes, all the singularities of $\phi(p)/p$ being to the left of $c\pm i\infty$.

† Full wave rectification in the electrical sense.

3. *Example.*—Suppose $f(t)=1$ from $t=0$ to π, and zero from $t=\pi$ to 2π, *i. e.*, a semi-infinite series of dots in the Morse code. The O.F. of the zeroth period is

$$\phi_0=p\int_0^{\pi}e^{-pt}\,dt+p\int_{\pi}^{2\pi}e^{-pt}[0]\,dt \quad . \quad . \quad (13)$$

$$=(1-e^{-p\pi}). \quad . \quad . \quad . \quad . \quad . \quad . \quad . \quad . \quad . \quad (14)$$

By (9) and (14) we obtain

$$f(t)=\frac{1}{2\pi i}\int_{c-i\infty}^{c+i\infty}\frac{e^{zt}\,dz}{z(1+e^{-z\pi})} \quad . \quad . \quad . \quad (15)$$

$$=\frac{1}{2}+\frac{2}{\pi}\sum_{n=0}^{\infty}\frac{\sin(2n+1)t}{(2n+1)}, \quad . \quad . \quad . \quad (16)$$

which also is a Fourier expansion, the function being repeated when $t<0$.

Fig. 1.

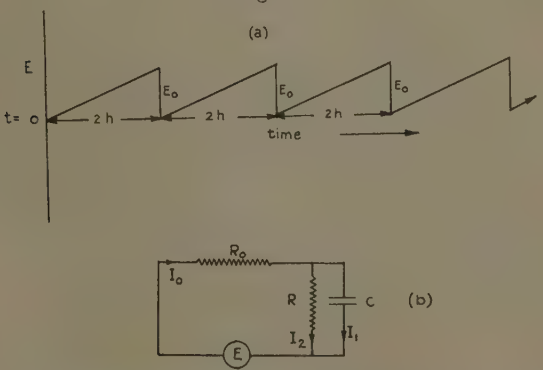

(*a*) Illustrating saw-tooth voltage wave form E.

(*b*) Circuit to which the saw-tooth wave form is applied.

4. *Electrical Application.*—As a final example, an application using the saw-tooth wave form common to television receivers (for scanning) may be of interest. At time $t=0$ an e.m.f. E having the form of fig. 1 (*a*) is applied to the circuit fig. 1 (*b*). The problem is to find the current I_2 in resistance R at any time $t>0$.

First we find the O.F. of E the iterated voltage wave form. For the zeroth period, $f(t)=E_0t/2h$ from $t=0$ to $2h$, so

$$\phi_0 = \frac{E_0}{2h} p \int_0^{2h} e^{-pt} t\, dt = \frac{E_0}{2ph} (1 - e^{-2ph}) - E_0 e^{-2ph}, \quad (17)$$

giving by (1)

$$\phi = E_0 \left(\frac{1}{2hp} - \frac{e^{-2hp}}{1 - e^{-2hp}} \right) \doteqdot E. \quad . \quad . \quad . \quad (18)$$

From fig. 1*b*, $$I_0 = I_1 + I_2. \quad . \quad . \quad . \quad . \quad . \quad . \quad (19)$$

The p.d.'s across C and R are equal, so

$$I_2 R = I_1 / Cp = E - I_0 R_0. \quad . \quad . \quad . \quad . \quad (20)$$

By (19), (20)

$$I_2 = (E/CRR_0)/(p+a), \quad . \quad . \quad . \quad . \quad . \quad (21)$$

where $a = (R + R_0)/CRR_0$. Substituting for E from (18) into (21), we have the operational solution

$$I_2 = \frac{E_0}{CRR_0} \left[\frac{1}{2hp} - \frac{e^{-2ph}}{(1 - e^{-2ph})} \right] \Big/ (p+a). \quad . \quad (22)$$

Interpreting this by aid of (8), we obtain

$$I_2 = \frac{(E_0/CRR_0)}{2\pi i} \int_{c-i\infty}^{c+i\infty} \frac{e^{zt}\, dz}{(z+a)} \left[\frac{1}{2hz^2} - \frac{e^{-2hz}}{z(1 - e^{-2hz})} \right]. \quad (23)$$

Evaluating (23) in the usual way gives

$$I_2 = \frac{E_0}{CRR_0} \left\{ \frac{e^{-at}}{a} \left[\frac{1}{2ha} - \frac{e^{2ha}}{(e^{2ha} - 1)} \right] \right.$$

$$\left. + \frac{1}{2a} - \frac{h}{\pi} \sum_{n=1}^{\infty} \frac{\sin\left(\frac{n\pi t}{h} - \tan^{-1} \frac{n\pi}{ah} \right)}{n(a^2h^2 + n^2\pi^2)^{\frac{1}{2}}} \right\}. \quad (24)$$

The transient is represented by the expression involving e^{-at}. The term $E_0/2CRR_0 a = E_0/2(R + R_0)$ is the mean value of the current after it is substantially steady, whilst the sigma terms represent the alternating components of the current. These and the constant term give the Fourier expansion of the current wave in resistance R during the steady state.

XCI. *The Use of Blue Filters in the Derivation of Candle-power Standards.* *By* H. Buckley, *M.Sc., F.Inst.P., National Physical Laboratory* *.

Summary.

The effect of field-size in the use of certain blue glasses employed to set up the candle-power unit at different colour temperatures is considered.

The experimental basis is the fact that in the photometry of high-pressure mercury vapour lamps by the colour-match filter method the result is about 7 per cent. higher if a small (2°) field is used than if a large (10°) field is used. This fact is shown to be consistent with the hypothesis that the visibility curve for the large field is identical in shape with that for a small field, but displaced 100 Å.U. in the direction of shorter wave-length.

The effect of this shift when the blue glass is used to set up standards of colour temperature 2360° K. from standards of colour temperature 2045° is shown to be about 0·5 per cent. As the standard visibility data were derived for a small visual field (3°) it would appear essential that, in default of evidence to the contrary, the small field should be used in the derivation of the standards of colour temperature 2360°.

Alternative methods of setting up the candle-power unit in terms of light of various colour temperatures consistently with the standard visibility data and without the use of blue glasses are considered.

PROPOSALS have been made and adopted by several national laboratories that standards of candle-power operating at a colour temperature of 2360° K. (vacuum tungsten lamps) should be derived from standards operating at a colour temperature of 2045° K. (carbon filament lamps) by means of certain blue glasses. These glasses are such that when used in conjunction with a source of colour temperature 2045° the radiation transmitted by the glass has the same colour as that emitted by a source of colour temperature 2360°. The integral transmission ratio of the blue glass, which is of fundamental importance in this method, is determined by means

* Communicated by the Author.

of calculations based on the standard internationally agreed visibility data, the spectrophotometric transmission data for the glass, and the distribution of energy in the spectrum of a black body at 2045° K.

By the use of the blue glass the colour difference between the sources compared is eliminated. The transmission of the blue glass throughout the spectrum is such, however, that although the colour difference is eliminated the distributions of energy in the spectra of the two sources compared are different. The colour match obtained by means of the blue glass is therefore a sensation colour match and is not due to an identity of spectral energy distribution.

The glasses are characterized by high transmission at both the red and blue ends of the spectrum, with a subsidiary maximum at wave-length 0·56 μ. They probably owe their colour to the presence of cobalt. They were prepared in 1928 under the direction of the Physikalisch-Technische Reichsanstalt for the purpose of the international comparison of methods of photometry agreed upon by representatives of the national laboratories of France, Germany, Great Britain and the United States of America at Bellagio in 1927. The integral transmission ratios were determined by each laboratory [1]. Transmission ratios throughout the spectrum were also determined by each laboratory, but only those obtained by Gibson [2] of the Bureau of Standards and by Preston and Cuckoo [3] of the National Physical Laboratory have so far been published. The spectral transmission curve of one of the glasses is shown in fig. 1.

It is well known in heterochromatic photometry that field size and Purkyně effects influence the results of measurements. The elimination of colour differences by the use of coloured glasses will not in general eliminate field size and Purkyně effects unless the glasses produce identity of spectral energy distribution in the sources under comparison. While it is to be expected that the production of a sensation colour match will reduce the field size and Purkyně effects it is by no means impossible that in particular cases they may be increased. The question therefore arises as to how the blue glasses which do not produce spectral energy identity should be used in practice, and in particular what should be the field-size conditions adopted.

Very little quantitative data are available on the variation of the visibility curve of the eye as a function

Fig. 1.

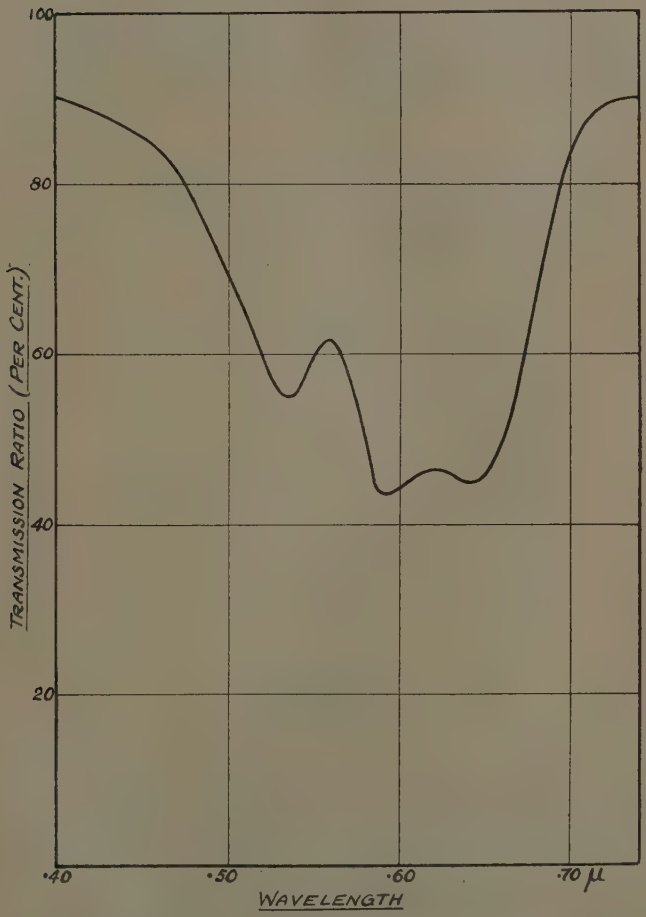

of the angular size of the visual field used. The main facts are that for large visual fields the eye is more blue-sensitive than for small fields ; that for large fields with reduction of field brightness the visibility curve moves

in the direction of shorter wave-length, probably without appreciable change of form ; and that the wave-length of maximum visibility moves from about 0·555 μ to about 0·505 μ.

It is possible on the basis of this information and the results of certain experiments on the field-size effect in the photometry of high-pressure mercury lamps to calculate the order of magnitude of the effect likely to be encountered.

Field-Size and Purkyně Effects in the Photometry of High-pressure Mercury Lamps.

In the photometry of high-pressure mercury lamps coloured filters have been used, which in conjunction

Fig. 2.

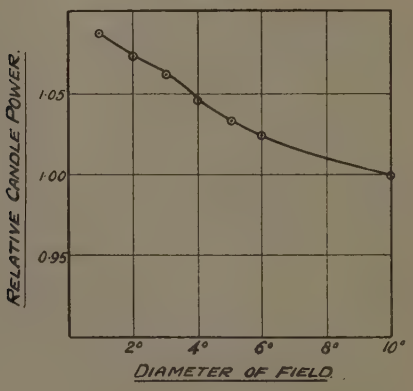

with tungsten lamps, produce colour matches in the photometric field. As the visible radiation from mercury lamps is confined mainly to radiation of two or three wave-lengths and the coloured filters transmit throughout the visible spectrum, the colour match produced is a sensation colour match and not an identity of energy match. In consequence it has been found by the author[4] that the candle-power deduced from observations utilizing a 2° visual field is higher by about 7 per cent. than that deduced from large field observations, even at field brightnesses of twenty millilamberts.

The variation in the candle-power of a high-pressure mercury lamp is shown in fig. 2 as a function of the angular field size. The field was circular, with a vertical central dividing line and black background. Ten observers were used.

If it is assumed that the difference in the results is due to a shift of the visibility curve without change of form, calculation enables the effect of any given shift to be determined.

Fig. 3.

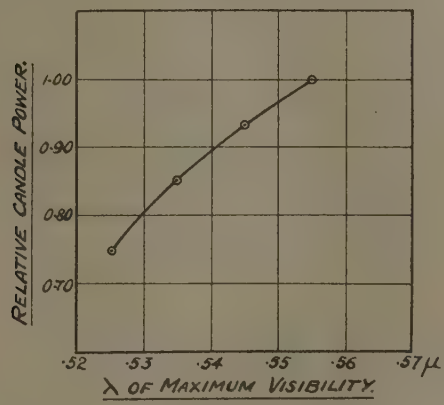

Calculation gave the results shown in fig. 3. They were obtained from evaluation of the ratio

$$\frac{\Sigma E_\lambda^H V_\lambda}{\int E_\lambda^T \tau_\lambda d\lambda}$$

for different sets of values of V_λ, where

E_λ^H = energy of high-pressure mercury lamp radiation at wave-length λ.

$E_\lambda^T d\lambda$ = energy in wave-length interval $d\lambda$ of tungsten lamp radiation at wave-length λ.

τ_λ = transmission ratio of colour-matching filter at wave-length λ.

V_λ = relative visibility of radiation of wave-length λ.

The standard visibility curve established for a small 3° field has its maximum at wave-length 0·555 μ. The other visibility curves used had the same shape, but their

maxima were displaced in 100 Å.U. steps to 0·565 μ, 0·545 μ, 0·535 μ, etc. The values of the energy in the various lines of the spectrum of the light from the mercury lamp were those obtained by Taylor and Kerr [5].

The curve gives the relative candle-power of a high-pressure mercury lamp as a function of the wave-length of maximum visibility. The value for the standard visibility curve with its maximum at 0·555 μ is taken as unity. It is immediately deducible from fig. 3 that a shift of the visibility curve of 100 Å.U. produces approximately a 7 per cent. change in the value assigned to the mercury lamp. Now 7 per cent. is the change which experimentally was found to be produced by a change in field size from 2° to 10°. It is therefore reasonable to assume that alteration of the field size from 2° to 10° is equivalent to a shift of the visibility curve of 100 Å.U. towards the blue end of the spectrum.

Observations of the Purkyně effect in the photometry of mercury lamps were found to be consistent with the existence of shifts of 300–400 Å.U. in the visibility curve, as was expected.

Field-size Effect in the Use of Blue Glasses.

It now becomes possible to calculate the effect of a shift corresponding to a change of field size from 2° to 10° in the use of the blue glasses to produce standards of colour temperature 2360° K. from standards of colour temperature 2045° K.

All that is required is to calculate for different sets of V_λ the ratio

$$\frac{\int E_\lambda^{T_1} V_\lambda d\lambda}{\int E_\lambda^{T_0} \tau_\lambda V_\lambda d\lambda},$$

where $T_0 = 2045°$ K. and $T_1 = 2360°$ K.

The results of the calculation are shown in fig. 4. In this the candle-power of a lamp of colour temperature 2360° K. as derived from a standard of colour temperature 2045° K. by means of a blue filter is expressed as a function of the wave-length of maximum visibility. The value obtained from the standard visibility curve with its maximum at 0·555 μ is taken as unity.

It can be seen that the candle-power depends on the field-size conditions used, and that the difference between

the results obtained with 2° and 10° fields is about 0·5 per cent., since the wave-lengths of maximum visibility in the two cases are 0·555 μ and 0·545 μ respectively on the assumption discussed above. Even if the assumed shift in the visibility curve is too large, and is reduced to one-third, the calculated result for a large field is still about 0·2 per cent. less than that derived for a small field.

In consequence it would appear desirable that small field conditions should be observed in the derivation of the standards of colour temperature 2360° K.

Experiments with a small number of observers seem to confirm these conclusions, but they cannot be regarded

Fig. 4.

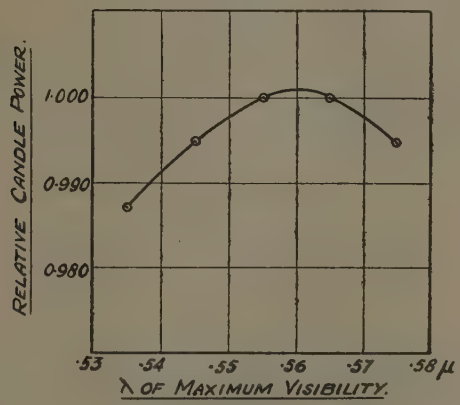

as definitive at the moment. Actual experimental verification may be difficult since individual observers may be expected to differ considerably in the amount of the effect they exhibit. For example, the work of Gibson and Tyndall [6] has shown that the position of the maximum of the visibility curves of fifty-two observers varied over a range of more than 200 Å.U. from 0·542 μ to 0·565 μ.

Thus the field-size effect for an observer whose wave-length of maximum visibility is 0·565 μ will be negligible, and for an observer whose wave-length of maximum visibility is 0·545 μ will be about 0·7 per cent.

An additional argument for using the small field is that for small fields the Purkyně effect is either non-

existent or very small, so that field brightness need not be considered. With large fields and low brightnesses the Purkyně effect will produce differences in results similar to those considered, since it also is due to bodily shifts of the visibility curve in the direction of shorter wavelengths, with decrease of field brightness.

General Considerations in the Use of Blue Filters.

The preceding considerations have shown that the particular blue filter which is being used in several national laboratories to derive candle-power standards of colour temperature 2360° gives results which depend on the observers and on the field-size conditions. The object of using the filter was to eliminate, or at any rate to reduce, the difficulties of heterochromatic photometry so that the results of photometric comparison should be independent of the observers and field-size conditions employed. This ideal is not achieved by the use of these filters. If the filter-transmission curve were of the form

$$T_\lambda = k e^{-\frac{C_2}{\lambda}\left(\frac{1}{T_1}-\frac{1}{T_0}\right)},$$

where

$$T_0 = 2045^\circ \text{ K.},$$

$$T_1 = 2360^\circ,$$

$$k = \text{constant},$$

then the colour match produced by the filter would also be accompanied by an energy match and only homochromatic photometry would be involved.

The uncertainties involved in the use of the blue filter are, however, much less than those involved in direct comparison of lamps of colour temperature 2045° and 2360°. The effect in this case is shown in fig. 5 by the full-line curve, which is deduced in the same way as the curve in fig. 4 from the ratio

$$\frac{\int E_\lambda^{T_1} V_\lambda d\lambda}{\int E_\lambda^{T_0} V_\lambda d\lambda}$$

for different sets of values of V_λ, where $T_0 = 2045^\circ$ K. and $T_1 = 2360^\circ$ K. Here it is seen that a shift of 100 Å.U., which is assumed to correspond to the change in field size from 2° to 10°, produces a change of about 2·5 per cent. in the relative candle-powers of the two sources.

The same results are also obtained analytically by expressing the visibility curve as a function of the form

$$(\lambda_m/\lambda)^n e^{n(1-\lambda_m/\lambda)}$$

suggested by Goldhammer[7], where λ_m is the wave-length of maximum visibility and n is a constant. If λ_m is taken as $0{\cdot}555\,\mu$ and n as 181 the resulting curve is a fair approximation to the visibility curve obtained by Nutting[8]. The effect of field size in the case under consideration can be determined from the ratio

$$\frac{\int \lambda^{-5} e^{-C_2/\lambda T_1}(\lambda_m/\lambda)^n e^{n(1-\lambda_m/\lambda)} d\lambda}{\int \lambda^{-5} e^{-C_2/\lambda T_0}(\lambda_m/\lambda)^n e^{n(1-\lambda_m/\lambda)} d\lambda}$$

Fig. 5.

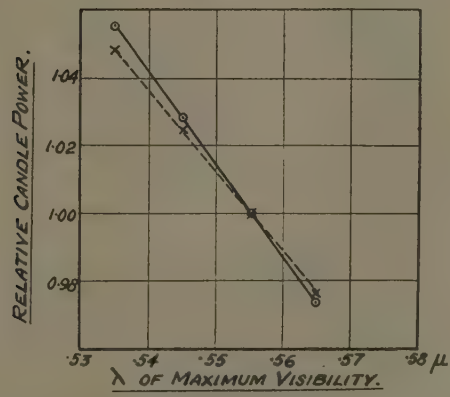

for different values of λ_m. For large values of n the expression

$$\int \lambda^{-5} e^{-C_2/\lambda T}(\lambda_m/\lambda)^n e^{n(1-\lambda_m/\lambda)} d\lambda = \frac{(n+3)(n+1)+2)(n\sqrt{2\pi n}}{(n\lambda_m)^4\left(1+\frac{1}{n\lambda_m}\frac{C_2}{T}\right)^{n+4}}.$$

So that the ratio to be evaluated becomes

$$1+\frac{1}{n\lambda_m}\frac{C_2}{T_0}\Big/1+\frac{1}{n\lambda_m}\frac{C_2}{T_1}.$$

The variation in this ratio is shown as the dotted line in fig. 5, which agrees very well with the full line previously obtained.

Since the spread of the observers' results may correspond to a spread of 200 Å.U. in λ_m it can be seen that the spread of the results of a large number of observers may be of the order of 5 per cent. Thus even with a colour difference which is considered small, for example that between the platinum standard of colour temperature 2045° K. and the carbon standards used to evaluate it, which at the National Physical Laboratory, the National Bureau of Standards, and the University of Strassburg had colour temperatures in the neighbourhood of 2110°, the spread of the observers' results might cover 1 per cent. unless the observers were all closely normal.

For a colour difference of 60° a group could be expected to obtain results differing by 0·5 per cent., depending on whether a small or a large field were used. Even if the 100° Å.U. unit shift which has been assumed to correspond to the effect of this change of field-size be regarded as much too large to be admitted, a shift of one-third of this amount produces a difference, viz., 0·2 per cent. approximately, which is significant in work of this character.

All the preceding considerations have been based on the assumption that the difference between large field results and small field results is due to a bodily shift of the visibility curve of about 100 Å.U. The existence of even larger shifts in connexion with the Purkyně effect is fairly well established, for instance by the work of König [9] and of Hecht and Williams [10]. Some alteration of the visibility curve must also correspond to the difference between large and small field vision, but the character of the alteration is not so definitely known. All that is asserted here is that a bodily shift of 100 Å.U. is consistent with observations made on high-pressure mercury lamps. It is conceivable that other alterations could be postulated which would be consistent with these observations and at the same time lead to smaller effects in the other cases considered, viz., the comparison of radiations of colour temperature 2045° K. and 2360 K. directly, and by means of the blue glass.

This does not alter the situation that changes in the visibility curve which will produce significant difference

between the large and small field results may exist. In default of reassuring information that the alteration in the visibility curve which does occur produces insignificant effects in the special cases here considered, it would be wise to use the small visual field since the standard visibility curve was established for a 3° field.

The reassuring information can come from past or future experiment. The question of the effect of field size in the comparison of carbon and tungsten lamps was investigated very carefully by Crittenden and Richtmyer in 1918[11]. It appears from their paper that they compared the results obtained by means of a Lummer-Brodhun contrast field in which attention was concentrated on the centre of the field ; the same field stopped down to a central vertically divided circular field of 2° diameter, the stop being illuminated ; and the 2° field of the flicker photometer with its surrounding bright field.

As between the first and second, even with 114 observers the authors found it difficult to be positive as to the existence of any effect. This is, perhaps, not surprising, since the difference in field size now under consideration is that between a large centrally divided circular field of 10° diameter and a similar one of 2° diameter, when both have a completely dark background. A light background to the 2° field used by Crittenden and Richtmyer might be expected to bring the eye to the same condition as does a background which consists of the rest of the Lummer-Brodhun contrast field.

It is therefore probably to future experiments that we must look for any reassuring information which may permit the use of the sensitive large photometric field in precision photometry of the type we are considering. As mentioned previously, experiments on a group of five observers did seem to show effects of the size anticipated in the use of the blue glasses. On the other hand, a limited number of experiments on a group of three observers on the effect of field-size in the direct comparison of lamps of colour temperature 2045° K. and 2360° K. gave results only about one-half of what was expected.

The matter is one which will have to be investigated, as it will occur again in the preparation of standards of colour temperature 2800° K. from those of colour temperature 2360° by a further use of the blue glass, the effect being cumulative.

Alternative Method of deriving Standards of Higher Colour Temperature from Standards of Lower Colour Temperature.

The proposal to use blue glass of the particular type which is being used to derive standards of one colour temperature from those of another was supposed by its authors to give a method of deriving a series of standards which should be consistent with the standard visibility curve. It was supposed that spectrophotometry and calculation would give the integral transmission factor of this glass and that the difficulties of heterochromatic photometry would be replaced by the adoption of the calculated value of the transmission ratio.

It has been shown above that the results obtained by means of the glass will not be independent of the observer nor of the method in which the glass is used It is therefore of interest to consider if there is any other method by which a series of tungsten candle-power standards may be derived in a way which is independent of the observer and the photometric conditions, and consistent with the internationally agreed visibility curve.

By "consistent with the visibility curve" is meant that the result obtained by the photometric procedure should be consistent with the evaluation of the ratio

$$\frac{\int E_\lambda^{T_1} V_\lambda d\lambda}{\int E_{\lambda_0}^{T} V^\lambda d\lambda},$$

where the denominator refers to the primary standard and the numerator to any other lamp radiating as a grey body. Incidentally the determination of the ratio of these and similar integrals without a knowledge of the various values of E_λ in the numerator appears to be the only definable problem of experimental photometry which has a unique meaning.

An alternative method has been described by Wensel, Roeser, Barbrow, and Caldwell[12]. The method consists in the determination of the brightness of a black body colour matching the standards in terms of the standards The brightness of the black body is then compared by measurements at one wave-length only with that of the brightness of the platinum primary standard of light whose brightness is known in terms of the unit of candle-power. Theoretically this method is independent of the

observer for narrow slit-widths of the spectrophotometer used in the comparison. It is also independent of the field-size conditions, since purely energy matches over a very narrow spectral region are involved. The method involves elaborate black body equipment, but is quite feasible for the derivation of the candle-power unit in terms of lamps having various colour temperatures.

Ribaud[13] has also described a similar process. He[14] has also described a simplification by means of which any two lamps of known colour temperature may be compared. The method amounts to a comparison at the Crova wave-length. A comparison of two brightnesses at this wave-length is equivalent to their comparison by means of an eye possessing the internationally agreed visibility data. Thus the photometric comparison is forced to give results consistent with the standard visibility curve by the use of this visibility curve in the calculation which determines the Crova wave-length. Ribaud, however, gives no experimental results.

The method was tried at the National Physical Laboratory[15] in 1935 and found to be fairly satisfactory. Lamps whose candle-powers were known at two voltages corresponding to colour temperatures of 2100° K. and 2300° K. were used to illuminate a magnesium oxide screen at a distance of about 6 inches from the lamps. Operation of each lamp at each of the two voltages produced brightnesses of the screen proportional to the candle-powers of the lamps at the two voltages. Observation by means of a spectrophotometer at the appropriate Crova wave-length then determined the ratio of the candle-powers independently of the observer and of the visual photometric conditions used.

This ratio was found to be about 1 per cent. different from the known candle-power ratio for each lamp and showed that the unit of candle-power as set up at the higher colour temperature was about 1 per cent. too small. This difference agrees with the similar difference which was found when lamps at the higher colour temperature were compared with lamps of approximately the same colour temperature derived by means of the blue glass at the National Bureau of Standards.

A number of small corrections had to be applied to the observed candle-power ratios, but they were very small and definite, as they depended on the physical character-

istics of materials and did not involve any unknown or uncertain properties of a sense organ.

It should be possible to use this method with photo-electric cells either by means of a spectroscope or a filter transmitting a very narrow spectral region in the neighbourhood of the Crova wave-length. A filter of this kind has been described by Gibson[16]. It would appear that for the setting up of the candle-power scale in terms of tungsten lamps this method might very well be the subject of extended investigation.

References.

(1) Nat. Bur. Stds., C.I.M.P., Pro. Verb. xvi. p. 296 (1933).
(2) Gibson, C.I.P.M., Pro. Verb. xvi. p. 370 (1933).
(3) Preston and Cuckoo, Proc. Phys. Soc. xlviii. p. 869 (1936).
(4) Buckley, Ill. Eng. xxvii. p. 148 (1934).
(5) Taylor and Kerr, Gen. El. Rev. xxxix. p. 342 (1936).
(6) Gibson and Tyndall, Bull. Bur. Stds. xix. p. 131 (1923).
(7) Goldhammer, *Ann. d. Phys.* xvi. p. 621 (1905).
(8) Nutting, Phil. Mag. xxix. p. 301 (1915).
(9) König, *Ann. d. Phys.* xlv. p. 604 (1892).
(10) Hecht and Williams, J. Gen. Phys. v. p. 555 (1923).
(11) Crittenden and Richtmyer, Bull. Bur. Stds. xiv. p. 87 (1918).
(12) Wensel, Roeser, Barbrow, and Caldwell, J. Res. xiii. p. 161 (1934).
(13) Ribaud, *Comptes Rendus*, cxcvi. p. 687 (1933).
(14) Ribaud, *Rev. d'Opt.* xii. p. 193 (1933).
(15) Nat. Phys. Lab., Ann. Report, p. 78 (1935).
(16) Gibson, J.O.S.A. xxv. p. 131 (1935).

XCII. *Deflexion of Thin Rectangular Plates clamped at the Edges and uniformly Loaded. By* B. C. Laws, *D.Sc., A.R.C.Sc., F.Inst.P.**

Relation between Experiment and Theory.

DURING recent years mathematicians have given a good deal of attention to the consideration of thin plates under the conditions here referred to.

Bryan [1] outlined a possible method of solution in 1894; subsequently a general study of the problem was presented to the Academy of Sciences, Paris, in a Mémoire by Hadamard [2] in 1906, followed by dissertations on the subject by Ritz [3] in 1909 and Hencky [4] four years later, while the underlying principles of solution

* Communicated by the Author.

are contained in Love's classic treatise [5] the 'Mathematical Theory of Elasticity,' in which are envisaged the difficulties of the problem.

The investigation of Ritz has not infrequently been referred to as a sound standard with which to compare deflexion values otherwise obtained experimentally or experienced in practice.

The theory is a little complex, perhaps too complex to appeal to the engineer, who rather desires some ready means—if that be possible—of estimating with a reasonable approach to accuracy such factors as "Maximum Stress" and "Maximum Deflexion."

Experiments have in a few instances been resorted to to ascertain by careful research what in fact does happen under the conditions cited. Of these the work of Crawford [6] and later of Montgomerie [7] are of particular importance.

In a paper [8] contributed to the 'Proceedings of the Inst. Civil Engineers,' the author described a series of experiments he carried out at the University of Leeds on mild steel plates of various dimensions. The object of the experiment was to determine the nature of the distribution of stress, and to arrive at a general expression for "Maximum Stress" *free from experimental error.* He also embodied in the paper an expression for "Maximum Deflexion" *in terms of measured deflexions*—

$$\delta = \frac{n^4}{n^4+2} \cdot \frac{wb^4}{32Et^3}.$$

To enable comparison to be made with theory it is therefore necessary to determine in what respect this expression requires to be modified to represent deflexion free from experimental error.

However carefully the experiments may be carried out it appears to be difficult to avoid the presence of certain factors—referred to later—the joint influence of which is to produce deflexions greater than they should be. The above-mentioned expressions—one giving the maximum stress which might be reached in practice under perfect conditions, the other the maximum deflexion which would probably result where imperfections of workmanship exist—are most useful in practical design, especially where compressive stresses in the plane of the plate have to be considered. In such cases the designer is

armed with the knowledge that he has to take into account the probable presence of deflexions *greater than those* which would exist under theoretical conditions.

It will be seen later that the discrepancy between "measured" and "theoretical or corrected" deflexion values may be considerable, and might reach a value of the order of 8 to 10 per cent. with plates of normal dimensions.

It is not easy, and perhaps impossible, in these experiments to so fix the plates that they are initially perfectly plane, ideally clamped, free from the possibility of slipping

Fig. 1.

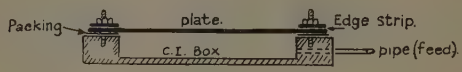

TABLE I.

	Plate. Dimensions $a'' \times b''$.	Plate. Thickness t''.	$n = \frac{a}{b}$.	Load in atmospheres. w.	$E - T/''\square$.	Poisson's ratio. σ.	Slope at end of short axis. θ.	Maximum measured deflexion.
(*a*) ..	36×14·5	·244	2·483	·69	13192	·343	5′ 20″	·03245″
(*b*) ...	,,	,,	,,	·912	,,	,,	7′ 30″	·04395″
(*c*) ...	27×18·3	·308	1·475	·75	11808	·363	5′ 14″	·03423″
(*d*) ..	18·3×7·3	,,	2·507	4·65	,,	,,	1′ 50″	·00717″
(*e*) ...	36·2×36·2	·268	1·000	·408	13112	·264	24′ 55″	·2224″

One atmosphere $\equiv$ ·006526 tons per sq. inch and $n \not< $ unity.

under the load, having zero slope at the boundary, and absence of initial stress in the material. In practice the load is generally applied hydrostatically, and was so applied in the experiments, in which the plates formed one side of an otherwise rigid box (fig. 1).

Particulars abstracted from the experimental data are given in Table I.

Deflexions were recorded optically by noting the rise and fall of a vertical needle—mounted independent of the plate—the lower end of which was kept lightly in contact with the plate surface.

The amount of slope was measured in two ways—by a mathematical analysis of the plate contours, and optically by means of two small mirrors mounted on a miniature three-legged table which could be set down at any position on the plate surface.

Fig. 2.

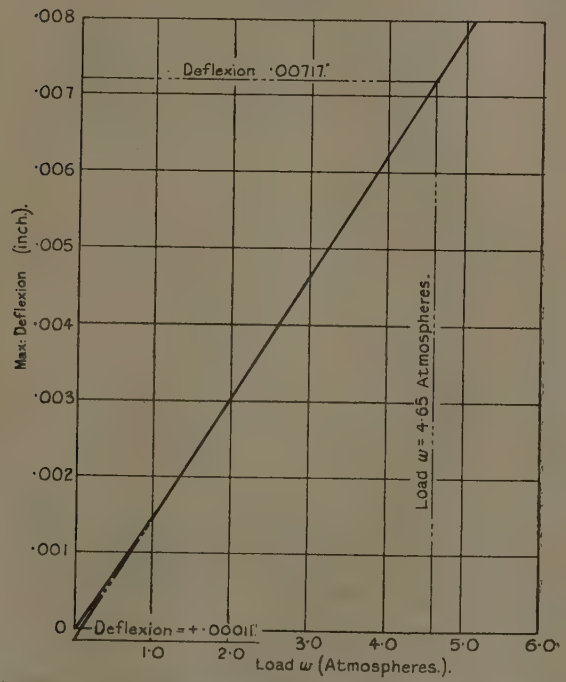

Relation of "max. deflexion" to "load." Case (*d*), Table II.

The maximum deflexion D corrected for slope is expressed by

$$D\left(\frac{1}{1+\frac{b}{d}\cdot\frac{\theta}{4}}\right),$$

in which θ is the slope at end of the shorter axis b of the plate and d is the maximum deflexion of a simple encrastre beam of thin plating of lengh "b" and unit width.

Apart from the question of slope a further correction was applied in respect to

Case (*d*) due to initial stress,
„ (*e*) „ „ deflexion,

illustrated in figs. 2 and 3 respectively.

Fig. 3.

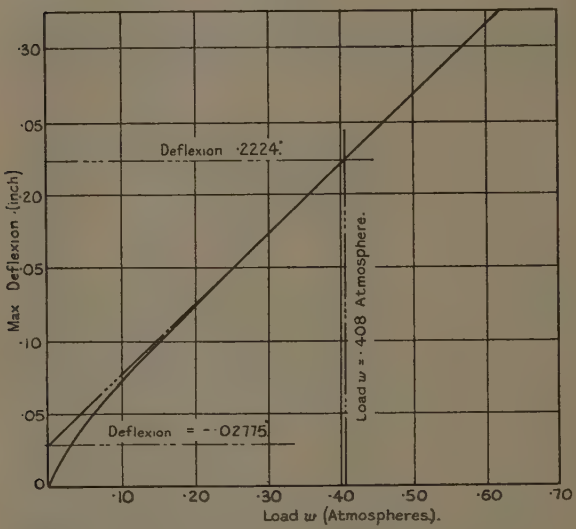

Relation of "max. deflexion" to "load." Case (*e*), Table II.

The details are set out below.

TABLE II.

	Maximum deflexion measured.	Corrections for initial stress.	Corrections for initial deflexion.	Corrections for slope.	Maximum deflexion corrected.
(*a*) ...	·03245"	..	..	—·00489"	·02756"
(*b*)	·04395"	..	..	—·00697"	·03698"
(*c*)	·03423"	..	..	—·0042"	·03003"
(*d*) ...	·00717"	+·00011"	..	—·0008"	·00648"
(*e*)	·2224"	..	—·02775	—·02024"	·1744"

The experiments showed that for any particular plate maximum deflexion $\propto$ load, and bore a constant relation (k) to the deflexion of a simple encastre beam of length=one of the sides of the plate, but that for plates of different size $k \propto f(n)$ which could be expressed in terms of a rapidly converging series $k=mf(n)=m(1-r)^{-1}$, where $m=\cdot 8586$ and $r=\dfrac{1\cdot 7866}{n^4}$, or very nearly by $k_1=m_1 f(n)$, where $m_1=6/7$ and $r=\dfrac{25}{14n^4}$.

Comparative values of k and k_1 are as follows :—

n.	k.	k_1
1	·3081	·3077
2	·7723	7719
3	·8401	8387
4	·8526	8512
5	·8581	·8567
∞	·8586	·8572

and for values of n given in Table I. the coefficients are

	(*a*).	(*b*).	(*c*).	(*d*).	(*e*).
k	·82006	·82006	·62333	·82145	·30812
k_1.....	·81876	·81876	·62235	·82007	·30770

The differences are small, and the expression for "Maximum Deflexion" may be written

$$\delta=\frac{\cdot 8586n^4}{n^4-1\cdot 7866}\cdot\frac{wb^4}{32Et^3}=\frac{6n^4}{7n^4-12\cdot 5}\cdot\frac{wb^4}{32Et^3}\text{ very nearly—}$$

giving a close approximation to the corrected experimental values.

With regard to theory, there are two factors which do not seem to have been included in the solution, nor does it appear to be possible to do so directly. They consist in the non-observance of the facts that : (1) the deformation of the plate brings into being stresses in the plane of the plate due to its change of form. (2) as a result of the deformation the direction of the load is continually altering from point to point of the plate surface, whereas by hypothesis the direction is assumed to be constant and at right angles to the initial plane of the plate.

These factors are not negligible : (2) may be so small as to exercise no great influence on the results, but (1) is

a measurable quantity and at least may be approximated to.

In a previous contribution [9] the author worked out the solution for a simple encastre thin plate beam, from which the derived expression for maximum deflexion is as follows :

$$D_1 = \frac{w.b.}{2m^3\,E.I.} \cdot \left(\frac{mb}{4} - \tanh\frac{mb}{4}\right) = \frac{mbt}{4\sqrt{2}},$$

and

$$t^4 = \frac{24\sqrt{2}}{m^4.E} \cdot \left(\frac{mb}{4} - \tanh\frac{mb}{4}\right),$$

Fig. 4.

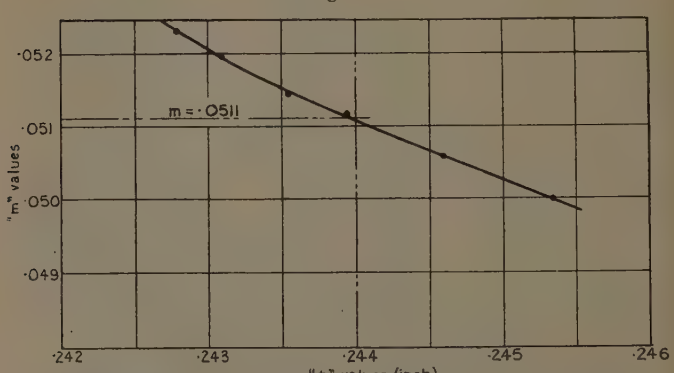

Simple encastre beam. Length 14·5″, thickness ·244″. w=·0045 T/□″. E=13192 T/□″. Pull along beam=P=m^2 E.I. Relation of "m" to "t."

where w=unit load on the beam, of span b and thickness t, and the pull along the beam =P=m^2 E.I.

E. g., for a beam corresponding to a strip taken along the minor axis of the plate referred to in case (*a*) Table I., in which b=14·5″, the following relation obtains (fig. 4) :

$$t = \cdot 244, \quad m = \cdot 0511, \quad P = \cdot 0417, \quad D_1 = \cdot 03196,$$

whereas by the usual encastre beam formula

$$t = \cdot 244, \quad m = 0, \quad P = 0, \quad D_1 = \cdot 03244,$$

showing a discrepancy in deflexion=1½ per cent. less

than that usually calculated—a matter which will be referred to later.

It is obvious, therefore, that any deflexion theoretically obtained needs to be reduced similarly, and it is not unreasonable to assume that the amount of reduction would be in like proportion to the above.

The problem involves the solution of the differential equation

$$\frac{\partial^4 z}{\partial x^4} + \frac{2\partial^4 z}{\partial x^2 \partial y^2} + \frac{\partial^4 z}{\partial y^4} = \frac{12w(1-\sigma^2)}{\mathrm{E} \cdot t^3},$$

in which z, the deflexion at any point, is zero at the boundaries, and the slope $\frac{\partial z}{\partial x}$, $\frac{\partial z}{\partial y}$, are also zero along the boundaries.

Fig. 5.

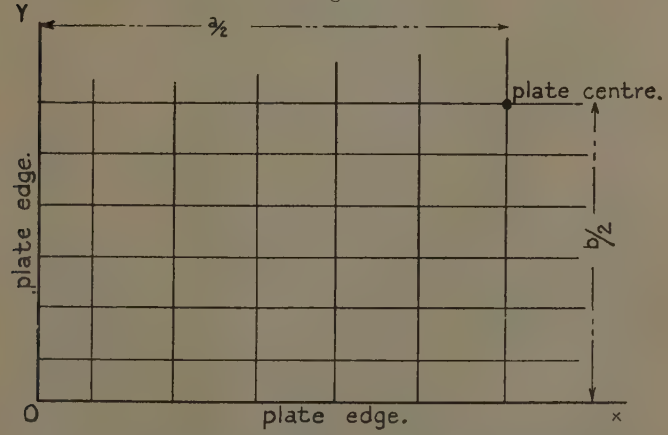

No exact solution appears to have been obtained.

In his method of approximation Ritz takes the origin at one of the corners of the plate, and the axes of coordinates x and y along the edges a and b respectively (fig. 5). The plate, of thickness t, is subject to a uniformly distributed unit load w, and σ = Poisson's ratio.

Deflexion at any point of the plate is expressed in a rapidly converging series $\Sigma\Sigma a_{mn}\xi_m(x)\eta_n(y)$, involving a set of functions

$$(x) = \alpha_m \left(Sh \frac{K_m x}{a} - \sin \frac{K_m x}{a} \right) - \left(Ch \frac{K_m x}{a} - \cos \frac{K_m x}{a} \right),$$

where m has values from unity upwards and K_m is the root of the equation $Ch K_m \cos K_m = 1$, and

$$\alpha_m = \frac{Ch K_m - \cos K_m}{Sh K_m - \sin K_m}.$$

$\eta_n(y)$ is similar to $\xi_m(x)$, in which n replaces m and $\frac{y}{b}$ is put in lieu of $\frac{x}{a}$.

The coefficient a_{mn} is found by solving a set of linear equations of the form

$$a_{\mu\nu}\left(K_\mu{}^4 \cdot \frac{b^2}{a^2} + K_\nu{}^4 \cdot \frac{a^2}{b^2} + 2\rho_{\mu\mu}\rho_{\nu\nu}\right) + 2\Sigma_m \Sigma_n a_{mn}\rho_{m\mu}\rho_{n\nu} = \frac{2\alpha_\mu \alpha_\nu}{K_\mu K_\nu} \cdot 10^4 l,$$

where

$$l = \cdot 0096 \frac{w \cdot a^2 b^2}{E \cdot t^3}(1 - \sigma^2),$$

and ρ_{mn} is obtained from the relation

$$\rho_{mn} = -\alpha_m{}^2 K_m{}^2 + 2K_m \alpha_m \ldots,$$

where $m = n$ and

$$\rho_{mn} = \frac{8K_m{}^2 K_n{}^2}{K_m{}^4 - K_n{}^4}(K_m \rho_m - K_n \rho_n),$$

where m and n are different.

The suffixes m and n are odd integers, and the degree of accuracy of the results depends upon how far we carry the numerals, 1, 3, 5, etc.

For the central deflexion—the point specifically dealt with in these notes, in which $\frac{x}{a} = \cdot 5, \frac{y}{b} = \cdot 5$—the factors involved, derived from the above expressions, are as follows :—

For m or n =	1.	3.	5.
K_m =	4·7300	10·9956	17·2787
α_m =	·98250	·99997	Unity.
$\mathrm{Sin}\ \frac{K_m}{2}$ =	·70085	−·70711	·70713
$\mathrm{Cos}\frac{K_m}{2}$ =	−·71330	·70711	−·70707
$\mathrm{Sh}\frac{K_m}{2}$ =	5·2752	122·08350	2825·13821
$\mathrm{Ch}\frac{K_m}{2}$ =	5·36915	122·0876	2825·13839
$\xi_m(x) = \eta_n(y) =$	−1·58815	1·40622	−1·41438

Values of ρ_{mn}.

ρ_{11}.	ρ_{33}.	ρ_{35}.	$\rho_{13}=\rho_{31}$.	$\rho_{35}=\rho_{53}$.	$\rho_{15}=\rho_{51}$.
−12·30207	−98·900	−263·99607	9·73067	24·50193	7·6154

The values of a_{mn}, depending on the ratio between the sides of the plate, vary with the conditions of the particular problem.

By way of comparison the following cases are considered :

Case (*a*) and (*b*).

Extreme case (*a*), *i. e.*, in which $\frac{a}{b}$ approximates to ∞.

Case (*e*).

The values of a_{mn} are given below :—

a_{mn}.	Case (*a*) & (*b*).	Extreme case (*a*).	Case (*e*).
11	·01374166	·0151592	·109003
13	·00025802	·0002272665	·0049941
31	·00308826	·00663693	do.
33	·00011216	·000099064	·000451518
15	·000027447	·00002371885	·000642807
51	·000733635	·00422371	do.
35	·0000142974	·000010384	·000079787
53	·000044218	·0000633194	do.
55	·0000064609	·00006608696	·00000319219

and $z=\Sigma\Sigma a_{mn}\xi_m(x)\eta_n(y)=$

	Case (*a*)	Case (*b*).	Extreme case (*a*).	Case (*e*).
Theoretical	·02901	·03849	·03251	·2561
Compared with :				
Experimental	·02756	·03698	—	·1744
Simple encastre beam .	·03244	·04290	·03246	·5661

TABLE III.

Deflexions at $x=\cdot5\ a$.

y values ...	0	1·65″	3·05″	4·45″	5·85″	7·25″
Ritz	0	·00474″	·01443″	·02104″	·02684″	·02901″
Hencky ...	0	·00470″	·01260″	·02050″	·02650″	·02860″
Experiment.	0	·00498″	·01219″	·01957″	·02521″	·02756″
Simple encastre beam.	0	·00490″	·01140″	·02020″	·02850″	·03244″

Applying the calculation to the surface of the plate the impression generally is that the form actually assumed by the plate is flatter, and the maximum deflexion at any particular section less, than that indicated by theory, typically illustrated in Table III. relating to the minor axis case (*a*), in which are also included relative figures obtained by Hencky's method of computation.

A significant point here is that in the limit, in which one side of the plate is relatively very long, the theoretical deflexion is identical with that for the simple encastre beam.

If, however, we consider, *e. g.*, a section along the minor axis of this plate the conditions of the problem are such as to lead us to anticipate a deflexion *at least* approximating to that in which lateral strain is prevented, or even less in view of the tension across the section consequent on the change in form of the plate, *i. e.*, less than $\cdot 02864 = \{\cdot 03246(1-\sigma^2)\}$ apart from the influence of factors referred to on p. 1077.

The conclusion, therefore, is that theory gives a value in excess of the real value. It is in agreement with what has been found from experiment, the results of which lead to the expression for maximum deflexion

$$\delta = \frac{6n^4}{7n^4 + 12 \cdot 5} \cdot \frac{wb^4}{32\,Et^3}.$$

References.

(1) Bryan, G. H., Trans. Inst. N.A. vol. xxxv. (1894).
(2) Hadamard, M. J., Paris, 1906.
(3) Ritz, W., Crelle's Journal, Berlin, 1909.
(4) Hencky, H., R. Oldenbourg, Berlin, 1913.
(5) Love, A. E. H., Cambridge, 4th edition, 1927.
(6) Crawford, W. J., Proc. R. S. Edin. vol. xxxii. (1911–12).
(7) Montgomerie, J., Trans. Inst. N. A., vol. lxi. (1919).
(8) Laws, B. C., Proc. Inst. C. E., vol. ccxiii. (1921–22).
(9) Laws, B. C., Phil. Mag. vols. xxxi. and xxxii. (1916).

24th August, 1937.

XCIII. *On some Operational Representations of Products of Parabolic Cylinder Functions and Products of Laguerre Polynomials.* *By* W. T. Howell, *M.Sc.**

§ 1. Dhar[1] has recently given a formula expressing the product of two parabolic cylinder functions $D_m(y \sin\alpha)D_n(y\cos\alpha)$ as a sum of the form $\Sigma c_r D_{n+m-2r}(y)$, where c_r involves a hypergeometric series. If we use the well-known operational representation of $D_n(y)$ we can write down at once the operational representation of the product $D_m(y\sin\alpha)D_n(y\cos\alpha)$. This has been

* Communicated by Sir Robert Pickard, F.R.S.

done for the special values $m=n$; $\alpha=\pi/4$ by Varma[2]. It will be observed that the arguments of the functions comprising the products are simply related to one another. It is the object of this paper to give some operational representations of the product when the arguments are not subject to this restriction.

In a previous paper [3] we have made use of the generating function of the Laguerre polynomial $L_n^{\alpha}(x)$ to deduce an operational representation for products of Laguerre polynomials, and have given some expansions of the products of Laguerre polynomials as sums of these polynomials. We passed over the Hille-Hardy generating function for products of Laguerre polynomials, as it was not sufficiently general for the sequel. We now propose to use this result as well as the corresponding generating function for products of the parabolic cylinder functions to deduce new operational representations of certain products of Laguerre polynomials with different arguments and of parabolic cylinder functions with different arguments. The operational representations so deduced enable us to write down at once integral representations of these products, and these in themselves may be regarded as a justification for finding the operational representations.

Curzon[4] was the first to point out a connexion between the functions of the parabolic cylinder and the Legendre functions, and his result has been generalized by Goldstein[5], while Meijer[6] has recently given some integral representations of products of parabolic cylinder functions, showing the connexion between these products and Bessel functions. We find in the following a connexion between products of parabolic cylinder functions and Legendre polynomials, a connexion between products of Laguerre polynomials and Gegenbauer polynomials, as well as a connexion between products of parabolic cylinder functions and Laguerre polynomials. The results given are only proved for positive integral values of n, except where more general values of n are specially indicated, and it is hoped to generalize the results for non-integral values in a future paper.

We remark that Weber's parabolic cylinder function $D_n(z)$ of integral order n may be defined by the relation

$$\sum_{n=0}^{\infty} \frac{t^n}{n!} D_n(x\sqrt{2}) = e^{-\frac{1}{4}(x^2+t^2)+xt\sqrt{2}}, \quad . \quad . \quad (1.1)$$

and that a generalization of this function is given by the Laguerre polynomial $L_n^{\alpha}(x)$ defined by

$$\sum_{n=0}^{\infty} t^n L_n^{\alpha}(x) = \frac{e^{-\frac{xt}{1-t}}}{(1-t)^{\alpha+1}}, \quad |t| < 1, \quad . \quad . \quad (1.2)$$

where the usual bracketing of α to show its non-index character has been discarded.

The following relations hold when n is a positive integer :

$$D_n(x) = (-)^n e^{\frac{1}{4}x^2} \frac{d^n}{dx^n} e^{-\frac{1}{4}x^2}, \quad . \quad . \quad . \quad . \quad . \quad . \quad . \quad (1.3)$$

$$L_n^{\alpha}(x) = \frac{e^x x^{\alpha}}{n!} \frac{d^n}{dx^n}(e^{-x} x^{n+\alpha}) = \sum_{r=0}^{n} \binom{n+\alpha}{n-r} \frac{(-x)^r}{r!}, \quad (1.4)$$

$$L_n^{-\frac{1}{2}}(x) = \frac{(-)^n}{2^n n!} e^{\frac{x}{2}} D_{2n}(\sqrt{2x}), \quad . \quad . \quad . \quad . \quad . \quad . \quad . \quad (1.5)$$

$$L_n^{\frac{1}{2}}(x) = \frac{(-)^n}{2^{n+\frac{1}{2}} n!} x^{-\frac{1}{2}} e^{\frac{x}{2}} D_{2n+1}(\sqrt{2x}), \quad . \quad . \quad . \quad . \quad (1.6)$$

$$L_n^{\alpha}(x) = \sum_{r=0}^{n} \frac{\Gamma(\alpha-\beta+r)}{r!\,\Gamma(\alpha-\beta)} L_{n-r}^{\beta}(x). \quad . \quad . \quad . \quad . \quad . \quad (1.7)$$

We note further a generating function involving products[7] of parabolic cylinder functions, namely

$$\sum_{n=0}^{\infty} \frac{t^n}{n! \sqrt{\frac{\pi}{2}}} D_n(x) D_n(y)$$

$$= \frac{1}{\sqrt{\left\{\frac{\pi}{2}(1-t^2)\right\}}} \exp\left\{\frac{4xyt-(x^2+y^2)(1+t^2)}{4(1-t^2)}\right\},$$

$$. \quad . \quad . \quad (1.8)$$

and the corresponding formula involving products of Laguerre polynomials :

$$\sum_{n=0}^{\infty} \frac{t^n n!}{\Gamma(n+\alpha+1)} e^{-\frac{1}{2}(x+y)} (xy)^{\frac{\alpha}{2}} L_n^{\alpha}(x) L_n^{\alpha}(y)$$

$$= \frac{t^{-\frac{\alpha}{2}}}{1-t} \exp\left\{-\tfrac{1}{2}(x+y)\frac{1+t}{1-t}\right\} I_{\alpha}\left(\frac{2\sqrt{xyt}}{1-t}\right); \quad |t| < 1.$$

$$. \quad . \quad . \quad (1,9)$$

It may not be out of place here to point out that this formula, associated with the names of Hillé, Hardy, and Kogbetliantz, was given by Bateman[8] in 1914.

§ 2. In virtue of the relation[9]

$$x^{\alpha}L_n^{\alpha}(\lambda x)L_m^{\alpha}(\mu x) \doteq \frac{\Gamma(n+m+\alpha+1)}{n!\,m!}\frac{(p-\lambda)^n(p-\mu)^m}{p^{n+m+\alpha}}$$

$$\times F\left\{-n,\ -m;\ -n-m-\alpha;\ \frac{p(p-\lambda-\mu)}{(p-\lambda)(p-\mu)}\right\}, \quad (2.1)$$

which holds for arbitrary values of λ and μ, for $\alpha > -1$ and (1.5) (1.6) we have

$$x^{-\frac{1}{2}}e^{\frac{1}{2}(\lambda+\mu)x}D_{2n}(\sqrt{2\lambda x})D_{2m}(\sqrt{2\mu x})$$

$$\doteq \frac{(-)^{n+m}\sqrt{\pi}(2n+2m)!}{2^{n+m}(n+m)!}\frac{(p-\lambda)^n(p-\mu)^m}{p^{n+m+\frac{1}{2}}}$$

$$\times F\left\{-n,\ -m;\ -n-m+\tfrac{1}{2};\ \frac{p(p-\lambda-\mu)}{(p-\lambda)(p-\mu)}\right\} \quad (2.2)$$

and

$$(\lambda\mu x)^{-\frac{1}{4}}e^{\frac{1}{2}(\lambda+\mu)x}D_{2n+1}(\sqrt{2\lambda x})D_{2m+1}(\sqrt{2\mu x})$$

$$\doteq \frac{(-)^{n+m}\sqrt{\pi}(2n+2m+2)!}{2^{n+m+1}(n+m+1)!}\frac{(p-\lambda)^n(p-\mu)^m}{p^{n+m+\frac{3}{2}}}$$

$$\times F\left\{-n,\ -m;\ -n-m-\tfrac{1}{2};\ \frac{p(p-\lambda-\mu)}{(p-\lambda)(p-\mu)}\right\}. \quad (2.3)$$

In order to obtain operational representations of products of type $D_{2n}(\sqrt{2\lambda x})D_{2m+1}(\sqrt{2\mu x})$ we can use the relation (1.7). It thus appears that there is no simple operational representation of such products in the case when λ and μ are arbitrary. When $n = m$ the above results simplify somewhat, and in this case it is interesting to show how the result can readily be deduced from (1.8), for we have at once

$$\sum_{n=0}^{\infty} t^n \int_0^{\infty} e^{-px}x^{-\frac{1}{2}}D_n(\sqrt{\lambda x})D_n(\sqrt{\mu x})\,dx$$

$$= 2\sqrt{\pi}\,n!\,\{(4p+\lambda+\mu)-4t\sqrt{\lambda\mu}+t^2(\lambda+\mu-4p)\}^{-\frac{1}{2}}, \quad (2.4)$$

from which it follows that

$$x^{-\frac{1}{2}}\mathrm{D}_n(2\sqrt{\lambda x})\mathrm{D}_n(2\sqrt{\mu x})$$

$$\doteqdot \frac{n\,!\,\sqrt{\pi}}{(p+\lambda+\mu)^{\frac{1}{2}}}\left(\frac{\lambda+\mu-p}{\lambda+\mu+p}\right)^{\frac{n}{2}}\mathrm{P}_n\left\{2\sqrt{\frac{\lambda\mu}{(\lambda+\mu)^2-p^2}}\right\}, \quad (2.5)$$

where $\mathrm{P}_n(z)$ is the ordinary Legendre polynomial.

§3. We may proceed to a few applications of the result (2.5).

We have

$$(2^n\,n\,!\,\sqrt{\pi})^{-1}\,x^{-\frac{1}{2}}\mathrm{D}_n(2\cos\alpha\sqrt{x})\mathrm{D}_n(2\sin\alpha\sqrt{x})$$

$$\doteqdot \sum_{r=0}^{m}(-)^r\frac{(2n-2r)\,!}{r\,!\,(n-r)\,!\,(n-2r\,!}\frac{p}{(p+1)^{\frac{1}{2}}}\left(\frac{1-p}{1+p}\right)^{\frac{n}{2}} \times\frac{(\sin 2\alpha)^{n-2r}}{\left\{(1+p)(1-p)\right\}^{\frac{n}{2}-r}}$$

$$\doteqdot \sum_{r=0}^{m}(-)^r\frac{(2n-2r)\,!}{r\,!\,(n-r)\,!\,(n-2r)\,!}(\sin 2\alpha)^{n-2r} \times\frac{p(1-p)^{n-r}}{(p+1)^{n-r+\frac{1}{2}}}\left(\frac{1}{2}\right)^{n-2r}\left\{1+\frac{p+1}{1-p}\right\}^{n-2r}$$

$$\doteqdot \sum_{r=0}^{m}(-)^r\frac{(2n-2r)\,!}{r\,!\,(n-r)\,!\,(n-2r)\,!}\left(\frac{1}{2}\right)^{n-2r}(\sin 2\alpha)^{n-2r} \times\sum_{s=0}^{n-2r}\binom{n-2r}{s}p\frac{(1-p)^{n-r-s}}{(1+p)^{n-r-s+\frac{1}{2}}},$$

where $m=\dfrac{n}{2}$ or $\dfrac{n-1}{2}$, whichever is integral.

Using the result

$$x^{-\frac{1}{2}}\mathrm{D}_{2n}(2\sqrt{x})\doteqdot\sqrt{\pi}\frac{(2n)\,!}{2^n\,n\,!}p\frac{(1-p)^n}{(1+p)^{n+\frac{1}{2}}},$$

we get, after a few reductions,

$$\mathrm{D}_n(2\cos\alpha\sqrt{x})\mathrm{D}_n(2\sin\alpha\sqrt{x})$$

$$=n\,!\sum_{r=0}^{\frac{n}{2}\text{ or }\frac{n-1}{2}}\sum_{s=0}^{n-2r}\frac{(-)^r(\sin\alpha\cos\alpha)^{n-2r}}{2^r\,r\,!\,(n-2r-s)\,!\,s\,!}\mathrm{D}_{2n-2r-2s}(2\sqrt{x}). \quad (3.1)$$

We have also from (2.5)

$$x^{-\frac{1}{2}}\mathrm{D}_n(\sqrt{2x})\mathrm{D}_n(i\sqrt{2x}) \doteqdot i^n\, n!\,\sqrt{\pi}p^{\frac{1}{2}}\mathrm{P}_n\left(\frac{1}{p}\right), \quad (3.2)$$

so that we get, on expanding and interpreting the right-hand side,

$$\mathrm{D}_n(\sqrt{2x})\mathrm{D}_n(i\sqrt{2x})$$

$$= i^n\, n!\,\sqrt{\pi}x^n \sum_{r=0}^{m} \frac{(-)^r(2n-2r)!\,x^{-2r}}{2^n\, r!\,(n-r)!\,(n-2r)!\,\Gamma(n-2r+\frac{1}{2})}, \quad (3.3)$$

where $m = \frac{n}{2}$ or $\frac{n-1}{2}$, whichever is integral.

We have also

$$\int_0^x \{\xi(x-\xi)\}^{-\frac{1}{2}}\mathrm{D}_n(\sqrt{2\xi})\mathrm{D}_n(i\sqrt{2\xi}) \times \mathrm{D}_m(\sqrt{2x-2\xi})\mathrm{D}_m(i\sqrt{2x-2\xi})\, d\xi$$

$$\doteqdot i^{n+m}\, n!\, m!\,\pi \mathrm{P}_n\left(\frac{1}{p}\right)\mathrm{P}_m\left(\frac{1}{p}\right). \quad . \quad . \quad (3.4)$$

Expanding the right-hand side by Adams'[10] formula we have, when $m \leqslant n$,

$$\doteqdot i^{n+m}\, n!\, m!\,\pi \sum_{r=0}^{m} \frac{\mathrm{A}_{m-r}\mathrm{A}_r\mathrm{A}_{n-r}}{\mathrm{A}_{n+m-r}} \times \left(\frac{2n+2m-4r+1}{2n+2m-2r+1}\right)\frac{1}{p}\cdot p^{\frac{1}{2}}\cdot p^{\frac{1}{2}}\mathrm{P}_{n+m-2r}\left(\frac{1}{p}\right);$$

interpreting this by the aid of the results

$$p^{\frac{1}{2}}\mathrm{P}_{n+m-2r}\left(\frac{1}{p}\right) \doteqdot \{i^{n+m-2r}(n+m-2r)!\,\sqrt{\pi}\}^{-1} \times x^{-\frac{1}{2}}\mathrm{D}_{n+m-2r}(\sqrt{2x})\mathrm{D}_{n+m-2r}(i\sqrt{2x})$$

and

$$\frac{1}{p^{-\frac{1}{2}}} \doteqdot \frac{x^{-\frac{1}{2}}}{\sqrt{\pi}}, \quad \mathrm{R}(x) > 0,$$

the left-hand side of (3.4) reduces to

$$\frac{n!\, m!}{(n+m-2r)!}\sum_{r=0}^{m}\frac{(-)^r\mathrm{A}_{m-r}\mathrm{A}_r\mathrm{A}_{n-r}}{\mathrm{A}_{n+m-2r}}\cdot\left(\frac{2n+2m-4r+1}{2n+2m-2r+1}\right) \times \int_0^x \mathrm{D}_{n+m-2r}(\sqrt{2\eta})\mathrm{D}_{n+m-2r}(i\sqrt{2\eta})\{\eta(x-\eta)\}^{-\frac{1}{2}}\, d\eta,$$

and using (3.3) we find

$$\int_0^x \{\xi(x-\xi)\}^{-\frac{1}{2}} \mathrm{D}_n(\sqrt{2\xi})\mathrm{D}_n(\iota\sqrt{2\xi})\mathrm{D}_m\{\sqrt{2(x-\xi)}\} \times \mathrm{D}_m\{\iota\sqrt{2(x-\xi)}\}\, d\xi$$

$$= \frac{\iota^{n+m}\sqrt{\pi}}{2^{n+m}} \sum_{r=0}^{m} \sum_{s=0}^{l} \frac{\mathrm{A}_{m-r}\mathrm{A}_r\mathrm{A}_{n-r}}{\mathrm{A}_{n+m-r}} \left(\frac{2n+2m-4r+1}{2n+2m-2r+1}\right) \cdot \frac{(-)^s(2n+2m-4r+2s)!\, 2^{2r}x^{n+m-2r-2s}}{s!\,(n+m-2r-s)!\,\{(n+m-2r-2s)!\}^2},$$

where $\mathrm{A}_m = \dfrac{1.3.5\ldots 2m-1}{m!}$

and $l = \dfrac{n+m-2r}{2}$ or $\dfrac{n+m-2r-1}{2}$, whichever is integral.

§4. If we write λx for x, μx for y throughout (1.9), multiply by $x^\beta e^{-px}$ and integrate both sides from zero to infinity we find that the integration on the left-hand side results in relatively simple functions for certain values of β. Subsequent expansion of these in ascending powers of t gives us a set of operational representations for various values of β out of which we can choose the best suited to the immediate purpose. If in the present instance β is taken equal to zero we arrive at a special case of the formula (2.1). The case of $\beta = \alpha$ is worth noting. We find

$$\sum_{n=0}^{\infty} \frac{t^n\, n!\, (\lambda\mu)^{\frac{\alpha}{2}}}{\Gamma(n+\alpha+1)} \int_0^\infty \exp\left[-x\{p+\tfrac{1}{2}(\lambda+\mu)\}\right] x^{2\alpha} \times \mathrm{L}_n^\alpha(\lambda x)\mathrm{L}_n^\alpha(\mu x)\, dx$$

$$= \frac{\Gamma(\alpha+\frac{1}{2})}{\sqrt{\pi}} \frac{(4\sqrt{\lambda\mu})^\alpha}{(1-t)^{-\alpha}} \left[\{p^2+p(\lambda+\mu)+\tfrac{1}{4}(\lambda+\mu)^2\} - 2t\{p^2-\tfrac{1}{4}(\lambda+\mu)^2+2\lambda\mu\} + t^2\{+p^2-p(\lambda+\mu)+\tfrac{1}{4}(\lambda+\mu)^2\}\right]^{-\alpha-\frac{1}{2}}.$$

Writing

$$a_1^2 = p^2+p(\lambda+\mu)+\tfrac{1}{4}(\lambda+\mu)^2,$$

$$b_1^2 = p^2-\tfrac{1}{4}(\lambda+\mu)^2+2\lambda\mu,$$

$$c_1^2 = +p^2-p(\lambda+\mu)+\tfrac{1}{4}(\lambda+\mu)^2,$$

and equating the coefficient of t^n on both sides, we find

$$e^{-\frac{1}{2}x(\lambda+\mu)}x^{2\alpha}L_n^{\alpha}(\lambda x)L_n^{\alpha}(\mu x)$$
$$\doteqdot \frac{\Gamma(n+\alpha+1)}{n!}\frac{\Gamma(\alpha+\frac{1}{2})}{\sqrt{\pi}}\frac{\Gamma(\alpha+1)}{2^{-2\alpha}}p$$
$$\cdot \sum_{r=0}^{\infty}\frac{(-)^r a_1^{-2\alpha-1}}{r!\,\Gamma(\alpha-r+1)}\left(\frac{c_1}{a_1}\right)^{n-r}C_{n-r}^{\alpha+\frac{1}{2}}\left(\frac{b_1^2}{a_1c_1}\right), \quad (4.1)$$

where $C_n^{\nu}(z)$ denotes, as usual, the Gegenbauer polynomial[11].

From (4.1) we get by the operational method

$$x^{2\alpha}L_n^{\alpha}(\lambda x)L_n^{\alpha}(\mu x)$$
$$\doteqdot \frac{\Gamma(n+\alpha+1)}{n!}\frac{\Gamma(\alpha+\frac{1}{2})}{\sqrt{\pi}}\frac{\Gamma(\alpha+1)}{2^{-2\alpha}}\cdot p$$
$$\cdot \sum_{r=0}^{\infty}\frac{(-)^r a^{-2\alpha-1}}{r!\,\Gamma(\alpha-r+1)}\left(\frac{c}{a}\right)^{n-r}C_{n+r}^{\alpha+\frac{1}{2}}\left(\frac{b^2}{ac}\right), \quad (4.2)$$

where

$$a^2=p^2,$$
$$b^2=p^2-(\lambda+\mu)p+2\lambda\mu,$$
$$c^2=\{p-\tfrac{1}{2}(\lambda+\mu)\}^2.$$

The summation terminates when α is integral or zero, and in the latter case we have

$$L_n(\lambda x)L_n(\mu x)$$
$$\doteqdot \left\{\frac{p-\lambda-\mu}{p}\right\}^n P_n\left[\frac{p^2-(\lambda+\mu)p+2\lambda\mu}{p(p-\lambda-\mu)}\right]. \quad (4.3)$$

§ 5. When n is integral we have the following contour integral for $D_n(z)$[12]:

$$D_n(z)=-\frac{n!\,e^{-\frac{1}{4}z^2}}{2\pi i}\int^{0+}\frac{e^{-zt-\frac{1}{2}t^2}}{(-t)^{n+1}}dt,$$

so that

$$2^{\frac{n}{2}}e^{\frac{x^2}{2}}D_n(x\sqrt{2})=\frac{n!}{2\pi\iota}\int_c\frac{e^{2x\xi-\xi^2}}{\xi^{n+1}}d\xi,$$

where c is a contour encircling $\xi=0$.

It follows that

$$\int_{-\infty}^{\infty} e^{2iax} D_n(x\sqrt{2}) D_m(x\sqrt{2})\, dx$$

$$= \frac{2^{-\frac{n}{2}-\frac{m}{2}}\, n!\, m!\, e^{-a^2}}{(2\pi i)^2}$$

$$\times \int_c \int_{c'} \int_{-\infty}^{\infty} \frac{e^{-\frac{1}{2}x-(ia+\xi+\eta)\}^2} e^{2\xi(ia+\eta)} e^{2ia\eta}}{\xi^{n+1}\eta^{m+1}} dx\, d\xi\, d\eta. \quad (5.1)$$

Inversion of the order of integration being permissible, we may integrate first with respect to x, then with respect to ξ, so that the right-hand side becomes

$$= \frac{\sqrt{\pi}\, m!\, 2^{\frac{n}{2}-\frac{m}{2}}\, e^{-a^2}}{2\pi i} \int_{c'} \frac{(ia+\eta)^n}{\eta^{m+1}} e^{2ia\eta}\, d\eta.$$

In virtue of the relation

$$\frac{n!}{\Gamma(n+\alpha+1)} L_n^{\alpha}(x) = \frac{1}{2\pi i} \int_c \left(1-\frac{x}{w}\right)^n \frac{e^w}{w^{\alpha+1}} dw$$

we have thus

$$\int_{-\infty}^{\infty} e^{2iax} D_n(x\sqrt{2}) D_m(x\sqrt{2})\, dx = n!\, (ia\sqrt{2})^{m-n} e^{-a^2} L_n^{m-n}(2a^2).$$

. . . (5.2)

§ 6. Using Whittaker's[13] integral for $D^n(z)$, viz.

$$D_n(z) = \frac{e^{-\frac{1}{4}z^2}}{\Gamma(-n)} \int_0^{\infty} u^{-n-1} e^{-zu-\frac{1}{2}u^2}\, du, \quad R(n)<0,$$

we may write

$$\Gamma(n) p e^{\frac{p^2}{4}} D_{-n}(p) \doteqdot x^{n-1} e^{-\frac{x^2}{2}}.$$

Using the product theorem of the operational calculus we have

$$\Gamma(n+1)\Gamma(m+1)\, \frac{p}{ab}\, e^{\frac{p^2}{4}\left(\frac{1}{a^2}+\frac{1}{b^2}\right)} D_{-n-1}\left(\frac{p}{a}\right) D_{-m-1}\left(\frac{p}{b}\right)$$

$$\doteqdot \int_0^x (a\xi)^n (bx-b\xi)^m e^{-\frac{a^2\xi^2}{2}-\frac{b^2}{2}(x-\xi)^2} d\xi$$

$$\doteqdot e^{-\frac{b^2x^2}{2}} \int_0^x (a\xi)^n [b(x-\xi)]^m e^{-\frac{(a^2+b^2)\xi^2}{2}+b^2x\xi} d\xi.$$

On developing the right-hand side by (1.1) we have

$$\doteqdot e^{-\frac{b^2x^2}{4}} \sum_{s=0}^{\infty} \frac{\mathrm{D}_s(bx)}{s!} b^{s+m} a^n \int_0^x \xi^{s+n}(x-\xi)^m e^{-\frac{a^2\xi^2}{2}}\, d\xi,$$

so that

$$\Gamma(n+1)\frac{p}{ab} e^{\frac{p^2}{4}\left(\frac{1}{a^2}+\frac{1}{b^2}\right)} \mathrm{D}_{-n-1}\left(\frac{p}{a}\right) \mathrm{D}_{-m-1}\left(\frac{p}{b}\right)$$

$$\doteqdot e^{-\frac{b^2x^2}{4}} (ax)^n (bx)^m \sum_{s=0}^{\infty} \frac{(bx)^s \mathrm{D}_s(bx)}{s!}$$

$$\times \sum_{r=0}^{\infty} \frac{(-)^r \Gamma(s+n+2r+1) a^{2r} x^{2r+1}}{2^r\, r!\, \Gamma(n+m+s+2r+2)}; \quad \mathrm{R}(n) > -1$$

. . . (6.1)

This result reduces to simpler forms in special cases; for example, taking $a = e^{-\frac{1}{4}\pi i}$, $b = e^{\frac{1}{4}\pi i}$, and $m = n$, we have

$$[\Gamma(n+1)]^2 p \mathrm{D}_{-n-1}(pe^{\frac{1}{4}\pi i}) \mathrm{D}_{-n-1}(pe^{-\frac{1}{4}\pi i})$$

$$\times \int_0^x \{\xi(x-\xi)\}^n e^{i\frac{x^2}{2} - ix\xi}\, d\xi,$$

and using the result

$$\mathrm{J}_\nu(z) = \frac{(\frac{1}{2}z)^\nu}{\Gamma(\nu+\frac{1}{2})\Gamma(\frac{1}{2})} \int_0^\pi e^{iz\cos\theta} \sin^{2\nu}\theta\, d\theta,$$

we obtain

$$\Gamma(n+1) p \mathrm{D}_{-n-1}(pe^{\frac{1}{4}\pi i}) \mathrm{D}_{-n-1}(pe^{-\frac{1}{4}\pi i}) \doteqdot \sqrt{\pi}\, \mathrm{J}_{n+\frac{1}{2}}\left(\frac{x^2}{2}\right).$$

. . . (6.2)

On interpretation this yields

$$\mathrm{D}_{-n-1}(ze^{\frac{1}{4}\pi i}) \mathrm{D}_{-n-1}(ze^{-\frac{1}{4}\pi i})$$

$$= \frac{\sqrt{\pi}}{\Gamma(n+1)} \int_0^\infty e^{-xz} \mathrm{J}_{n+\frac{1}{2}}\left(\frac{x^2}{2}\right) dx; \quad \mathrm{R}(n) > -1. \quad (6.3)$$

As a further example take $a = 1$, $b = -1$, and $m = n$; we get on reduction

$$\Gamma(n+1) p \mathrm{D}_{-n-1}(p) \mathrm{D}_{-n-1}(-p)$$

$$\doteqdot (-)^n \sqrt{\pi}\, \mathrm{I}_{n+\frac{1}{2}}\left(\frac{x^2}{2}\right); \quad \mathrm{R}(n) > -1. \quad (6.4)$$

By the application of the operational calculus to (6.2) and (6.4) integral representations analogous to those given by Meijer[6] may be readily deduced.

§ 7. Bailey [14] has recently given the relation

$$L_n^{\alpha}(x)L_n^{\alpha}(y) = \frac{\Gamma(1+\alpha+n)}{n!} \sum_{r=0}^{n} \frac{(xy)^r}{r!} \frac{L_{n-r}^{\alpha+2r}(x+y)}{\Gamma(1+\alpha+r)}.$$

When $y=x$ this gives an expression for the square of the Laguerre polynomial as a series involving $L_m^{\beta}(2x)$. There is, however, a neater result than this, which has hitherto escaped notice. It is

$$[L_n^{\alpha}(x)]^2 = \frac{\Gamma(n+\alpha+1)}{2^{2n}\, n!} \sum_{l=0}^{n} \frac{(2n-2l)!\,(2l)!}{\Gamma(1+\alpha+l)\,[(n-l)!]^2} L_{2l}^{2\alpha}(2x). \quad . \quad . \quad . \quad (7.1)$$

In order to deduce this result, we note that in virtue of (1.9),

$$\sum_{n=0}^{\infty} \frac{t^n\, n!}{\Gamma(1+\alpha+n)} \int_0^{\infty} \exp\{-x(p+1)\} x^{2\alpha} [L_n^{\alpha}(x)]^2\, dx$$

$$= \frac{\Gamma(\alpha+\frac{1}{2})}{\sqrt{\pi}}\, 2^{2\alpha}(1-t)^{-\frac{1}{2}}(p+1)^{-2\alpha-1} \left\{ 1 - t\left(\frac{p-1}{p+1}\right)^2 \right\}^{-\alpha-\frac{1}{2}}.$$

On equating coefficients of t^n, we have

$$\int_0^{\infty} e^{-px} e^{-x} x^{2\alpha} [L_n^{\alpha}(x)]^2\, dx$$

$$= \frac{\Gamma(1+\alpha+n)}{2^{2n}\, n!} \sum_{l=0}^{n} \frac{\Gamma(2l+2\alpha+1)\,(2n-2l)!}{\Gamma(l+\alpha+1)\,[(n-l)!]^2} \frac{(p-1)^{2l}}{(p+1)^{2l+2\alpha+1}},$$

or

$$e^{-x} x^{2\alpha} [L_n^{\alpha}(x)]^2$$

$$\doteqdot \frac{\Gamma(n+\alpha+1)}{2^{2n}\, n!} \sum_{l=0}^{n} \frac{\Gamma(2l+2\alpha+1)\,(2n-2l)!}{\Gamma(l+\alpha+1)\,[(n-l)!]^2} p \frac{(p-1)^{2l}}{(p+1)^{2l+2\alpha+1}}.$$

The result given follows immediately in virtue of

$$e^{-x} x^{\alpha} L_n^{\alpha}(2x) \doteqdot \frac{\Gamma(n+\alpha+1)}{n!} p \frac{(p-1)^n}{(p+1)^{n+\alpha+1}}.$$

As a consequence of the result (7.1) Watson's integral equation [15] for the square of a Laguerre polynomial, viz.,

$$e^{-x} x^{\alpha} [L_n^{\alpha}(x)]^2 = (-)^n \int_0^{\infty} J_{2\alpha}(2\sqrt{xs})\, e^{-s} s^{\alpha} [L_n^{\alpha}(s)]^2\, ds,$$

follows by mere summation from the simple result

$$e^{-x}x^{\alpha}\mathrm{L}_n^{\alpha}(2x) = \int_0^{\infty} \mathrm{J}_{\alpha}(2\sqrt{xs})e^{-s}s^{\alpha}\mathrm{L}_n^{\alpha}(2s)\,ds.$$

The corresponding result for products of Parabolic Cylinder Functions has already been given by Dhar [16].

References.

(1) S. C. Dhar, Journal London Math. Soc. x. pp. 171–175 (1935).
(2) R. S. Varma, Phil. Mag. p. 926 (May 1937).
(3) W. T. Howell, Phil. Mag. (In the press.)
(4) H. E. J. Curzon, Proc. London Math. Soc. (2) xii. pp. 233–259 (1913).
(5) S. Goldstein, Proc. London Math. Soc. (2) xxxiv. p. 118 (1932).
(6) C. S. Meijer, *Proc. Kon. Akad. Wet.* xl. p. 259.
(7) F. G. Mehler, *Journal für Math.* lxvi. pp. 161–176 (1866).
(8) H. Bateman, ' Electrical and Optical Wave Motion,' p. 102, equation 214 (Cambridge, 1914).
(9) W. T. Howell, Phil. Mag. (In the press.)
(10) Whittaker and Watson, ' Modern Analysis,' 3rd edit. p. 331, ex. 11 (Cambridge, 1920).
(11) *Ibid.* p. 329, paragraph 15.8.
(12) *Ibid.* p. 350, paragraph 16.7
(13) E. T. Whittaker, Proc. London Math. Soc. (1) xxxv. pp. 417–427 (1903).
(14) W. N. Bailey, Proc. London Math. Soc. ser. 2, xli. p. 219.
(15) G. N. Watson, Journal London Math. Soc. ii. p. 256.
(16) S. C. Dhar, *loc. cit.* equation (9).

XCIV. *Thermionic Emission.* *By* E. W. B. Gill, *B.Sc., M.A., Fellow of Merton College, Oxford* *.

THE number of electrons emitted per second by a hot filament depends upon its temperature, and for a fixed temperature, if the electric force between the collecting electrodes and the filament is great enough to overcome the field due to the space charges, the current flowing is said to be saturated, this term implying that the current remains constant however much more the field is increased. All, however, who have taken valve curves experimentally are aware that this state of constancy is never attained in practice.

As the voltages across the valve are increased there is a rapid rise in current in the region where the space charges are operative, and beyond that the curve certainly

* Communicated by Prof. J. S. Townsend, F.R.S.

flattens out, but it never becomes quite flat, though the increase of current per volt continually decreases as the volts are increased.

In some cases this effect is partly accounted for by secondary emission from some of the electrodes, but in a triode with the grid at a potential only slightly different from the filament, and always in a diode, secondary emission has no effect, and some other cause must be operative. The emission from a heated filament in fact does not depend only on the temperature of the filament, but depends to a lesser extent on the electric force at the surface.

Practically the only theory put forward on the subject is that of Schottky, who regarded an electron leaving the filament as a charge in the presence of a conductor, and as, therefore, being acted on by the retarding force due to an equal and opposite charge at its image *.

This led him to the expression for the emission

$$i_0 e^{\frac{4\cdot39\sqrt{E}}{T}},$$

where i_0 is the emission for zero field, T the temperature, and E the electric force (volts/cm.) at the surface.

It is claimed that this expression has been verified by experiment for "bright" emitters, and so far as can be ascertained it has never been questioned, though, for some not understood reason, it is not accurate for coated filaments.

The experiments to be described, however, appear to show that the true expression for the emission is simpler than that above, and the new expression has in its favour that it applies equally to bright emitters and to coated filaments. (It is difficult to see why the image theory if it applies to one does not apply to the other.) The main experimental difficulty is that in the so-called saturation portion of the curve the increase of current is very minute for very considerable increases in voltage, and these current increases have therefore to be measured with very considerable accuracy. It seemed that the solution of the problem would be to work with emissions not of the order of milliamperes (the usual working

* An excellent summary of the present knowledge of the subject and a very complete bibliography is given by T. J. Jones in Methuen's monographs on physical subjects—Thermionic Emission.

condition of wireless valves) but with currents of the order of microamperes only, for the following reasons :—

1. Only 2 or 3 volts are required to overcome the space charge effect.

2. (Very important.) The energy dissipated at the anode by electron bombardment is so small that there is no appreciable heating. For larger emissions the anode gets heated for large values of V, the filament has its temperature raised by the radiation from the anode, and an error is introduced which it is very difficult to allow for.

3. The current being read on a mirror galvanometer scale can be read with a much higher percentage accuracy than with a milliammeter. The scale was 50 cm. in length, or at least five times as long, and therefore five times more accurate than a milliammeter.

4. The filament has only to be at a low temperature to emit a microamp. At this temperature a slight fluctuation in filament current has little effect on the emission ; but at the higher temperatures required for the emission of milliamperes the same proportionate fluctuation has an enormously greater effect on the emission.

Most experimenters know that even with every care with accumulators, contacts, and especially resistances, it is a matter of extreme difficulty to keep an emission of milliamperes constant to, say, 1 part in 500 for any length of time. With microamps it was quite easy. The disadvantage is that several hundred volts used in conjunction with a galvanometer responding to fractions of a microamp needs exceptionally good insulation in all the circuits, and only certain valves could be used.

The main danger to be guarded against is the possibility that the valve containing the filament and anode has not a good enough vacuum. Any appreciable trace of gas results in ionization when V is large, and the anode current now gives a measure not of the emission but of the emission plus the products of ionization.

For this reason commercial transmitting valves were generally used, as these are very carefully degassed in the process of manufacture ; and as an additional precaution triodes and not diodes were used as a test, for ionization

is possible with the former. A split anode diode can, however, be tested, and one of these was used. Transmitting valves have also very good electrical insulation.

The chief measurements were made on three different valves, the first two kindly given by the Marconi Company.

Valve A, known as a split anode, had a tungsten filament 6·5 cm. in length (*i. e.*, it was a bright emitter). The anode was a concentric cylinder of radius 1 cm., this anode being split into two equal halves by cuts parallel to the filament, with separate leads through the glass envelope. In the actual experiments it was used simply as a diode, the two halves being connected, but the splitting of the anode has the advantage that a test for ionization is possible ; to conduct such a test one anode was put at a very high positive potential above the filament and the other negative to it. If there is ionization this negative electrode should receive positive charge, but with the most sensitive galvanometer no trace could be detected even when the filament was heated to give 20 milliamps emission.

Valve B was of the type known as Det. 1, a small transmitting triode. It had a thoriated dull emitter filament of hairpin type and a fairly open grid. The anode and grid were both of the flattened cylinder type common in modern valves.

Valve C was a Mullard type 354V. This is a triode with an indirectly heated filament which has the advantage that the emitting electrode is an equipotential.

Both valves B and C were tested for ionization by the usual method of having the grid highly positive to the filament and the anode slightly negative to it. Any positive current reaching the anode indicates ionization of residual gas in the valve.

Valve B showed no trace of ionization up to 1000 volts across it, but valve C showed a slight trace for voltages exceeding 100. (This valve was only a receiving valve and would not be expected to have the high vacuum of the other two.) For the emission measurements in the two latter valves the anode and grid were joined and put at the same potential V above the filament. The total current to these electrodes gave the filament emission.

For greater accuracy the D'Arsonval galvanometer used for measuring the emission had its scale pasted

on an arc of a circle of radius 1 metre placed 1 metre from the galvanometer mirror. Tests showed this arrangement produced a deflexion most accurately proportional to the current.

In an experiment the valve filament was heated by a constant current, and the current-EMF characteristic was taken between the filament and anodes.

Typical results were :—

Valve A. Current unit 250=1 microamp.

[V was measured from the negative end of the filament.]

TABLE I.

Anode volts V.	4	8	20	36	64	100	144	200	256	400	600	900
Anode current i.	122	190	231	246	260	274	280	290	296	312	328	350

In the case of all three valves it was found that if i was plotted against $\sqrt{V}$ the curve was found to be a straight line for the higher values of V, but fell below it for the lower values (see figure).

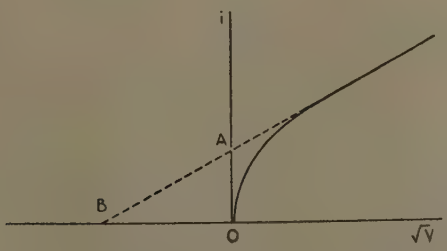

This gives the formula (for larger values of V)

$$i = i_0 + a\sqrt{V}, \quad . \quad . \quad . \quad . \quad . \quad . \quad (1)$$

where i_0 and a are constants for a given filament temperature ; whereas according to Schottky

$$i = i_0 e^{b\sqrt{V}} \quad . \quad . \quad . \quad . \quad . \quad . \quad . \quad (2)$$

for the electric force E outside the filament is in general proportional to V.

When expanded equation (2) gives

$$i=i_0\left(1+b\sqrt{V}+\frac{b^2}{2}V+\ldots\right),\ldots\quad\ldots\quad(3)$$

and as b is in practice small equation (3), to a first approximation, gives the same result as equation (1).

The test of the rival formulæ thus obviously requires extremely accurate measurement.

There are two methods of comparison; according to equation (2) $\log i=\log i_0+b\sqrt{V}$, and hence $\log i$ instead of i plotted against $\sqrt{V}$ should give a straight line.

The curves of i against $\sqrt{V}$ and $\log i$ against $\sqrt{V}$ were therefore plotted, and it was found that the former gave the better straight line; but the differences are so small that it would be imperceptible on a small diagram. Both curves deviated from the straight for the lower values of $\sqrt{V}$.

The second method, more suitable for publication, is to calculate the currents, finding the values of the constants from two values of the current. In the table below these values were found from the currents for $V=400$ and $V=900$.

TABLE II.

Valve A.

V	4	8	20	36	64	100	144	200	256	400	600	900
Actual I	122	190	231	246	260	274	280	290	296	312	328	350
Calculated from $i=236+3{\cdot}8\sqrt{V}$.	244	247	253	258	266	274	282	290	297	312	329	350
Calculated from log. $i=2{\cdot}126+{\cdot}283\sqrt{V}$ ..	163	171	204	222	241	256	270	283	293	312	330	350

There is no doubt from this table that the agreement is better for all the higher values of V with the formula $a+b\sqrt{V}$ than with Schottky's log formula. The deviation of both formulæ for the lower values of V will be discussed later.

It should, however, be remarked that in deriving the log formula from Schottky's equation the electric force E is only proportional to V for a uniform filament, which

has been assumed. If the filament is rough with small projecting points the value of E is large at these points, and Schottky's equation would lead to a sum of terms made of emissions from every element of the filament, the value of E at these points depending on the shape of the filament there. It is, however, inconceivable that the sum of a series of exponential terms should give the simple result $a+b\sqrt{V}$ for a filament with random roughness. The log formula above has been fitted to agree with the points on the curve given by V=400 and V=900, but no better result can be obtained by fitting it to agree with any other two points.

The results discussed so far are for a bright emitter to which Schottky's theory is supposed to apply. The figures in the next table are for *Valve B*, the thoriated dull emitter filament, and show that the formula $a+b\sqrt{V}$ fits these equally well for the larger values of V.

TABLE III.

Scale for i . . . 150 =1 microamp.
i calculated from formula $i=131+20{\cdot}1\sqrt{V}$.

V	10	17	36	64	100	144	196	256	324	400	600	800
i observed	148	176	234	285	332	374	414	453	492	533	623	701
i calculated ...	194	214	251	292	332	372	413	453	493	533	624	700

The log formula was in worse agreement with this than it was for the bright emitter.

The curves for the lower values of V are rather puzzling. Space charge effects for the minute emissions employed are quite ineffective when V exceeds 2 or 3 volts, unless the filament contains tiny cavities where the electric force is much reduced.

One disturbing factor is that in valves A and B there was a potential drop down the filament of about 4 volts, and the potential across the valve thus ranged between V and V–4. As was therefore expected, better agreement for lower values of V was obtained with valve C, with its equipotential dull emitter filament, as shown in Table IV.

It is, however, possible that the improved agreement is not due solely to the equipotential, but is to do with the fact that an indirectly heated filament is of much

larger diameter than a plain wire filament, and the forces around it are in consequence very different.

Unfortunately, as mentioned above, the vacuum in this valve was not good enough to get reliable results above $V=100$.

Referring to the figure, the curve $i=i_0+a\sqrt{V}$ has intercepts on the axes $OA=i_0$ and $OB=-i_0/a$. The former may be taken as a true measure of the temperature emission uninfluenced by electric force, and, of course, increases very rapidly with the temperature of the filament.

TABLE IV.

Scale for i . . . 1000=1 microamp.

Calculated from formula $i=100+26{\cdot}2\sqrt{V}$.

Valve C.

V	2	4	6	8	10	20	40	63	100
i observed	120	148	163	174	181	216	262	303	362
i calculated	137	152	164	174	183	217	265	308	362

For emissions not differing unduly OB has the same value for the straight lines, for different emissions all pass through the same point B, hence i_0/a is constant, so that the emission current can, to a first approximation, be taken as $i_0(1+b\sqrt{V})$, where i_0 alone depends on the filament temperature and b is a constant.

The point B is not easy to obtain accurately, for a slight change in the slope of the lines alters it a good deal, but some very careful experiments with a dull emitter valve showed that as the emission is increased OB is not quite constant but does increase slightly.

For the valve in question for $i_0=\frac{1}{10}$ microamp OB was -15, and as i_0 was increased OB rose continuously till when $i_0=200$ microamps OB was -25. This increase is not considerable, seeing that i_0 was varied by a factor of 2000.

In all cases OB is much larger for a bright than for a dull emitter, so that the increase with anode voltage of the emission current is less for a bright than a dull. Thus for bright emitter valve A the curve cuts the axis

for $\sqrt{V}=-62$, while for currents of the same order for dull emitter valve B the point is given by $\sqrt{V}=-6{\cdot}5$, and for dull emitter valve C by $\sqrt{V}=-4$.

The experiments thus appear to show that the emission from a hot filament is given by an expression $i_0(1+b\sqrt{V})$, where V is the potential between the filament and the collecting electrode and i_0 and b are both functions of the temperature, but b only varies very slightly with it.

These expressions apply equally to bright and dull emitters. There is no previous theory to explain this result, and the following general idea is put forward with reserve.

The expression $\sqrt{V}$ suggests that the velocity of the electrons is in some way involved. If the electrons were started from a region of constant volume density σ the current flowing would be proportional both to σ and to their velocity at any point of their path. The velocity at the anode is proportional to $\sqrt{V}$, so that the current would be proportional to $\sigma\sqrt{V}$. Thus if a hot filament not only ejected an emission current i_0 but also set up just round it a constant concentration of electrons of density proportional to i_0, then the total emission current would be of the form $i_0(1+b\sqrt{V})$.

In all theories of emission the electrons are shot out of the filament with various velocities, and accepting the image theory of Schottky, in the absence of any external field, the slower ones are, after a short excursion, attracted back to the filament and the faster ones have enough energy to get away.

The latter might represent the current i_0, and the former would give an average volume density of electricity just round the filament proportional to i_0. In the absence of an electric field this volume density remains constant, because in unit time as many electrons return to the wire as leave it. If, however, some of these electrons are removed by the application of an external electric field the explanation above demands that the number of electrons leaving the wire per second should increase, to maintain the density around the filament at its proper value; for the contribution to this density which the removed electrons would have made on their passage back to the filament has been lost.

A novel idea of thermionic emission is therefore required;

a hot wire must not be regarded as emitting per second a fixed number of electrons depending on its temperature, but as maintaining, just outside it, a distribution of free electrons whose volume density depends on the temperature. The emission adjusts itself to maintain this state of affairs, however many electrons may be removed by external agencies.

The problem practically becomes one of diffusion, being somewhat similar to that of contact differences of potential between two dissimilar metals or between a metal and a liquid.

The $\sqrt{V}$ law does not operate in these latter cases if current passes, because the velocity of the electrons or ions depends on V and not on $\sqrt{V}$.

The analogy is very close with the case of a current flowing in a circuit which contains a junction of dissimilar metals; the electron concentration on one side of the junction which gives rise to the contact potential difference is maintained constant whatever the current, for as fast as they are removed by the current others cross the junction to take their place.

There is one objection to Schottky's theory. The image theory should, presumably, apply equally to photoelectric emission, but in a photo-cell, provided the vacuum is sufficiently high, a true saturation current can be obtained which is independent of the applied voltage. The theory outlined above would, on the other hand, not be expected to apply to photoelectric emission.

In the suggested theory the electrons causing the phenomenon are all very close to the filament, and the current due to them will only be proportional solely to $\sqrt{V}$ if the electrons are removed from the whole region they occupy. But for the lower values of V only the outer layers will be removed, as there will be a reverse field in the region due to the electron space charge in it. This would account for a deviation from the $\sqrt{V}$ law for the lower values of V.

To summarize, it is suggested that there is a constant contact potential difference between a hot filament at a fixed temperature and an external vacuum, the electrons producing this potential being available for removal from the vicinity of the filament under an external field. If they are removed an equal number come from the filament to maintain the contact potential at its con-

stant value. The majority of the electrons from the filament take part in this process, but a smaller number pass from the filament with a higher velocity and leave its vicinity completely unless forced back by a sufficiently large opposing external field.

It is the presence of these higher velocity electrons which alone distinguishes the phenomenon from the contact potential between two dissimilar metals, or between a metal and a liquid.

The theory is consistent with the fact that the bright emitter curves are flatter than the dull emitter, for at the higher temperatures the proportion of the higher velocity electrons escaping to those which maintain the contact potential is greater than at the lower temperatures, and the flatness of the curves depends on the ratio of these two quantities.

The difference between the theory suggested and that of Schottky is that the latter supposes the external field to neutralize the retarding image field at the wire, and in effect to reduce the virtual work function, while on this theory the image field is bound up with the maintenance of the volume density just outside the wire.

My thanks are due to Prof. Townsend, in whose laboratory the experiments were made, and also to Mr. E. B. Moullin, who has kindly looked through this paper.

XCV. *Measurements of Thermal Diffusion in Gas Mixtures.*

By Dr. Grete Blüh, Dr. O. Blüh, *and* M. Puschner (Physics Department, German University, Prague)*.

1. *Introduction.*

THE separation produced in a uniform mixture of two gases by a gradient of temperature was termed by Chapman thermal diffusion. According to the theory the heavier molecules diffuse towards the cooler side and the lighter ones to the hotter side. The amount of the effect is greatest if the two gases are mixed in nearly equal proportions by volume and if the components are very unequal in masses and sizes. The total separation

* Communicated by T. L. Ibbs.

ΔA, the change in composition on both sides, is, according to Chapman's theory *, proportional to $\log T_2/T_1$, *i. e.*, $\Delta A = k_t . \log T_2/T_1$; T_1 is the absolute temperature of the cold side, T_2 the absolute temperature of the hot side, and k_t is defined as the ratio of the coefficient of thermal diffusion D_t to the coefficient of ordinary diffusion D_{12} : $k_t = D_t/D_{12}$. If ΔA is found from experiment and T_2/T_1 is known, k_t may be calculated. Moreover, the theory gives interesting relations between the amount of separation and the repulsive forces of the molecules. If q is the index in the law of repulsive force ($K = 1/r^q$), the theory of thermal diffusion indicates that the effect vanishes altogether if $q = 5$, while for $q = \infty$ the effect is greatest. In the latter case the molecules behave like rigid elastic spheres. For $q = \infty$ Chapman and Hainsworth † give a theoretical formula for k_t, whose value may be compared with the k_t exp. The ratio k_t exp./k_t theor. $= R_t$ offers a possibility of judging the difference of q from $q = \infty$. Chapman gives a formula to calculate q from the k_t exp. values in the special case when the masses and diameters of the molecules of the two gases are very different, but from this approximate values only of q can be obtained. The first experiments on thermal diffusion were made by Chapman and Dootson ‡ with a mixture of hydrogen-carbon dioxide with a difference of temperature of about 200° C. More exact experiments were made by Ibbs and collaborators § by means of a katharometer method of analyzing the gas mixture before and after the process of thermal diffusion. The results are in agreement with the theory. Variations in k_t have been found in some mixtures if the cold side is cooled to very low temperatures. In mixtures containing carbon dioxide Ibbs and Wakeman found a difference at about 145° C. which they believe to be due to a change in the nature of the repulsive forces of the molecules.

* S. Chapman, Proc. Roy. Soc. Lond. A, xciii. p. 1 (1916) ; Phil. Mag. xxxiv. p. 146 (1917).

† S. Chapman and W. Hainsworth, Phil. Mag. xlviii. p. 602 (1924).

‡ S. Chapman and F. W. Dootson, Phil. Mag. xxxiii. p. 268 (1917).

§ T. L. Ibbs, Proc. Roy. Soc. Lond. A, cvii. p. 470 (1925) ; T. L. Ibbs and L. Underwood, Proc. Phys. Soc. xxxix. p. 227 (1927) ; T. L. Ibbs, K. E. Grew, and A. Hirst, Proc. Phys. Soc. xli. p. 456 (1929) ; T. L. Ibbs and K. E. Grew, Proc. Phys. Soc. xliii. p. 142 (1931) ; T. L. Ibbs and A. C. R. Wakeman, Proc. Roy. Soc. cxxxiv. p. 613 (1932) ; K. E. Grew and B. E. Atkins, Proc. Phys. Soc. xlviii. p. 415 (1936).

2025-01-09

It seemed to be interesting to observe the phenomenon of thermal diffusion also with another experimental method, especially with the intention of watching the process continuously until it reached the steady state. An interferometer method was therefore developed, and measurements were made with the following pairs of gases : hydrogen-carbon dioxide, hydrogen-nitrogen, helium-argon, and helium-neon, chiefly between room-temperature and higher temperatures *.

2. *The Experimental Method.*

In the Jamin interferometer which was used the chief features are (fig. 1) the two glass plates P_1 and P_2, silvered at the back, the slit-tube S_1 with a lamp, the telescope S_2,

Fig. 1.

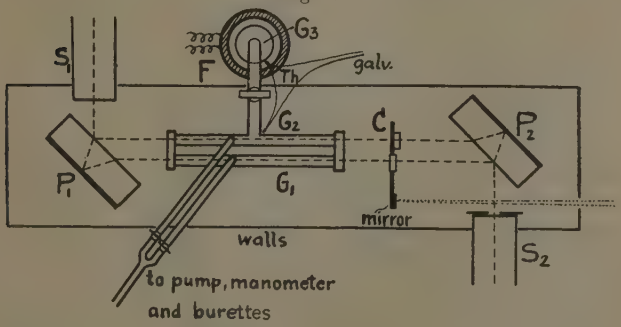

the Jamin compensator C, and the gas-tubes G_1 and G_2, which are closed with plane parallel glass plates. In fig. 1 is shown a scheme of the apparatus and the way which light takes through the two glass tubes. The tube G_2 communicates by a wider tube with stopcock with the vessel G_3, which may be heated by an electric furnace F or cooled by a cooling mixture. The temperature in G_2 was measured with a mercury thermometer, the difference of temperatures between G_2 and G_3 was measured with a thermocouple Th and a galvanometer. If G_1 and G_2 are filled with the same gas or gas mixture at the same pressure one observes in the telescope a system of fine parallel interference fringes ; in the case

* G. and O. Blüh, *Zeitschr. f. Physik*, xl. p. 12 (1934); M. Puschner, *Zeitschr. f. Physik* (in print).

of white light the fringes are coloured with an achromatic line in the centre of the system, in the case of monochromatic light (*e. g.*, sodium D) the fringes are dark on the yellow background. If there is any change in composition of the gas mixture in G_2 the interference system begins to move in consequence of the change in the refractive index of the medium and consequently of the optical pathway in G_2. By means of the compensator one can bring the interference system to the former state, using the achromatic line. The zero point is fixed by means of a second system of interference fringes arising from two beams of light going through air. The compensator must be gauged in wave-length of monochromatic light, in our case with the help of a sodium-arc lamp. In order to read off the motion of the compensator very accurately a mirror and scale were employed (see fig. 1).

By means of two gas burettes the gas mixtures were made in the desired composition, and the mixture was admitted into the diffusion chamber, consisting of the tube G_2 and the vessel G_3. G_2 remained at room-temperature, while G_3 was heated or cooled. In consequence of this the pressure varied, and by means of one of the burettes the pressure was brought to its original atmospheric value. If the temperature gradient is steady the thermal diffusion is observable as a change of the refractive index n of the mixture, and can be calculated from the formula $\Delta n = z\lambda/l$, where z is the number of fringes which moved in homogeneous light of wave-length λ, and l the length of the tube (20 cm.). From Δn it is possible to calculate the new composition of the mixture when equilibrium is reached. According to the Biot-Arago formula the refractive power $n-1=\beta_3$ of the gas mixture is equal to the sum of the partial refractive powers β_1 and β_2 of each pure gas :

$$\beta_3 = \beta_1 \frac{\lambda_1}{100} + \beta_2 \frac{\lambda_2}{100},$$

where λ_1 and λ_2 are the proportions of the two gases in the mixture. The values of β_1 and β_2 are known, and therefore it is possible to calculate with the same formula the new composition of the mixture (λ_1' and λ_2') if $\beta_3' = [(n \pm \Delta n) - 1]$ of the new composition was found.

The separation in G_3, which could not be measured, must be calculated from the value for the separation in G_2.

The volumes of G_2 and G_3 were made equal, so it is only necessary to consider the ratio of the absolute temperatures on both sides. If $\Delta\lambda_c$ is the percentage separation on the cold side G_2, the total separation is $\Delta\Lambda = \Delta\lambda_c(1+T_2/T_1)$, while in the case of G_2 being the warmer side and G_3 cooled the formula is $\Delta\Lambda = \lambda_h(1-T_1/T_2)$.

Fig. 2.

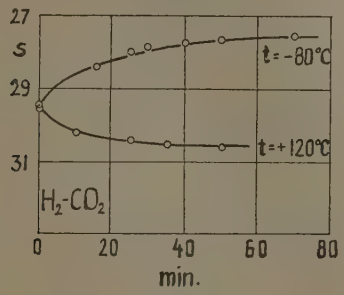

Fig. 3.

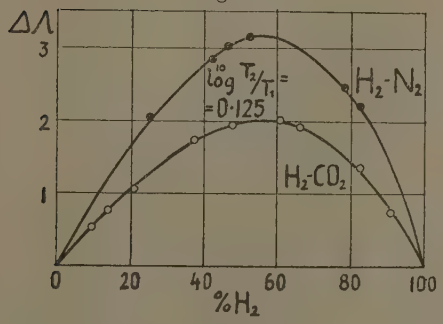

3. *Experimental Results.*

a. *Hydrogen-carbon dioxide mixtures.*—We first made measurements on mixtures of hydrogen and carbon dioxide at pressures of about 74 cm. of mercury. In all experiments the tube G_2 has been at room-temperature, while G_3 was cooled to $-80°$ C. or heated to 120° C. or 180° C. Fig. 2 shows for these mixtures the progressive separation with time; the steady state is reached in about 40 minutes (*s* denotes the scale of compensator). From the results of the experiments shown in fig. 3 it

will be seen that the total separation $\Delta\Lambda$ depends upon the percentage of hydrogen in the mixture. The relation between $\Delta\Lambda$ and $\log_{10} T_2/T_1$ is shown for two mixtures in fig. 4. It may be considered that the points for $T_2=120°$ C. and for $T_1=-80°$ C. (carbon dioxide snow

Fig. 4.

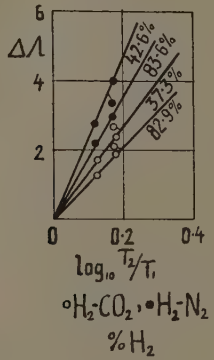

Fig. 5.

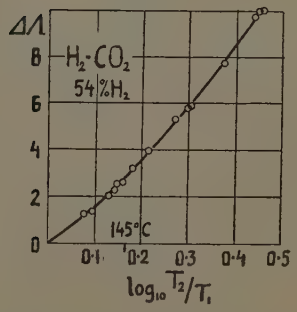

in toluene) can be connected by a straight line through the origin, while the point for $T_2=180°$ C. is situated above. Ibbs found an edge in the $\Delta\Lambda-\log_{10} T_2/T_1$ curve, and this appears to be supported by Lugg's * results. To test this we have made experiments with hydrogen-carbon dioxide mixtures with the higher

* J. W. H. Lugg, Phil. Mag. viii. p. 1019 (1929).

temperatures up to $T_2 = 587°$ C. The results in mixtures of about 54 per cent. H_2 are shown in fig. 5. In agreement with Ibbs and Lugg we find an increasing of the slope of the curve, but not a distinct edge at about 145° C. In fig. 6 is shown the dependence of k_t exp. upon the composition, and in the same diagram the relation between k_t exp. and k_t theor. calculated from the Chapman and Hainsworth formula. The ratio of these values, R_t, shows a small dependence upon the percentage of hydrogen.

Fig. 6.

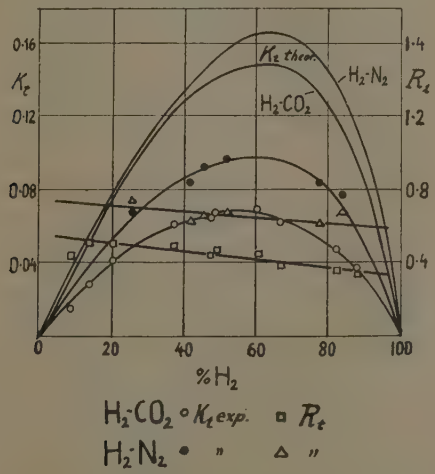

b. *Hydrogen-nitrogen mixtures.*—Using the same temperature-gradients experiments were made with hydrogen-nitrogen mixtures (see fig. 3). Fig. 4 shows the $\Delta\Lambda - \log_{10} T_2/T_1$ graph for two mixtures. There the points for the higher temperatures are in a straight line with the origin, but the point for $T_1 = -80°$ C. lies below the line. That indicates variations in k_t at low temperatures, which are yet easier to observe, if T_1 has been produced with help of liquid air (−180° C.). Also these results are in good agreement with those of Ibbs. Fig. 6 shows the dependence of k_t exp. upon the composition and the behaviour of R_t. There is again a small dependence of R_t upon the percentage of hydrogen in the mixture.

c. *Helium-argon Mixtures.*—These mixtures were observed only at high temperatures up to 352° C. The lower

Fig. 7.

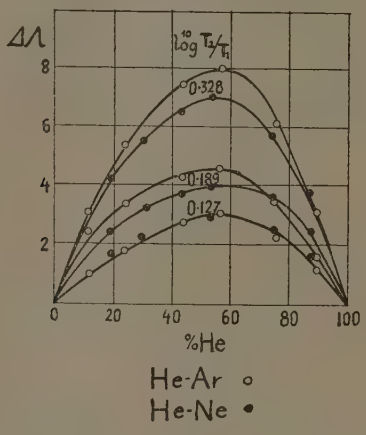

Fig. 8.

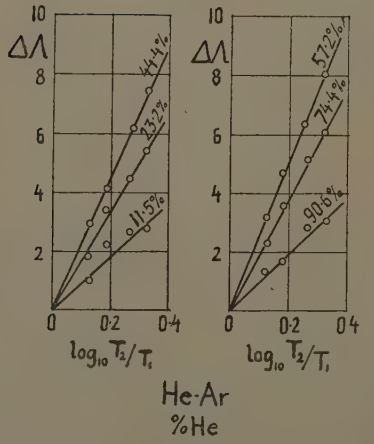

temperature was room-temperature. Fig. 7 shows the $\Delta\Lambda$—per cent. He graph for certain values of $\log_{10}T_2/T_1$. In fig. 8 are the $\Delta\Lambda$—$\log_{10}T_2/T_1$ graphs, which show

with some exceptions a good agreement with the demand of the theory, with a straight line joining the points. The calculated values of k_t and its dependence on the compo-

Fig. 9.

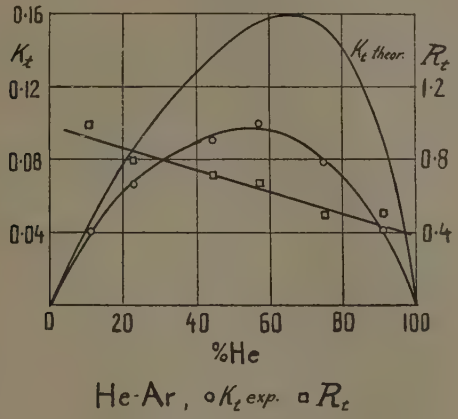

Fig. 10.

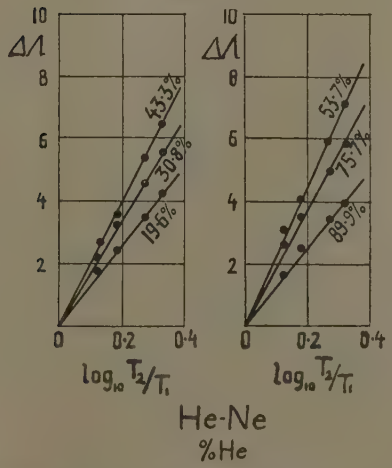

sition is shown in fig. 9. It also shows the relation of k_t exp. with kt theor. The values of R_t demonstrate a remarkable dependence upon the percentage of helium in the mixture.

d. Helium-neon mixtures.—Experiments were made with helium-neon mixtures under the same conditions. the diagrams for which are shown in figs. 7, 10, 11.

Fig. 11.

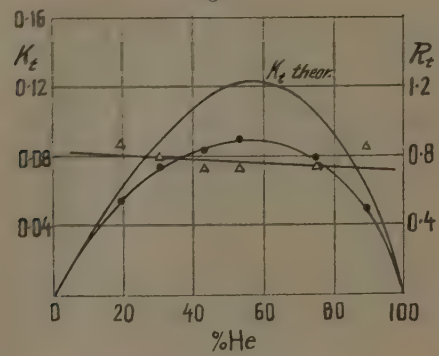

He-Ne, • K_t exp. △R_t

4. Discussion of Results.

The experiments generally show good agreement with the theory. The values of k_t exp. are in all cases rather smaller than the k_t theor., calculated from Chapman's formula. This means that the molecules of the gases in question are not rigid elastic spheres. On the other hand, the existence of the effect of thermal diffusion shows clearly that the exponent in the inverse power law for the repulsvie forces is greater than five. To calculate the value of q it is only possible to employ a formula which is strictly valid only for the case $m_1/m_2 = \infty$ and $\sigma_1/\sigma_2 = \infty$, where m_1 and m_2 are the masses and σ_1 and σ_2 the diameters of the molecules. The following approximate values of q are obtained from our experimental data, using Chapman's formula :—

Mixture.	T_3.	q.
H_2-CO_2	+100° C.	6·4
	+280	7·3
	+420	8·4
H_2-N_2	+180	10·0
He—Ar	+380	15·0
He—Ne	+380	10·5

For the hydrogen-carbon dioxide mixtures we note three values of q for three different temperatures. Ibbs believes that there is an edge in the curve at about 145° C., which also appears to be shown by Lugg's results, and he interprets Archer's * results on the thermal conductivity of carbon dioxide in the same sense. In his opinion the carbon dioxide molecule shows two types of field. hard about 145° C. and soft below that temperature. Our experiments give indications that the molecules become harder with increasing temperature, but apparently continuously. At lower temperatures the carbon dioxide molecules are quadrupoles corresponding with the heat of adsorption †, but at higher temperatures they seem to become temporary dipoles by the thermal impacts.

The molecules of nitrogen are much more rigid, and there we found q in good agreement with viscosity measurements (9.3). In comparing the rigidity of the nitrogen molecule with that of the molecule of carbon dioxide it is interesting to note that the total separations obtained with nitrogen-hydrgoen mixtures are greater than for carbon-dioxide-hydrogen mixtures of the same concentration, in spite of the fact that the ratio of molecular weights of the former pair is smaller ($N_2/H_2 = 14$, $CO_2/H_2 = 22$).

For the mixtures of the inert gases the mass-ratio of the molecules are still smaller (Ar/He = 10, Ne/He = 5); nevertheless the values of q are in good agreement with those of other authors. Simon and v. Simson ‡ studied the crystalline structure of solid argon, and calculated from the compressibility the index of repulsive force $q = 15$. The q-value we found for the helium-neon mixture is possibly small because of the unfavourable mass-ratio.

The dependence of R_t upon concentration, which is especially great for the helium-argon mixtures, is probably due to the fact that the coefficient of the ordinary diffusion changes with concentration; but the number of measurements in this direction is not sufficient to justify a discussion of the results.

* C. T. Archer, Phil. Mag. xix. p. 901 (1935); T. L. Ibbs, Phil. Mag. xxi. p. 508, Suppl. (1936).

† N. Stark & O. Blüh, *Physikal. Zeitschr.* xxviii. p. 502 (1927).

‡ F. Simon and Cl. v. Simson, *Zeitschr. f. Physik*, xxv. p. 160 (1924).

5. *Summary.*

By means of an interferometer method, which is described, thermal diffusion in gas mixtures (H_2-CO_2, H_2-N_2, He–Ar, He–Ne) was observed, and the effect found generally to agree with Ibbs's experiments. From the measured total separations the values of the indices of repulsive forces of the molecules were calculated according to Chapman's theory, and found to be in good agreement with the values obtained by other methods.

6. *Acknowledgement.*

We desire to express our thanks to Dr. T. L. Ibbs for many interesting discussions by letter, and for his kind help in connexion with the publication of this paper.

Prag.
July 5th, 1937.

XCVI. *Extensions of the new Family of Wing Profiles.* *By* R. W. Piper, *M.Sc.**

1. *Introduction.*

RECENT development † has established a convenient method of conformally transforming the flow past a circular boundary to that past aerofoils which closely resemble aeroplane wings. By suitable location of the two singular points the profiles can be varied in shape to meet aeronautical requirements. In this respect the method can be extended without great complication in two directions, one of which is immediately important, whilst the other may soon become so. These extensions are developed in the present paper. The new family of profiles has been shown to have a smaller travel of the centre of pressure with variation of incidence, or inclination of the section to the wind, than its predecessors. But to confine this travel within the very narrow limits desirable for weight economy in wing construction requires, as is well known, that the tail of the section be slightly

* Communicated by Dr. N. A. V. Piercy.

† Piercy, Piper, and Preston, "A new Family of Wing Profiles," Phil. Mag. vol. xxiv. Sept. 1937, p. 425. References to this paper are denoted by P.P.P.

reflexed. This is the first modification of shape studied. The second modification in view relates to the shape of the nose of the section. As far as may be judged, this part of the contour already accords closely with modern aeronautical practice. If aircraft speeds continue to increase, however, the compressibility of the fluid will cease to be negligible, and it may result from this or other causes that the shape of the nose now characterizing the family will become too blunt. Means for sharpening the nose are therefore investigated in later paragraphs of the paper.

Fig. 1.

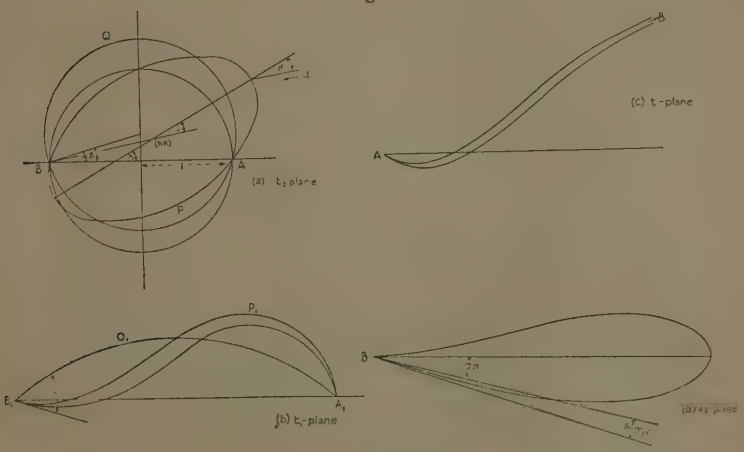

2.

Referring to the sequence of transformations developed in P.P.P., any simple closed continuous curve passing through suitably chosen singular points will transform into an aerofoil shape. The curve originally chosen was circular. In order to obtain a reflexed tail in the final profile, the circle is now replaced by the ellipse. Consequent changes are easily traced as follows.

With the notation of P.P.P., let A, B be the singular points on the unit circle in the t_2-plane. Let 0, tan $\frac{1}{2}\beta'$ be the centre of the circle AQB through A and B, which in the original paper was transformed into a cambered profile, and let this circle cut the ellipse ABP passing through A and B at an angle $\frac{1}{2}f$ at the point B (fig. 1 (*a*)).

Then as the first transformation $t_1=t_2+1/t_2$ maps the eccentric circle ABQ into the circular arc $A_1B_1Q_1$, so it maps the elliptic boundary into the curves $A_1B_1P_1$, shown in fig. 1 (*b*), the angle between the tangent to this curve at B_1 and B_1A_1 being f. Inversion with respect to B by the second transformation $t(t_1+2)=\lambda$ (P.P.P.(25)) gives the curve shown in fig. 1 (*c*), where at infinity the curves make angle f with the real axis. In this plane

$$t=p+iq=\epsilon'+i\delta'+\cosh\frac{w-i\sigma\pi}{1-\sigma} \quad \text{(P.P.P. (19))}$$

Hence

$$\tan f=q/p \ (\lim p \rightarrow \infty)$$

$$= \frac{\sinh\dfrac{u}{1-\sigma}\sin\dfrac{v-\sigma\pi}{1-\sigma}}{\cosh\dfrac{u}{1-\sigma}\cos\dfrac{v-\sigma\pi}{1-\sigma}} \qquad \lim|u| \rightarrow \infty$$

$$= \tan\frac{v-\sigma\pi}{1-\sigma} \qquad \text{as } u \rightarrow +\infty$$

$$= -\tan\frac{v-\sigma\pi}{1-\sigma} \quad \text{as } u \rightarrow -\infty .$$

Thus $v=\sigma\pi\pm(1-\sigma)f$, according as u (large) is positive or negative. In the plane of the hyperbola (the z_1-plane of P.P.P., fig. 1), the curve corresponding to the ellipse is therefore parallel at infinity to the lines $\dfrac{y}{x}=\sigma\pi\pm(1-\sigma)f$.

The tail-angle of the aerofoil, equal to the angle between the asymptotes in the hyperbola plane, is still $2\sigma\pi$, but is turned through an angle $(1-\sigma)f$ (fig. 1 (*d*)). The angle f in the t_2-plane is a measure, therefore, of the amount of reflexure of the tail of the profile.

3. *Mapping the Profile.*

To regard the circle as the limiting case of the ellipse presents difficulties in complex variable analysis, the degeneration of the ellipse $x+iy=C\cosh(\xi+i\eta)$, $\xi=\xi_0$ into a circle involving the limits $C \rightarrow 0$, $\xi=\xi_0 \rightarrow \infty$. For this reason circular functions were necessary in P.P.P. despite the frequent use of elliptic coordinates in the transformations. Clearly in the present application,

however, it is convenient to recast the analysis and use elliptic coordinates throughout. We take

$$t_2=h+ik+Ce^{i\lambda}\cosh(\xi_0+i\eta) \quad . \quad . \quad . \quad (1)$$

as the general equation of an ellipse in the t_2-plane, and we assume that the constants are adjusted so that it passes through A and B, the singular points of the unit circle $|t_2|=1$. We take η_1, η_2 as the eccentric angles of A and B respectively; then with the notation of fig. 1 (*a*)

$$\left.\begin{aligned}\tan j&=-\tanh\xi_0\tan\eta_2,\\ \tan(\lambda-j)&=\frac{k}{1+h}.\end{aligned}\right\} \quad . \quad . \quad . \quad (2)$$

As before, the circle which maps into the cambered profile with tail-angle $2\sigma\pi$ in P.P.P. has its centre at 0, $\tan\frac{1}{2}\beta'$.

The transformations (P.P.P. (19), (21), (22))

$$t_1=t_2+1/t_2,$$
$$t(t_1+2)=4(1-\cosh p_c),$$
$$t=-\cosh p_c+\cosh\frac{w-i\sigma\pi}{1-\sigma},$$

where

$$p_c=\frac{w_c-i\sigma\pi}{1-\sigma}, \quad w_c=u_c+iv_c \quad \text{(P.P.P. (20), (17))}$$

give

$$\cosh\frac{w-i\sigma\pi}{1-\sigma}-1=(\cosh p_c-1)\left(\frac{t_2-1}{t_2+1}\right)^2.$$

Hence

$$\sinh\frac{w-i\sigma\pi}{2(1-\sigma)}=\sinh\tfrac{1}{2}p_c\left(\frac{t_2-1}{t_2+1}\right), \quad . \quad . \quad . \quad (3)$$

there being no ambiguity of sign since the upper parts of the ellipse and profile boundaries correspond.

By using tables of hyperbolic functions of complex arguments, equation (3) is readily solved for w in terms of η for points on the boundary. Or, alternatively, let

$$\sinh\frac{w-i\sigma\pi}{2(1-\sigma)}=[(1+\epsilon')\sec\beta']^{\frac{1}{2}}e^{\frac{1}{2}i\beta'}\frac{t_2-1}{t_2+1}=R_1e^{i\theta_1},$$

$$\cosh^2\frac{w-i\sigma\pi}{2(1-\sigma)}=1+R_1^2e^{2i\theta_1}=R_2^2e^{2i\theta_2}.$$

Then

$$\left.\begin{aligned} e^{\frac{\mu}{1-\sigma}} &= R_1^2+R_2^2+2R_1R_2\cos(\theta_1-\theta_2), \\ \tan\frac{v-\sigma\pi}{2(1-\sigma)} &= \frac{R_1\sin\theta_1+R_2\sin\theta_2}{R_1\cos\theta_1+R_2\cos\theta_2}, \end{aligned}\right\} \quad . \quad (4)$$

where

$$R_2^4=1+R_1^4+2R_1^2\cos 2\theta_1,$$

$$\tan 2\theta_2=\frac{R_1^2\sin 2\theta_1}{1+R_1^2\cos 2\theta_1}$$

and

$$R_1^2=(1+\epsilon')\sec\beta'\frac{\sin^2(\eta-\eta_1)}{\sin^2(\eta-\eta_2)}\cdot\frac{\cosh 2\xi_0-\cos(\eta+\eta_1)}{\cosh 2\xi_0-\cos(\eta+\eta_2)},$$

$$\tan(\theta_1-\tfrac{1}{2}\beta')=\frac{\sinh 2\xi_0\sin\frac{1}{2}(\eta_1-\eta_2)}{\cosh 2\xi_0\cos\frac{1}{2}(\eta_1-\eta_2)-\cos(\eta+\frac{1}{2}\eta_1+\frac{1}{2}\eta_2)}.$$

Using the values of u and v given by (4) and the formulæ P.P.P. (36), (38), the profile can be plotted.

4. *S-symmetrical Profiles.*

Cases in which $h=k=0$ and $\beta'=0$ (and therefore $u_c+iv_c=i\pi$) are described, for short, as S-symmetrical profiles. The analysis is particularly simple in their case, as follows :—

Equation (2) with $u_c+iv_c=i\pi$ becomes

$$\sinh\frac{w-i\sigma\pi}{2(1-\sigma)}=\frac{it_2-1}{t_2+1},$$

or

$$\sin\frac{iw+\sigma\pi}{2(1-\sigma)}=\frac{1-t_2}{1+t_2}=\cos\frac{\pi}{2}-\frac{iw+\sigma\pi}{2(1-\sigma)} \quad . \quad (5)$$

Hence

$$\left.\begin{aligned} t_2 &= \tan^2\frac{\pi(1-2\sigma)-iw}{4(1-\sigma)} \\ &= Ce^{i\lambda}\cosh(\xi_0+i\eta) \\ &= R^2e^{2i\theta}, \end{aligned}\right\} \quad . \quad . \quad . \quad . \quad . \quad (6)$$

where

$$R^4=\tfrac{1}{2}C^2(\cosh 2\xi_0+\cos 2\eta),$$

$$\tan(2\theta-\lambda)=\tan\eta\tanh\xi_0.$$

From (6)

$$\tan\frac{(1-2\sigma)\pi+v-iu}{4(1-\sigma)}=\mathrm{R}e^{i\theta}$$

(θ being a discontinuous function of η at B),

and this leads to

$$\left.\begin{aligned}\tan\frac{\pi(1-2\sigma)+v}{2(1-\sigma)}&=\frac{2\mathrm{R}\cos\theta}{1-\mathrm{R}^2},\\ \tanh\frac{u}{2(1-\sigma)}&=\frac{-2\mathrm{R}\sin\theta}{1+\mathrm{R}^2}.\end{aligned}\right\}\quad\ldots\quad(7)$$

u and v can now be calculated readily for specified points on the ellipse, and the profile at once follows from equations P.P.P. (36), (38). Fig. 2 shows the profile obtained by taking $\sigma=1/18$ and $f=5°$.

Fig. 2.

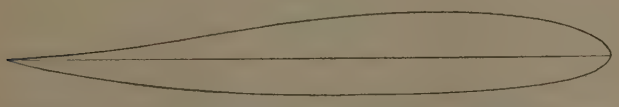

S-symmetrical section, with $\sigma=1/18$, $\lambda=\pi/4$, $f=5°$, and $\mathrm{K}_{m_0}=0{\cdot}0021$. *Cf.* cambered section (P.P.P., fig. 4*a*) with $\sigma=1/18$, $\mathrm{K}_{m_0}=0{\cdot}034$.

5. *Flow past the Aerofoil.*

It is known that the two-dimensional flow past a cylinder of elliptic section, $\xi=\xi_0$, about which is a circulation K, is given by the complex potential

$$\mathrm{W}=\phi+i\psi=-\mathrm{CU}'e^{\xi_0}\cosh(\zeta-\zeta_0)-\frac{i\mathrm{K}}{2\pi}(\zeta-\zeta_0),\quad(8)$$

where $\zeta=\xi+i\eta$, $\zeta_0=\xi_0+i\eta_0$, and U′ is the velocity, $\eta_0=\alpha$ the inclination to the major axis of the section, of the flow at infinity. In order to calculate velocities and pressures at points on the boundary of the profile, it is necessary to evaluate

$$\left|\frac{d\mathrm{W}}{dz_2}\right|=\left|\frac{d\mathrm{W}}{dt_2}\right|\left|\frac{dt_2}{dw}\right|\left|\frac{dw}{dz_2}\right|\quad\text{for }\xi=\xi_0.$$

From (8)

$$\frac{d\mathrm{W}}{dt_2}=-\left(\mathrm{CU}'e^{\xi_0}\sinh(\zeta-\zeta_0)+\frac{i\mathrm{K}}{2\pi}\right)\Big/\mathrm{C}e^{i\lambda}\sinh\zeta,$$

where K is usually determined by Joukowski's hypothesis, viz., that B is a stagnation point in the t_2-plane.

This gives

$$K = -CU' 2\pi e^{\xi_0} \sin(\eta_2 - \alpha), \quad . \quad . \quad . \quad (9)$$

and then

$$\left|\frac{dW}{dt_2}\right|_{\xi=\xi_0} = U' e^{\xi_0} \left| \frac{\sin(\eta-\eta_0) - \sin(\eta_2-\eta_0)}{(\sinh^2\xi_0 + \sin^2\eta)^{\frac{1}{2}}} \right|. \quad (10)$$

From (3)

$$\frac{1}{2(1-\sigma)} \cosh \frac{w - i\sigma\pi}{2(1-\sigma)} \frac{dw}{dt_2}$$

$$= 2 \sinh \tfrac{1}{2} p \frac{1}{(t_2+1)^2}$$

$$= 2 \sinh \tfrac{1}{2} p_c \frac{1}{C^2 e^{2i\lambda} [\cosh(\xi_0 + i\eta) - \cosh(\xi_0 + i\eta_2)]^2}$$

$$= \frac{\sinh \frac{1}{2} p_c}{2C^2 e^{2i\lambda} \left[\sinh\left(\xi_0 + \frac{i}{2}(\eta+\eta_2)\right) \sin(\eta-\eta_2) \right]^2}.$$

Hence

$$\left|\frac{dt_2}{dw}\right| = \frac{C^2 \left| \cosh \frac{w - i\sigma\pi}{2(1-\sigma)} \right| \sin^2(\eta-\eta_2)(\sinh^2\xi_0 + \sin^2\tfrac{1}{2}(\eta+\eta_2))}{(1-\sigma) \left| \sinh \frac{1}{2} p_c \right|}.$$

$$. \quad . \quad . \quad (11)$$

From P.P.P. (16)

$$\left|\frac{dw}{dz_2}\right| = \frac{1}{x_2^2 + y_2^2} \left| \operatorname{cosech} w \right|.$$

Thus the velocities and the pressures may be calculated.

6. *Pitching Moment.*

To calculate the pitching moment of the wing it is necessary to evaluate the complex integral $\oint \left(\frac{dW}{dz}\right)^2 z\, dz$, taken round a closed contour entirely surrounding the profile.

Now

$$\frac{dW}{dt_2} = -\left(CU' e^{\xi_0} \sinh(\zeta - \zeta_0) + \frac{iK}{2\pi} \right) \Big/ Ce^{i\lambda} \sinh \zeta.$$

When the lift is zero, K=0, i. e. $\alpha=\eta_2-\pi$, and we have

$$\left(\frac{dW}{dt^2}\right)^2 = U'^2 e^{2\xi_0-2i\lambda}(\cosh^2\zeta_0+\sinh^2\zeta_0\coth\zeta - 2\cosh\zeta_0\sinh\zeta_0\coth\zeta)$$

$$= U'^2 e^{2\xi_0-2i\lambda}\left(\cosh^2\zeta_0+\sinh^2\zeta_0\left(1+\frac{C^2e^{2i\lambda}}{t_2^2}\right)^{-1} - \sinh 2\zeta_0\left(1+\frac{C^2e^{2i\lambda}}{t_2^2}\right)^{-\frac{1}{2}}\right)$$

$$= A_0+\frac{A_1}{t_2}+\frac{A_2}{t_2^2}+\ldots,$$

where

$$\left.\begin{aligned} A_0 &= U'^2 e^{-2i(\lambda+\alpha)},\\ A_1 &= 0,\\ A_2 &= \frac{U'^2C^2}{2}(e^{2\xi_0}-e^{-2i\alpha}),\end{aligned}\right\} \quad \ldots\ldots \quad (12)$$

In P.P.P. (31), (58) it was shown that if

$$z_2 = a_0 t_2 + a_1 + \frac{a_2}{t_2}+\ldots,$$

the pitching moment M_0 is given by

$$M_0 = \rho\pi I.P.\left(2A_0\frac{a_2}{a_0}+A_1\frac{a_1}{a_0}+A_2\right),$$

where

$$\frac{a_2}{a_0} = 1+\frac{(1-\cosh p_c)^2}{4\sinh^2 p_c}\left\{(1-\sigma)^2\left(\frac{1}{3}+\frac{1}{\sinh^2 w_c}\right) - \left(\frac{1}{3}+\frac{1}{\sinh^2 p_c}\right)\right\}.$$

Using the values of A_0, A_1, A_2 given in (12), since the first part of A_2 is wholly real, we get

$$M_0 = -\pi\rho U'^2 I.P.\left\{\frac{a_2}{a_0}e^{-2i(\lambda+\alpha)}-\frac{C^2}{2}e^{-2i\alpha}\right\}. \quad (13)$$

For a specified σ and u_c+iv_c, the factor $\frac{a_2}{a_0}$ is constant, and when once it is evaluated in prescribed circumstances (for a chosen λ, say) the equation $M_0=0$ in ξ_0 may be

solved graphically. Thus may be obtained cambered sections with a stationary centre of pressure.

Referring to the S-symmetrical aerofoils of § 4, we have for this type

$$\frac{a_2}{a_0} = 1 + \frac{16}{\sinh^2 p_c}\left\{(1-\sigma)^2\left(\frac{1}{3} + \frac{1}{\sinh^2 w_c}\right) - \left(\frac{1}{3} + \frac{1}{\sinh^2 p_c}\right)\right\},$$

when $w_c \rightarrow i\pi$ and $p_c \rightarrow i\pi$.
This is readily evaluated to

$$1 + \frac{16}{15}\{(1-\sigma)^4 - 1\},$$

whence the pitching moment at once follows as

$$M_0 = \rho\pi U'^2\left\{-\left[1 + \frac{16}{15}((1-\sigma)^4 - 1)\right]\sin(2\lambda + 2\alpha) + \frac{C^2}{2}\sin 2\alpha\right\}. \quad (14)$$

With the condition that the ellipse passes through B,

$$\frac{\cos^2\lambda}{\cosh^2\xi_0} + \frac{\sin^2\lambda}{\sinh^2\xi_0} = C^2$$

and (2),

$$\tan\eta_2 = \tan\alpha = -\coth\xi_0 \tan\lambda,$$

M_0 is a function of ξ_0 and λ for a specified σ, and vanishes when $\tanh\xi_0$ and $\tan\lambda$ satisfy

$$t^4 - At^3 - (1-A)(1-\tan^2\lambda)t^2 + A\tan^2\lambda \,.\, t - \tan^2\lambda = 0,$$

where

$$t = \tanh\xi_0 \quad \text{and} \quad \tfrac{1}{2}A = \frac{a_2}{a_0} = 1 + \frac{16}{15}((1-\sigma)^4 - 1).$$

Thus with an arbitrary value of λ, ξ_0 can be chosen to yield a profile with a stationary centre of pressure.

Increase of Curvature at the Nose.

7. *Direct Method.*

The curvature near the nose of the new wing profile, whether derived from a circle or an ellipse, can be varied by two alternative methods. In the first method, now

to be described, the modification is obtained by a suitable choice of position of the centre of inversion.

The circle of curvature of the nose of the profile is the inverse of the circle of curvature of the vertex of the boundary curve in the hyperbola plane. To fix ideas we shall suppose that the curve is a hyperbola and the aerofoil is then not reflexed at the tail. Thus, if we denote their respective radii by ρ and R, and the camber be small,

$$(c-2\rho)\left(\frac{1}{c}+2\mathrm{R}\right)=1,$$

where c is the chord of the aerofoil (P.P.P.(8)), whence

$$\frac{c}{\rho}=\frac{1}{c\mathrm{R}}+2. \quad . \quad . \quad . \quad . \quad . \quad . \quad . \quad (15)$$

For a given tail-angle R is constant and the non-dimensional quantity ρ/c becomes smaller, and the nose of the profile becomes sharper, as $1/c=\mathrm{CA}=(\epsilon+\cos\sigma\pi)/\cos\beta$ (P.P.P. (8)) increases. Since the constants β and σ are determined by the camber and tail-angle of the section respectively, ϵ can now be determined from (15) to give an arbitrary value to ρ/c, so that, by this method, a profile with specified camber, tail-angle and curvature at the nose, can be plotted.

In P.P.P., § 4 *b*, it is shown that, in the case of a thin symmetrical aerofoil, the position of the maximum ordinate moves towards the tail as ϵ increases. There is also no difficulty in showing that, in the case of thin symmetrical aerofoils, the fineness ratio increases with ϵ; for with the notation of P.P.P.

$$y_2=\frac{-y_1}{x_1^2+y_1^2}\triangleq-\frac{y_1}{x_1^2} \quad \text{for a thin section,}$$

$$\triangleq\frac{-\sin\sigma\pi\left[\left(\frac{x_1-\epsilon}{\cos\sigma\pi}\right)^2-1\right]^{\frac{1}{2}}}{x_1^2};$$

hence

$$\text{max.}\ \frac{y_2}{c\sin\sigma\pi}\triangleq\frac{2(1+\epsilon)[(\epsilon+\sqrt{\epsilon^2+8})^2-4]^{\frac{1}{2}}}{(3\epsilon+\sqrt{\epsilon^2+8})^2}.$$

provided σ is small.

The graph (fig. 3) shows the variation of $\dfrac{y_2}{c\sin\sigma\pi}$ and $\dfrac{x^2}{c}$,

and the decrease in the radius of curvature, with ϵ, for a constant small value of the tail angle.

TABLE I.

ϵ.	1.	2.	3.	5.	8.
max. $y_2/c \sin \sigma\pi$..	·385	·340	·317	·294	·279
ρ/cR	·500	·333	·250	·167	·111
x_2/c	·667	·634	·613	·578	·554

From fig. 3 it is evident that the movement of the centre of inversion produces a sharp variation in the curvature of the nose, accompanied by only slight variations in the position and magnitude of the maximum ordinate.

Fig. 3.

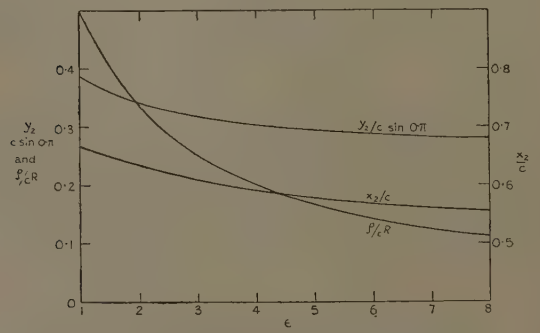

Variation of position of maximum thickness, fineness ratio, and curvature of nose with ϵ, $\beta=0$.

8.

Thinning the nose of the section can, alternatively, be accomplished without moving the centre of inversion by suitably modifying the curve in the z_1-plane from a hyperbola. This is most simply done by applying a Joukowski transformation with respect to a circle lying entirely within the hyperbola and with the singular

points on the real axis. If this circle is near to the nose, and hence small, the effect of the transformation is concentrated at the nose both in the hyperbola plane and in the plane of the section. The thinning is then localized and a large change in the curvature will result in concavities in the aerofoil profile. However, such exaggeration is readily avoided if the centre of curvature of the vertex of the hyperbola be taken as centre of the circle, and ρ', its radius, be ascribed a fraction (less than $\frac{1}{2}$) of the radius of curvature in the hyperbola plane; the Joukowski circle will then give a profile free from undesired concavities, with the curvature at the nose increased up to twice its normal amount (fig. 4).

Fig. 4.

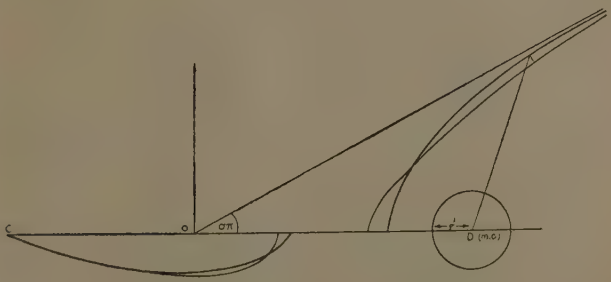

Using Trefftz's geometrical construction or a linkage for the Joukowski transformation, the profile may still be plotted graphically or mechanically from a hyperbola.

In order to calculate pressures, pitching moments, and other details, however, we may proceed analytically as follows. Equation P.P.P. (6) must be modified to

$$\frac{e^{i\beta}}{z_2} = z_1{}^1 = z_1 + \frac{\rho'^2}{z_1 - \epsilon - i\delta - m},$$

where $(m, 0)$ are the coordinates of D, the centre of the circle in the z_1-plane, with corresponding alterations to all results depending on this equation.

Fig. 5 shows in detail the nose of a normal P.P.P. symmetrical profile, $\sigma = 1/18$, together with the nose of the corresponding profile obtained by using this additional transformation.

Comparing the methods of §§ 7 and 8; from the first method results an aerofoil section with a nose sharpened to any desired extent, and with a slightly larger fineness ratio. The analysis remains essentially unchanged. The second method gives a section in which only the nose is modified, being sharpened to a limited, but adequate, extent. Here the analysis involves one additional transformation.

Fig. 5.

Normal and sharpened nose of symmetrical profile: $\sigma = 1/18$, $\epsilon = 1$.

9. *Summary.*

In this paper the use of the transformations of "A new Family of Wing Profiles" has been extended, (*a*) to reflex the tail of the aerofoil and so restrict or eliminate the travel of its centre of pressure; (*b*) to produce a section with an arbitrarily sharpened nose. The extensions developed separately, for simplicity, are not mutually exclusive, and may be combined, if desired, to give a cambered profile with a stationary centre of pressure and an arbitrarily sharpened nose.

The writer has pleasure in acknowledging the interest and advice of Dr. N. A. V. Piercy in the preparation of this paper.

XCVII. *The Two-dimensional "Ice-pail."*

By E. P. Adams, *Princeton, New Jersey* *.

THE problem of the electrification of a freely charged two-dimensional "ice-pail" was solved by Prof. Morton and Miss Macdonald † by transforming the z-plane of the conductor into the interior of a circle in a w-plane by Schwarz's method. In order to get numerical results by this method it was necessary to use mechanical quadrature, and there was difficulty when the ratio of the lengths of the sides to the base was greater than about 0·6. If advantage be taken of the

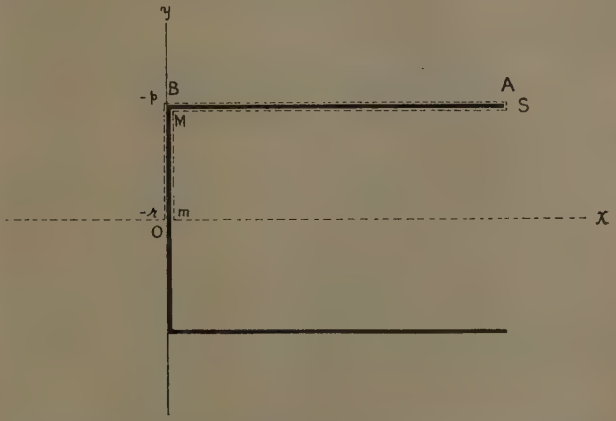

symmetry of the conductor and half the z-plane be transformed to the upper half of the t-plane by the method of Schwarz-Christoffel, the problem may be solved with the aid of elliptic functions, and numerical results obtained for any values of the ratio of the lengths of the sides to the base.

The interior of the polygon, enclosed within the dotted lines in the accompanying figure, is transformed to the upper half of the t-plane by means of the equation

$$\frac{dz}{dt} = \mathrm{A}\,\frac{(t+p)^{\frac{1}{2}}(t-s)}{(t+r.t-n.t-m)^{\frac{1}{2}}},$$

* Communicated by the Author.

† Phil. Mag. viii. p. 761 (1929).

where

$$-\infty < -r < -p < s < n < m < +\infty ,$$

and $z=\infty$, $t=\infty$ are corresponding points. This equation may be solved with the aid of the substitution

$$t = \frac{\operatorname{sn}\lambda}{1-k\operatorname{sn}\delta\operatorname{sn}\lambda},$$

where δ is real and lies between $-\mathrm{K}$ and $+\mathrm{K}$, K being the complete elliptic integral, to the modulus k, of the first kind. With corresponding values given by

$t=$	$-r$	$-p$	n	m	∞	$s,$
$\lambda=$	$-\mathrm{K}+i\mathrm{K}'$	$-\mathrm{K}$	K	$\mathrm{K}+i\mathrm{K}'$	$i\mathrm{K}'+\delta$	$u_0,$
$z=$	0	ib	ib	0	∞	$a+ib,$

the solution is found to be

$$\mathrm{Z} = \frac{2\mathrm{K}b}{\pi}\left\{ Z(\lambda) - \frac{k\operatorname{sn}\delta\operatorname{cn}\lambda\operatorname{dn}\lambda}{1-k\operatorname{sn}\delta\operatorname{sn}\lambda}\right\} + ib,$$

together with

$$1+k\operatorname{sn}\delta = \frac{\mathrm{K}k'^2}{\mathrm{E}},$$

and

$$s = \frac{1+k\operatorname{sn}\delta}{k^2\operatorname{cn}^2\delta\operatorname{dn}^2\delta}\left(\operatorname{dn}^2\delta - \frac{\mathrm{E}}{\mathrm{K}}\right).$$

The ratio of the lengths of the sides, AB$=a$, to the base, 2BO$=2b$, is given by

$$\frac{a}{2b} = \frac{\mathrm{K}}{\pi}\left\{ \mathrm{Z}(u_0) - \frac{k\operatorname{sn}\delta\operatorname{cn}u_0\operatorname{dn}u_0}{1-k\operatorname{sn}\delta\operatorname{sn}u_0}\right\}.$$

Z is Jacobi's zeta function, and u_0 is the real value of λ, lying between $-\mathrm{K}$ and $+\mathrm{K}$, that corresponds to the edge A. u_0 is given by

$$\operatorname{sn}u_0 = \frac{s}{1+sk\operatorname{sn}\delta}.$$

For large values of the ratio $a/2b$ the modular angle is large. Up to modular angles of 89° tables of elliptic functions may be used to calculate this ratio. For larger values of the modular angle the approximate value of this ratio is given by

$$\frac{a}{2b} = \frac{\mathrm{K}}{\pi}\left\{ \frac{u_0}{\mathrm{K}} + \frac{2(\mathrm{K}-1)}{2\mathrm{K}-1}\right\},$$

where

$$u_0 = \frac{1}{2M} \log \frac{2}{Kk'^2(4K-3)},$$

and

$$M = \log e.$$

For values of the complementary modulus, k', less than 10^{-3}, we may use the approximation

$$\log K = \log \log 4/K' + 0{\cdot}3622157.$$

The logarithms are all to the base 10.

If the complex potential be taken as

$$\chi = \phi + i\psi,$$

ϕ being the real potential, the χ-plane for the freely charged conductor is transformed to the t-plane by means of the equation

$$\frac{d\chi}{dt} = -\frac{2Q}{(t+r.t-m)^{\frac{1}{2}}},$$

where Q is the charge on unit length of the conductor. The solution of this equation that satisfies the conditions

$$\chi = 0 \text{ for } t = -r,$$

$$\chi = 2\pi i Q \text{ for } t = m,$$

taking the potential of the conductor as 0, is

$$\chi = 2\pi i Q - 4iQ \sin^{-1}\left(\frac{m-t}{m+r}\right)^{\frac{1}{2}}.$$

If we take

Q_1 = charge on inside of the bottom,
Q_2 = charge on inside of the sides,
Q_3 = charge on outside of the sides,
Q_4 = charge on outside of the bottom,

so that

$$Q = Q_1 + Q_2 + Q_3 + Q_4,$$

we find

$$\pi Q_1/2Q = \phi_1,$$

$$\pi Q_2/2Q = (\phi_2 - \phi_1),$$

$$\pi Q_3/2Q = (\phi_3 - \phi_2),$$

$$\pi Q_4/2Q = \left(\frac{\pi}{2} - \phi_3\right),$$

where

$$\sin\phi_1=\left\{\frac{1-k.1+\operatorname{sn}\delta}{2(1-k\operatorname{sn}\delta)}\right\}^{\frac{1}{2}},$$

$$\sin\phi_2=\left\{\frac{\frac{E}{K}(1+k\operatorname{sn}\delta)-(1-k)\operatorname{dn}^2\delta}{2k\operatorname{dn}^2\delta}\right\}^{\frac{1}{2}},$$

$$\sin\phi_3=\left\{\frac{1+k.1+\operatorname{sn}\delta}{2(1+k\operatorname{sn}\delta)}\right\}^{\frac{1}{2}}.$$

For large values of the modular angle the approximate values of ϕ_1, ϕ_2, and ϕ_3 are given by

$$\sin\phi_1=\frac{k'^2}{4}(2K-1)^{\frac{1}{2}},$$

$$\sin\phi_2=\left(\frac{1}{4K}\right)^{\frac{1}{2}},$$

$$\sin\phi_3=\left(\frac{2K-1}{2K}\right)^{\frac{1}{2}}.$$

The distribution of the charges on the four surfaces is shown in the following two tables. The calculations

TABLE I.

θ.	$a/2b$.	Q_1/Q.	Q_2/Q.	Q_3/Q.	Q_4/Q.
0	0	·5	0	0	·5
45°	·2039	·1602	·1228	·3424	·3746
70° 33·4′ ..	·6026	·0370	·1713	·4941	·2976
85°	1·3189	·0031	·1615	·5998	·2356
89°	2·2251	·0002	·1374	·6662	·1962

TABLE II.

θ.	$a/2b$.	Q_1/Q.	Q_2/Q.	Q_3/Q.	Q_4/Q.
89°	2·2178	·0002	·1375	·6661	·1962
89·5°	2·6199	·0000	·1295	·6860	·1845
89·9°	3·5688	·0000	·1151	·7213	·1636
$k'=10^{-3}$ ...	3·9009	·0000	·1109	·7312	·1579
$k'=10^{-4}$ ...	5·2877	·0000	·0982	·7624	·1394
$k'=10^{-12}$ ..	16·739	·0000	·0592	·8570	·0838

for the first table were made with the aid of Legendre's and the Smithsonian Tables of Elliptic Functions. For

a modular angle of approximately 70° 33·4′ the value of s is zero, and it becomes negative for larger angles. This modular angle corresponds to the maximum of the charge on the inside surfaces of the sides of the conductor. The calculations for the second table were made by using the approximate values that have been given for large modular angles. The first column gives the modular angle or the complementary modulus, k'.

If the conductor be placed in a uniform electric field parallel to the sides the complex potential is given as the solution of the equation

$$\frac{d\chi}{dt} = \frac{C(t-s')}{(t+r.t-m)^{\frac{1}{2}}},$$

that satisfies the conditions

$$\chi=0 \text{ for } t=m \text{ and } t=-r.$$

The potential of the conductor is taken as 0, and $t=s'$ corresponds to the point of equilibrium. The solution is found to be

$$\chi=iC(t+r\,.\,t-m)^{\frac{1}{2}}$$

with

$$s'=\frac{m-r}{2}=\frac{2\,\mathrm{sn}\,\delta}{k\,\mathrm{cn}^2\,\delta}.$$

The constant C must be determined so that at infinity the potential shall be

$$\phi=-Fx+\text{const.}$$

for a uniform field of intensity F in the direction of the x-axis. We therefore find

$$C=-\frac{2FKkb}{\pi}\,\mathrm{cn}\,\delta\,\mathrm{dn}\,\delta.$$

The charges induced on the four surfaces of the conductor may be found by dividing the differences of the values of ψ at the points $t=m,\ n,\ s,\ -p,\ -r$ by 2π. The point of equilibrium, $t=s'$, always lies upon the outer surface of the side of the conductor.

For a uniform field parallel to the y-axis the complex potential is given by

$$\chi=-iCt.$$

The value of C, determined so that the potential at infinity shall be

$$\phi = -Fy + \text{const.}$$

is given by the same expression as that for the field parallel to the x-axis.

XCVIII. *Notices respecting New Books.*

Engineering Mechanics. Statics and Dynamics. Two vols. By Professors S. Timoshenko and D. H. Young. [Statics : pp. xiv+334 ; Dynamics : pp. xii+323.] (McGraw-Hill Publishing Co., Ltd. Price 15*s*.)

SINCE the present trend of engineering industry requires the engineer to be increasingly scientific, engineering students will welcome these two books, as they are more than conventional treatises on Statics and Dynamics. The authors have emphasized the importance of fundamental principles in the study of mechanics, and have devoted very special attention to the application of such principles to a large number of varied and practical engineering problems. Many of the topics considered may be found in one or other of the now numerous books on mechanics, but the arrangement and contents differ from those in elementary textbooks. Thus in the volume on Statics the laws of friction are presented in the first chapter and are then applied in problems throughout the book ; the theory of statically determinate trusses is discussed, with the object of establishing a closer connexion between theoretical statics and its applications in the theory of structures, while in the end of the volume the principle of virtual displacements is given for the solution of certain types of problems in statics. In the volume on Dynamics it is gratifying to find that the authors have included several articles dealing with the important subject of vibration. Problems of torsional vibration are of great practical importance and, as the authors indicate, an elementary course in dynamics should now include an introduction to vibration problems in engineering.

The books are intended for readers with no extensive knowledge of advanced mathematics, and a clear exposition is obtained by full explanation of the various steps in the detailed treatment. The value of the books is much enhanced by copious illustrative problems, together with an excellent selection of instructive problems at the end of each chapter.

A very high standard of logical sequence is maintained in the two books and, on the whole, the authors have achieved their object with conspicuous success. The books can be strongly recommended to both engineering and mathematical students.

Atomic Structure of Minerals. By W. L. Bragg. [Pp. xiii+ 292.] (Published by Humphrey Milford, Oxford University Press, 1937. Price 18*s.* net.)

This is a book of first-rate importance which is likely to remain a standard work for many years. Professor W. L. Bragg was the first to apply Laue's discovery of X-ray diffraction to the analysis of crystal structures. In the subsequent development of methods of analysis, and also in their application to more and more complex structures, the work of W. L. Bragg and his co-workers in Manchester has been of the greatest importance. In particular their work on the silicates, which occupies a large part of the present book, is of outstanding interest. The complexity of the structures of these substances makes it exceedingly difficult for those who are not specialists in crystal analysis to appreciate the significance of the results obtained. To chemists and mineralogists this book will be specially welcome, for the X-ray results have largely revolutionized the earlier chemical views of the atomic structures of the silicates, and, as Professor Bragg says in his preface, the generalizations which have been established may be useful to mineralogists in coordinating their intimate knowledge of the vast variety of forms displayed by natural minerals. The book is complete in itself, and presupposes no previous knowledge of X-ray methods or results on the part of the reader. In three short preliminary chapters a brief account is given of the methods of crystal analysis, the geometry of crystal lattices and the general principles of mineral structures. We then come to the main part of the book, pp. 43–272, giving the results which have been obtained by X-ray methods. Passing fairly quickly over elements and simpler substances, we come on p. 139 to the silicate structures, and the rest of the book is then mainly devoted to the wide variety of structural forms exhibited by the silicate minerals. The reader is conducted from the earliest stages of the work to the latest developments, and nothing of importance is omitted on the way. The book is liberally furnished with diagrams and these have been drawn in such a way as to assist the reader in building up scale models of the structures. The book is a very valuable addition to the literature of the subject, and can be strongly recommended.

The Discovery of Specific and Latent Heats. By D. McKie, Ph.D., B.Sc., and N. H. de V. Heathcote, B.Sc. With foreword by E. N. da C. Andrade, D.Sc., Ph.D., F.R.S. [Pp. 155.] (Arnold & Co. Price 6*s*.)

This account of the foundation of the quantitative science of heat is based on a comprehensive and careful study of the original papers of the eighteenth century investigators, and the sources are freely quoted. The authors are to be commended not only for their selection and arrangement of the material, but for their scholarly and interesting presentation.

After an account of the work of Black they take some pains to establish his priority in the conception of latent and specific heats (although apparently he did not actually use the latter term), but at the same time they do ample justice to other workers, and in particular to Wilcke, to whose work quite a considerable portion of the book is devoted. Good use is made of extracts of some of the most important of the original experimental results and the arguments based on them.

This readable little book, about which the least interesting point is perhaps the title, is well worth a study by physics students in general, as well as those who are mainly interested in the history of science.

The Retardation of Chemical Reactions. By K. C. Bailey. [Pp. viii+479.] (Edward Arnold & Co., 1937. Price 26*s*.)

Although the subject dealt with in this book has not been entirely neglected in several of the standard works on chemical kinetics published during the last decade, it has, generally speaking, been accorded insufficient attention, or at the best has been discussed in relation to a very restricted series of reactions. Professor Bailey's book marks the first attempt to deal systematically with this class of phenomena, and it thus fills an evident gap in the literature on chemical reactions. A comprehensive treatise has not been attempted, and would obviously be impossible in the space of less than five hundred pages, and the author has chosen to exclude certain fields, rather than give a necessarily more sketchy survey embracing everything that could legitimately be included under the title. The subjects omitted include enzyme reactions, salt effects, and intensive drying, which are all treated adequately elsewhere.

In any discussion of retardation the theory of chain reactions must occupy a prominent place, and this is introduced early in an excellent chapter, which provides a sound basis for the consideration of the experimental data given later. Thereafter the order of chapters follows that of types of reaction.

Oxidation takes nearly the first half of the book, and subsequent chapters are devoted to anti-knock compounds, the protection of rubber, the prevention of metallic corrosion, the setting of plaster of Paris and cement, and the stabilization of hydrogen peroxide. This accounts for about three-quarters of the book, the remainder being given to a discussion of reactions involving decomposition, addition and substitution, polymerization, isomeric change, etc.

The author writes in a clear and pleasant style, and displays throughout a quite unusual degree of impartiality. On the whole he shows discrimination in his selection of material, but in certain chapters the reviewer felt that the text was rather overloaded with detail, not all of which was entirely relevant. The general impression gained, however, was that of a well-balanced book in which the author had avoided, with some skill, the danger of presenting a mere miscellany of chemical reactions. A feature that can be unreservedly commended is the historical development of the individual fields, which is particularly thorough.

The bibliography is extensive, and contains references to more than sixteen hundred papers on retardation alone. It is well up to date, and only once did the reviewer notice the omission of an important recent paper.

The book is essentially one for research workers, but there is much to sustain the interest of the general reader.

OBITUARY.

JOHN ROBINSON AIREY.

By the passing of John Robinson Airey we lose one who made his mark in the fields of Science and Education.

He died on September 16th, 1937, aged sixty-nine, at Newtown, Montgomeryshire, where he had been living with his wife and daughter since his retirement in 1933 from his post as Principal of Leeds City Training College.

Born in Leeds in 1868, his foundational education at the Blenheim Board School, Leeds, was followed by further instruction at the Leeds Central High School. Then, after training for the teaching profession at the Borough Road Training College, London, from 1888 to 1889, he joined the staff of the Central High School in Leeds, continuing his studies in the evenings at the then Yorkshire College and taking the degree of B.Sc. as an external student of the University of London in 1894.

From 1896 to 1903 he was second master at Porth Intermediate School, Glamorganshire, and the end of this period

marks a courageous and decisive step in his career, for at the age of thirty-five he went up to St. John's College, Cambridge, as an undergraduate, to read for the Natural Sciences Tripos.

He often referred with characteristically modest satisfaction and happy reminiscence to his three years of work at Cambridge, and to the encouragement he got at College, where he was awarded prizes and a scholarship on his Tripos results, for he took a First Class in Part I. in 1905, and a First Class also in Part II. the following year. He took his B.A. degree in 1906, proceeded to the M.A. in January 1910, and was awarded the Sc.D. degree in 1926. The D.Sc. of London was awarded in 1915.

It is said of him as an undergraduate that he was surprisingly fresh and resilient in mind and was at the same time an extremely careful worker, qualities which marked his work at all times.

One of his Cambridge lecturer friends relates that Airey was very despondent after his Tripos Part II. examination—asserting that it was a shame that none of the questions to which he had given attention was included in the papers—he would burn his books! His friend counselled patience—"Wait," he said, "until the results are out and then you can burn your books at the bottom of my garden"! There was, of course, no bonfire.

It was during his residence at Cambridge that he showed his liking for computation in general, which later was to earn him so high a reputation in scientific circles.

His early interest in Bessel and allied functions was undoubtedly stimulated by Cambridge contacts, particularly perhaps with G. F. C. Searle and R. R. Webb. He loved to tell how, in the garret of his house, he used to perform experiments with bicycle chains, following up those he did at the Cavendish Laboratory, Cambridge. The results of these experiments and calculations, involving both Bessel and Neumann functions, were published in the 'Philosophical Magazine' of 1911—as a matter of fact, the same volume which contains Rutherford's famous paper on α-ray scattering.

Airey's interest in his chosen branch of Mathematics scarcely waned with the years. There are a number of publications to his credit, including those important tables published in Volume I. of the British Association Mathematical Tables (1931), which had previously appeared in the BritishAssociation reports between 1916 and 1928.

He was a member of the British Association Mathematical Tables Committee uninterruptedly for twenty-six years, until his death, and it was within this period that he actively engaged in his computations.

It is not only as a mathematical physicist that Airey will be remembered, for he earned his living not as a scientific worker, but as an educationist, and an unusually successful one.

He well and truly laid the educational foundations of Morley Grammar School as its first headmaster—1906 to 1912—and then became Principal of West Ham Technical College, where he stayed until his appointment in 1919 as Principal of Leeds City Training College, Beckett Park, a post from which he retired at the age of sixty-five in 1933.

This later phase of his working life was one in which he found himself beset with many post-war difficulties which he always successfully surmounted. The high position he won for himself in the regard of all his associates and students cannot better be recorded than in the words of the testimonial handed to him in 1933. It says: "Your portrait hangs in the College Hall as a symbol of our affection and esteem. In this little book we wish to translate that symbol into words. As Principal of the College you have ever been jealous for its interests and have at all times safeguarded its good name.

"Not only by your own achievements, but in your own addresses to us, you have held up the torch of learning—learning which can only be won by persistent and earnest effort.

"Serene in calm and storm, you have at all times steered a straight course, your actions characterized by sincerity of purpose and a love of what is right.

"You will live in our memories as a Principal and a friend whose words were few, and whose happy and kindly disposition shone out so brightly that even your reproofs were tinged with humour. Not least we shall cherish your memory because you showed us a religion based on simple faith and a reverential search for truth."

It is particularly fitting in this place to record the good work done by Airey as an Advisor to this Journal. No inconsiderable part of his time in retirement was devoted to editorial work on behalf of the 'Philosophical Magazine.' He spared no pains in the reading of MSS. and proofs.

His selfless devotion to this work and his gentle unobtrusive personality will be missed no less in this sphere than in others.—R. W.

[*The Editors do not hold themselves responsible for the views expressed by their correspondents.*]

INDEX TO VOL. XXIV.

ACOUSTICAL experiments with telephone receivers.—Part I., 665; Part II., 905.
Adams (E. P.), the two-dimensional ice-pail, 1127.
Airey (Dr. John R.), the converging factor in asymptotic series, and the calculation of Bessel, Laguerre, and other functions, 521.
Alkali halides at low concentrations, the refractive index of the, 890.
Alternating magnetic fields, experiments on supraconductors in, 361.
—— stress systems and a stress criterion of the fatigue limit, note on certain combined, 695.
Atomic forces of solid states, 466.
Auroral region of the atmosphere, the temperature distribution within the, 588.
Bailey (J. E.), Makinson (R. E. B.), and Somerville (J. M.), the behaviour of electrons in bromine, 177.
Bate (Dr. A. E.), the end-correction of an unflanged pipe, 453.
Baudisch (Oskar) and Welo (Lars A.), transformations from γ-FeOOH and γ-Fe_2O_3 to α-Fe_2O_3 at lower temperatures and the irreversible transition γ-FeOOH to α-FeOOH, 80.
Baxter (Dr. A.) and Brentano (Dr. J. C. M.), the effect of discontinuities of the background on the evaluation of the intensities of X-ray reflexions from crystalline powders, 473.
Bell (R. P.), some properties of Bessel function zeros derived from the wave functions for a particle in an enclosure, 299.
Bessel, Laguerre, and other functions, the converging factor in asymptotic series and the calculation of, 521.
Bessel function zeros, some properties of, derived from the wave functions for a particle in an enclosure, 299.
—— product functions, 888.
Beta-rays, the diffraction of, 953.
Bickley (Dr. W. G.) and Rutland (V. D. H.), the flow past a flat plate, to Oseen's approximation, 704.
Blue filters, use of, in the derivation of candle-power standards, 1059.
Blüh (Dr. Grete), Blüh (Dr. O.), and Puschner (M.), measurements of thermal diffusion in gas mixtures, 1103.
Blüh (Dr. O.), Puschner (M.), and Blüh (Dr. O.), measurements of thermal diffusion in gas mixtures, 1103.
Bond (Dr. W. N.) and Puls (H. O.), the change of surface tension with time, 864.
Books, new :—F. C. Champion and N. Davy's Properties of Matter, 207; Sir A. S. Eddington's Relativity Theory of Protons and Electrons, 208; A. H. Wilson's The Theory of Metals, 325; Lord Rutherford's The Newer Alchemy, 327; A. C. Candler's Atomic Spectra and the Vector Model.—Vol. I. Series Spectra, Vol. II. Complex Spectra, 327; F. W. J. Taylor and Wilson Baker, Sidgwick's The Organic Chemistry of Nitrogen, 519; Dr. J. E. Shrader's Manual of Experiments in Physics, 712; Sir Frank Dyson and R. v. d. R. Woolley's Eclipses of the Sun and Moon, 824; Profs. S. Timoshenko and D. H. Young's Engineering Mechanics. Statics and Dynamics, 1132; Prof. W. L. Bragg's Atomic Structure of